65-70-AD

AD 670984

PRELIMINARY INVESTIGATION OF BALLUTE-FLEXIBLE ROTOR CONCEPT FOR LOW-ALTITUDE CARGO AIRDROP -

Final Report

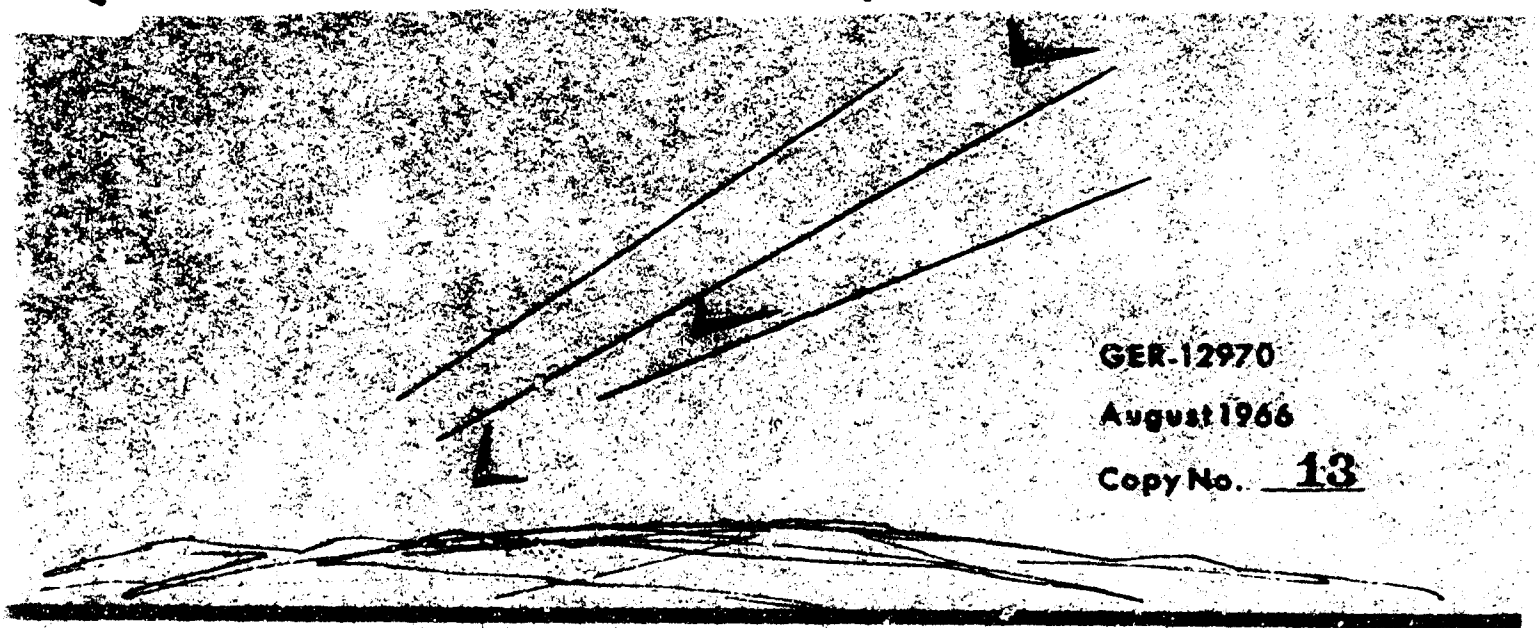

GER-12970

August 1966

Copy No. 13

Prepared by D. L. MANSFIELD

GOODYEAR AEROSPACE CORPORATION AKRON, OHIO

for

U.S. ARMY NATICK LABORATORIES, NATICK, MASSACHUSETTS

Contract DA19-129-AMC-857(N)

[illegible]

116

PRELIMINARY INVESTIGATION OF BALLUTE-FLEXIBLE ROTOR CONCEPT FOR LOW-ALTITUDE CARGO AIRDROP

D. L. Mansfield

Goodyear Aerospace Corporation
Akron, Ohio

August 1966

GOODYEAR AEROSPACE
CORPORATION

AKRON, OHIO 44315

TECHNICAL REPORT
68-70-AD

PRELIMINARY INVESTIGATION OF
BALLUTE-FLEXIBLE ROTOR CONCEPT
FOR LOW-ALTITUDE CARGO AIRDROP -
FINAL REPORT

GER-12970 August 1966

TABLE OF CONTENTS

TABLE OF CONTENTS

LIST OF ILLUSTRATIONS

LIST OF ILLUSTRATIONS

LIST OF TABLES

LIST OF SYMBOLS

A = disk area swept by rotor blades = πR^2 (sq ft)

A_f = surface area of decelerator

A_r = projected area of rotor during deployment

b = blade chord length (ft)

C_1, C_2 = constants of integration

CF = centrifugal force (lb)

C. F. = unit coating weight

C_{D_B} = drag coefficient as referenced to a BALLUTE

C_{D_R} = drag coefficient for rotor system

C_T = rotor thrust coefficient

C_f = coating and/or construction factor

C_l = section-lift coefficient

D_B = BALLUTE diameter (ft)

D. F. = total meridian design factor

D_f = total fabric design factor

d = vertical distance (ft)

E = pressure bottle energy (ft-lb)

FS = factor of safety

F_P = power required for flare

LIST OF SYMBOLS

f_f = design stress due to design inflation pressure and decelerator radius

g = acceleration due to gravity (ft/sec^2)

H = number of meridians

h = blade height = 0.12b (ft)

I = moment of inertia

K = strength-to-weight ratio of material (in.)

KE = kinetic energy (ft-lb)

K_f = envelope fabric strength-to-weight ratio

$$K_1 = \int_o^R \frac{dm}{dR} R^2 dR \Big/ \int_o^R \frac{dm}{dR} R dR$$

$$K_2 = \int_o^R \frac{dm}{dR} \Big/ \int_o^R \frac{dm}{dR} R dR$$

$$K_D = C_{D_R} \rho b/2$$

$$\bar{K}_D = \int_o^R \frac{dK_D}{dR} R^3 dR \Big/ \int_o^R \frac{dm}{dR} R dR$$

$$K_L = C_l \rho b/2$$

$$\bar{K}_L = \int_o^R \frac{dK_L}{dR} R^3 dR \Big/ \int_o^R \frac{dm}{dR} R dR$$

L = length of each meridian (ft)

LF = load factor

LF_o = load factor after completion of flare maneuver

LIST OF SYMBOLS

L_T = total blade lift (lb)

l_r = lift at point r along blade span (lb)

M = total mass (lb)

M_{cg} = moments about center of gravity

m = rotor mass (lb)

N = number of blades

P = absolute pressure (psia)

p = internal pressure (psi)

Q = tip weight (lb)

Q_C = constant applied torque (ft-lb)

$$\bar{Q} = Q / \int_o^R \frac{dm}{dR} \, RdR$$

Q_{TOT} = weight of total tip system

$q = \frac{\rho}{2} V_D^2$ (psf)

R = blade radius (ft)

R_B = radius of the BALLUTE = $D_B/2$ (ft)

R_l = local radius arm along rotor blade (ft)

R_X = component of forces in X direction at hub (lb)

R_Y = component of forces in y direction at hub = thrust of one blade (lb)

r = any point along blade span (ft)

T = meridian design tension load (lb)

$T_R = \sqrt{(R_X)^2 + (R_Y)^2}$ (lb)

t = time (sec)

V = volume of air (cu ft)

V_{AF} = actual airfoil volume (cu ft) = V_{blade}

V_D = vertical descent velocity (fps)

V_{FA} = volume of flat AIRMAT (cu ft)

V_f = final impact velocity (fps)

V_I = initial deployment velocity (fps)

V_T = tip speed (fps)

W = gross system weight (lb)

W_{AIR} = weight of air in the blade (lb)

W_B = weight of the BALLUTE (lb)

W_{BP} = AIRMAT weight for pressure (lb)

W_{BT} = total blade weight (lb)

W_C = blade coating weight (lb)

W_D = disk loading = $W/\pi R^2$ (psf)

W_{FA} = weight of flat AIRMAT (lb)

W_f = weight of fabric (lb)

W_{HUB} = weight of hub assembly (lb)

W_{LE} = material weight required at leading edge for mass balance (lb)

LIST OF SYMBOLS

W_m = weight of meridian (lb)

W_{PB} = air storage bottle weight (lb)

W_R = rotor system weight (lb)

W_{RS} = blade weight and tip weight = $W_{BT} + Q$ (lb)

W_r = weight of elemental disk of AIRMAT at radius r

w = weight per unit length of blade (ppf)

X = radius of rotor hub

$\bar{X}$ = centroidal distance (ft)

$\underline{\bar{X}} = \frac{r}{R}$ = percent blade length

X_T = tip horizontal coordinate = $R \cos \theta_o$ (ft)

x = horizontal coordinate = $r \cos \theta$ (ft)

$\underline{\bar{Y}} = \frac{l_r R}{L_T}$; R (ft)

α = blade angle of attack (deg)

θ = blade pitch angle (angle of blade relative to its rotational plane) (deg)

θ_o = coning angle (deg)

λ = advance ratio = $V_D / R\,\Omega$

ρ = air density (slugs/cu ft or pcf)

σ = rotor solidity = ratio of blade area to disk area or stress (lb/in.)

ϕ = rotor deployment angle (deg)

Ω = rotor angular velocity (radians per second)

LIST OF SYMBOLS

Subscript

f = final value for deployment

Miscellaneous

$(')$ = differentiation with respect to time

SUMMARY

Goodyear Aerospace Corporation (GAC) was awarded U.S. Army Contract DA19-129-AMC-857(N) to perform an exploratory investigation of a BALLUTE[a] flexible rotor system for a low-altitude airdrop mission. In this concept the BALLUTE extracts the rotor and payload, and induces initial spin into the rotor; then the inflatable fabric rotor system decelerates the cargo to the required impact velocity.

The evaluation of the BALLUTE-flexible rotor system was performed in a series of dependent steps. A definition of the system concept as required by this application was first established and then a detailed design of the system components was generated. The final phase determined the design weights of the BALLUTE and rotor system. Existing performance data and state-of-the-art structural analysis techniques were used in evaluating the final size and weight tradeoffs.

The rotor was studied only as a drag device; its basic L/D (glide) capability was not considered. One reason for neglecting the forward flight ability is the requirement for a highly complex mechanism to control blade pitch angle. The only advantage in having a glide capability is the ability to fly the cargo to a desired touchdown point. At this time the low-altitude requirement restricts the distance of forward flight to a minimum. These two reasons have eliminated L/D from further consideration.

The results of this study indicate that the delivery of cargo payloads from 2,000 to 35,000 lb can be accomplished without exceeding a gross weight allowance of 20 percent for rotor system weight. A majority of the payloads can be delivered at a weight penalty of less than 15 percent. Payloads greater than 8,000 lb must descend at a velocity greater than the required 22-fps landing speed value. To meet the required impact value, a "flare" maneuver must be performed. During the flare, the blade's angle of attack is increased to produce more lift and then the cargo is decelerated to the proper impact velocity. Experimental investigation with a 5-ft diameter inflatable model was conducted and demonstrated small-scale functional feasibility of flexible rotors for vertical-descent autorotative applications.

While this exploratory study provided analytical data indicating full-scale feasibility, further experimental verification clearly is required to prove the validity of assumptions made.

[a]TM, Goodyear Aerospace Corporation, Akron, Ohio. Citation of the registered trademark BALLUTE in this report does not constitute an official endorsement or approval by the Government of the BALLUTE.

SUMMARY

Three significant factors to be established deal with (1) the transient spin-up time required by the rotor to reach its steady autorotative state, (2) the effect of gyroscopic motion of the rotating system. Since the rotational motion of the rotor will restrict the rate of change of its flight path angle, the possibility exists that the rate of change of the cargo's flight path angle will be greater than that of the rotor and result in the cargo colliding with the rotor. A suitable coupling between the rotor and the cargo to prohibit the relative motion of one to the other is required, and (3) the motion of the rotor after the cargo has made impact. While the rotor is more likely to fall away from the payload, the possibility exists that the rotor will descend vertically and fall on the cargo.

In conclusion, further exploratory design and verification in these performance areas is needed to properly assess the rotor concept's applicability to meet the subject application.

SECTION I - INTRODUCTION

The primary function of airdrop in the Army mission is surprise assault by mass air transport of men and equipment. The requirement for surprise dictates minimum reliance on drop zone improvement. The requirement for mass transport demands airdrop system reliability, simplicity, and economy. The ideal airdrop system concept could be defined therefore, as that concept which realizes the advantages of low-altitude airdrop with minimum compromise of the above requirements.

Low-altitude airdrop from heights under 500 ft is desirable because of its potential for improvement in drop accuracy and in reduction of aircraft vulnerability to hostile action. In addition to replacing the present 1500-ft cargo drop altitude, the requirement to investigate, in a more complete manner, a possible improved delivery method was established. A more complete evaluation consists of not only functional feasibility studies, but also considering other operating suitability characteristics such as reliability, environmental effects, and logistics. Other considerations include such nonoperating characteristics as cost, maintenance, training requirements, human factors, handling, and readiness for operation.

The preliminary investigation of the BALLUTE-flexible rotor has been directed toward a system design compatible with the requirements for a low-altitude airdrop system for supplies and equipment weighing from 2000 to 35,000 lb. The designation of low altitude for the airdrop mission stipulates a drop initiation point relative to the ground of 500 ft or less. As indicated, the concept is comprised of two basic components designed to fulfill their respective requirements. The BALLUTE extraction system will produce a maximum extraction force of 1.5 g's at aircraft velocities of 110 to 150 knots, at altitudes relative to sea level up to 5500 ft. The rotor system has been designed to satisfy a sea level vertical impact velocity of 22 fps.

Experimental investigations have demonstrated the feasibility of inflatable fabric rotors for autorotative applications. In addition to the packaging capability, the inflatable rotor offers the ability to change rotational energy through a flare maneuver into a form that will reduce the impact velocity to a value lower than that experienced at steady-state terminal descent conditions. The intent of this study has been to establish design criteria that would provide projected weight and anticipated system operating characteristics.

Evaluation of the concept to utilize an autorotating decelerator for the low-altitude delivery of military cargo was performed for both the functional and operational aspects of the system. The objectives of the functional analysis were to determine the performance characteristics and to evaluate the conceptual design. Operational considerations were used to establish the reasonable and acceptable extremes as applied to this specific mission. Reliability, ground handling, and maintenance then were considered for the remaining operating regime.

SECTION II - SYSTEMS DESIGN AND FUNCTIONAL ANALYSIS

1. GENERAL

The exploratory development of the inflatable rotor system for the air-drop mission was performed in a series of discrete steps. As with any development program, a definition of the system concept and the function of various components has been established and can be found in Item 2. After formulating the conceptual design, it was necessary to establish size criteria based on state-of-the-art performance data. These data are presented in Item 3. The detailed design analysis of the various system components then was performed to establish projected weight information and limitations that might restrict the use of the system for this application.

Final weight and size determination evaluation can be found in Item 4.

2. CONCEPTUAL DESIGN

a. Evaluation

Presented in other sections of this document are the various theoretical performance characteristics that can be obtained with a BALLUTE and a rotating decelerator. The practical limitations of the concept for this application are dictated by the personnel responsible for the handling and preparation of the systems. In order to evaluate the concept, therefore, the system and the requirements for preparing it prior to the airdrop operation must be described.

b. Deployment Sequence

The deployment sequence selected as the most applicable for this initial study is presented in Figure 1. The deployment sequence is initiated by the release of a small pilot chute from its attachment point on the ceiling of the aircraft cargo compartment. Upon release, the chute pack falls through the doorway and into the airstream. Once in the air, aerodynamic forces remove the bag from the chute, thus allowing the chute to inflate.

The chute then extracts a package that contains the BALLUTE and rotor system. This package moves rearward, out the door, and into the airstream.

As this package reaches the end of the riser line attached to the cargo,

a lanyard becomes tight and pulls a pin from a time-delay, reefing-line type cutter located at the front of the blade deployment bag. Then the riser becomes tight from the pull of the pilot chute; the drag force is concentrated on the BALLUTE deployment bag. The appropriate restraints between the BALLUTE deployment bag separates and deploys the BALLUTE. As soon as the BALLUTE is in the airstream, inflation begins. When full inflation is approached, rotation begins and within a predetermined amount of time the system is at the maximum rotational velocity. When the required 1.5-g extraction force is obtained, the cargo begins to move out of the aircraft.

As the cargo is moving through the aircraft, the BALLUTE reaches its maximum rotational velocity and the previously initiated rotor bag release cutter fires, starting blade deployment. As the deployment of the blades begins, the cargo is passing across the door, and the static line releases the extraction force from the extraction attachment point on the platform. The actual load on the riser at this time is relatively small, resulting from the release of the BALLUTE for blade deployment.

When the deployment bag and rotor hub are at a predetermined separation distance, a lanyard connected to the initiator pin of the pyrotechnic manifold release valve is pulled. As the pin is removed, the pyrotechnic charge fires and severs a diaphragm located in the manifold assembly. The air in the storage bottles then is released into the blades.

During the time that the blades are being deployed and inflated, the cargo leaves the door and undergoes a free-flight condition until the blades are completely deployed. As the deployment bag leaves the bladetips, the rotational energy induced by the rotating BALLUTE takes over and the centrifugal force generated throws the blade tips outward. The combination of this initial torque and aerodynamic forces accelerate the blades to their steady-state autorotating condition. The accelerating force on the blades reduces the system velocity to an intermediate or terminal descent velocity.

Prior to ground impact of the descending system, a flare maneuver, if required, is initiated to further decrease the descent velocity. Flare would be initiated by a ground-sensing probe; the exact location and attachment would be determined during a development program. When the probe would touch the ground, a signal would be transmitted to the rotor blade tips and an appropriate cutter device would be activated to release restraint at the blade tips, allowing a change in the angle of the attack, α. The airdrop item then would impact at 22 fps.

Eliminating the flare maneuver was another recovery method considered. This could be accomplished with larger rotor blades (relative to a given payload weight) to lower the design terminal velocity of the descending

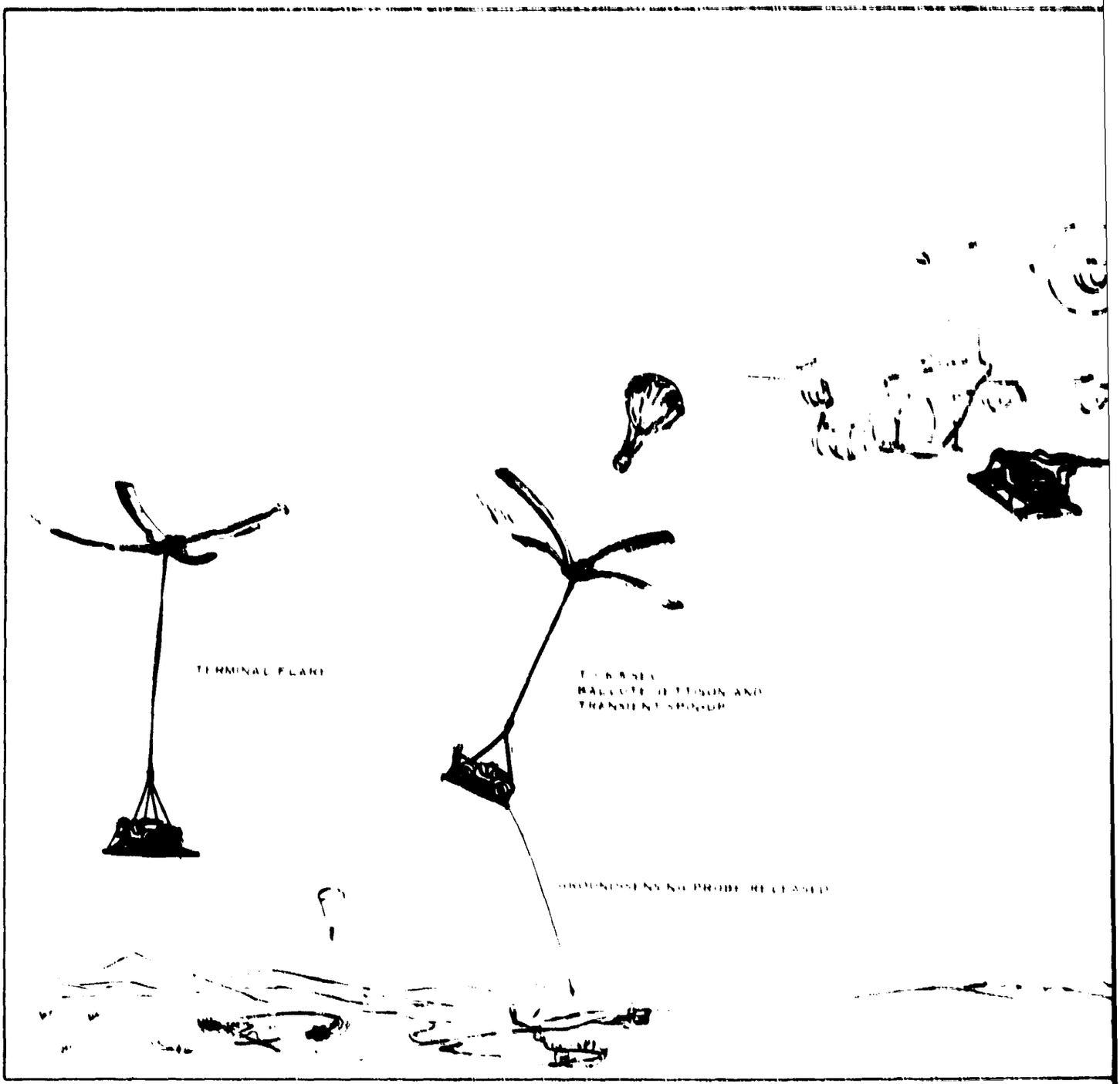

A.

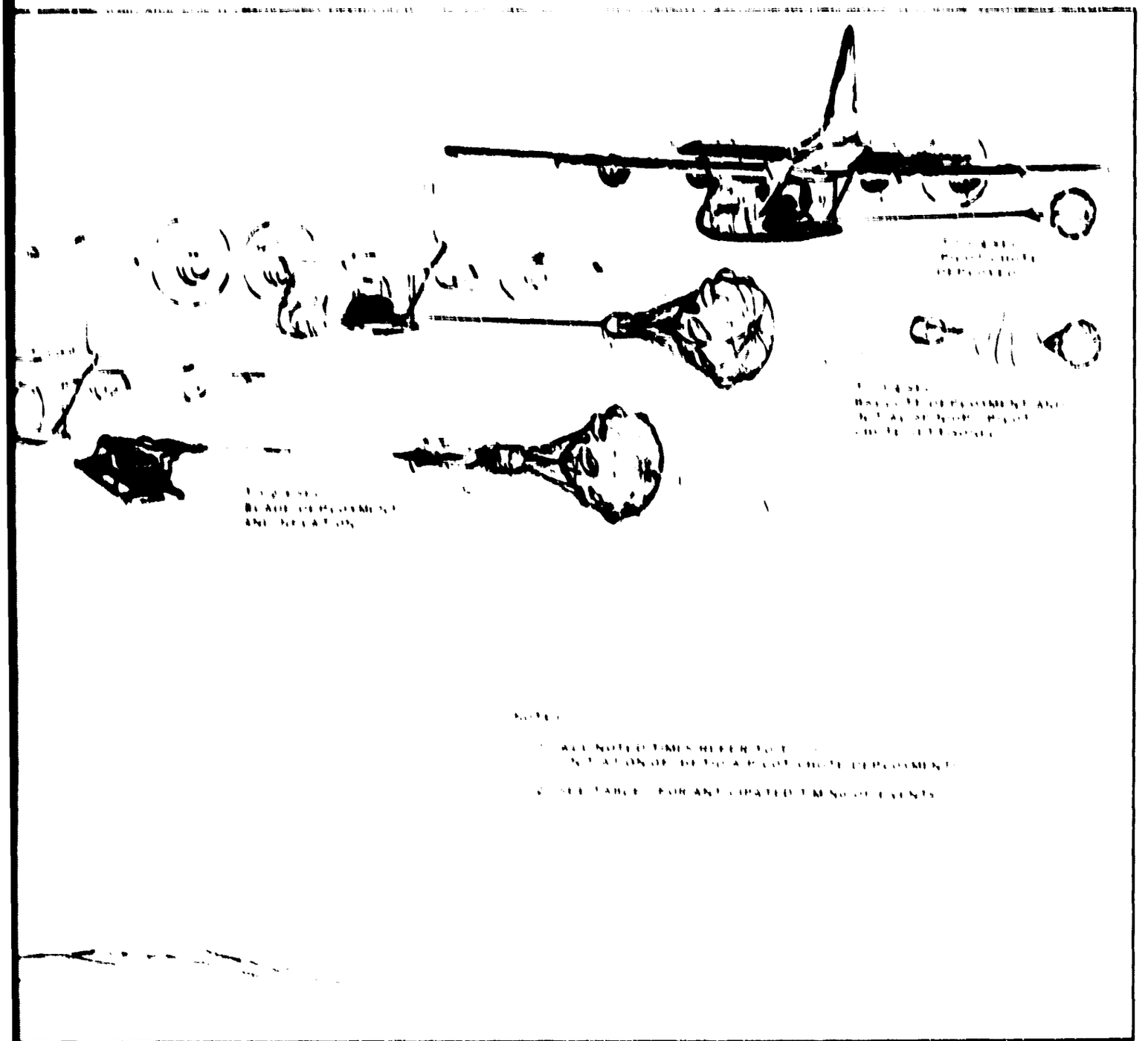

Figure 1 - Deployment Sequence

B.

system to the required 22 fps minimum. The advantage would be one less sequencing stage and less design complexity. The original purpose of the flare maneuver was to reduce the blade size and hence the weight. Subsequent weight studies of payloads greater than 8000 lb indicated a significant weight saving by using a flare maneuver. Studies for payload weights between 2000 and 8000 lb indicated the flare system weight saving of only about two percent and hence justifies utilizing the system without flare to deliver the smaller payloads because of its simplicity.

The changes that were made in the present parachute system include replacing the parachute extraction device with a BALLUTE and the main parachutes with a rotor blade system. One feature of this system not used with most existing systems is the requirement for a small pilot chute to deploy the BALLUTE.

Presented in Table I are the anticipated times that will be experienced during the drop operation. The values are relative to the release of the pilot chute. The values are reasonable approximations of the values that would be necessary for successful operation of the system as applied to the low-altitude mission.

TABLE I - ANTICIPATED TIMING OF EVENTS

Event	Time (sec)
Initiation of command signal (3-ft pilot drogue released from aircraft ceiling)	0
Three-foot drogue reaches "line-stretch" and begins to extract rotor package	0.4
BALLUTE rotor package reaches "line-stretch"	0.6
Drogue chute strips off bag and BALLUTE reaches full inflation (cargo leaves door)	1.4
Blades completely deployed and inflated	2.4
Blades at steady-state conditions	8.4

Further description of the BALLUTE and rotor are given in Items 3 and 4.

c. BALLUTE Description

In general, a BALLUTE is a woven-fabric ram-air-inflated pressure

vessel of isotensoid design. The basic principle underlying the operation of the BALLUTE is that the ram-air inlet oriented into the airflow allows internal pressurization of the body to a level equal to the sum of the dynamic and ambient pressures of the flow. This internal pressure acting normal to the membrane is always greater than a combination of the external ambient pressure and the dynamic forces that act externally and obliquely on the membrane. The inflated shape determines the effectivity of the BALLUTE as a stable drag device. Presented in Figure 2 is a picture of a presently developed BALLUTE. The inflated structure is primarily pear-shaped except for the large circumferential burble "fence" at, or just aft of, the maximum diameter. Ram air enters through a series of symmetrically located side inlets or through a single large nose inlet. The fence is inflated through numerous small ports located around the decelerator proper and beneath the envelope of the fabric fence. The inflated height of the fence is up to 10 percent of the maximum inflated diameter of the model.

For application to this program, a modification will be incorporated into the burble fence so that the BALLUTE will spin. Figure 3 shows a spinning BALLUTE in free fall. This demonstration model shows the segmented burble fence that imparts the spin. Because this BALLUTE is stable, the canted segments are maintained at a constant angle of attack. Since each segment has a constant lift-to-drag ratio, the spin rate will be directly proportional to velocity of the air impinging on the BALLUTE. The resultant rotational energy will be transferred to the rotor package through a geodesically arranged attachment riser. A representation of this method can be found in Figure 1.

At this time a parachute type device has been excluded from evaluation due to certain advantages of the BALLUTE. Its stability in an aircraft's wake while closely coupled is of major importance. This stability also is important to the anticipated deployment sequence described in this section. Experience has shown that the BALLUTE opening shock can be minimized with proper design to achieve a gradual drag buildup to a maximum at full inflation. Gradual drag buildup minimizes shock loads to the aircraft.

In addition to providing the required drag for extraction, the addition of vanes to the periphery of the BALLUTE makes it capable of autorotating so that the proper rotation energy is obtained to spin the packed rotor blades for their subsequent deployment. Because of the low-altitude requirement, the transient spin-up deployment time clearly must be minimized. Here again the BALLUTE's performance capability appears to be superior to a spinning parachute because it not only is capable of producing larger magnitudes of torque, but also develops this torque in a more repeatable manner. Forecasting higher torque values is based upon the fact that both the vanes and the basic BALLUTE envelope structure are nonporous. This results first in higher aerodynamic pressure

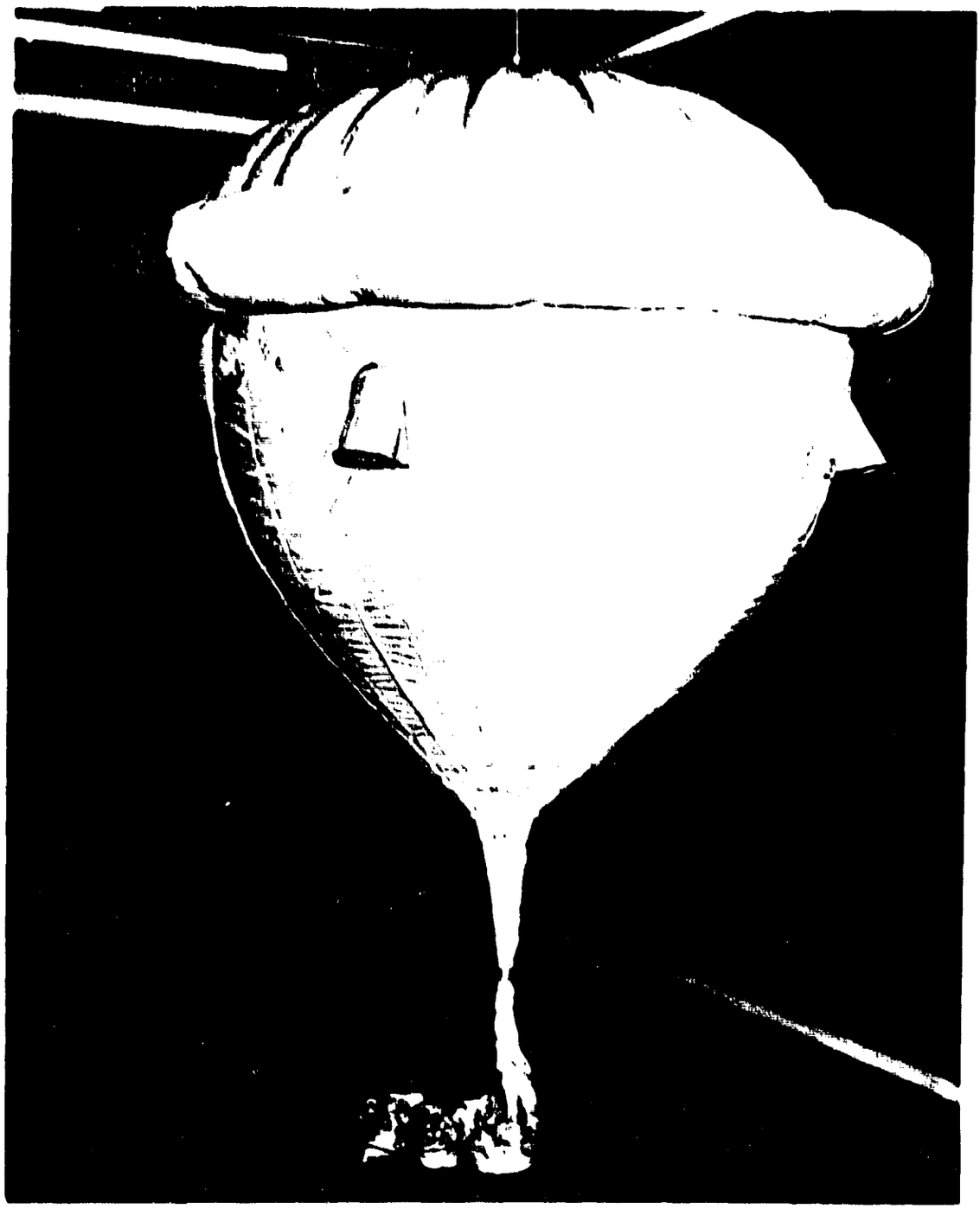

Figure 2 - Conventional BALLUTE Configuration

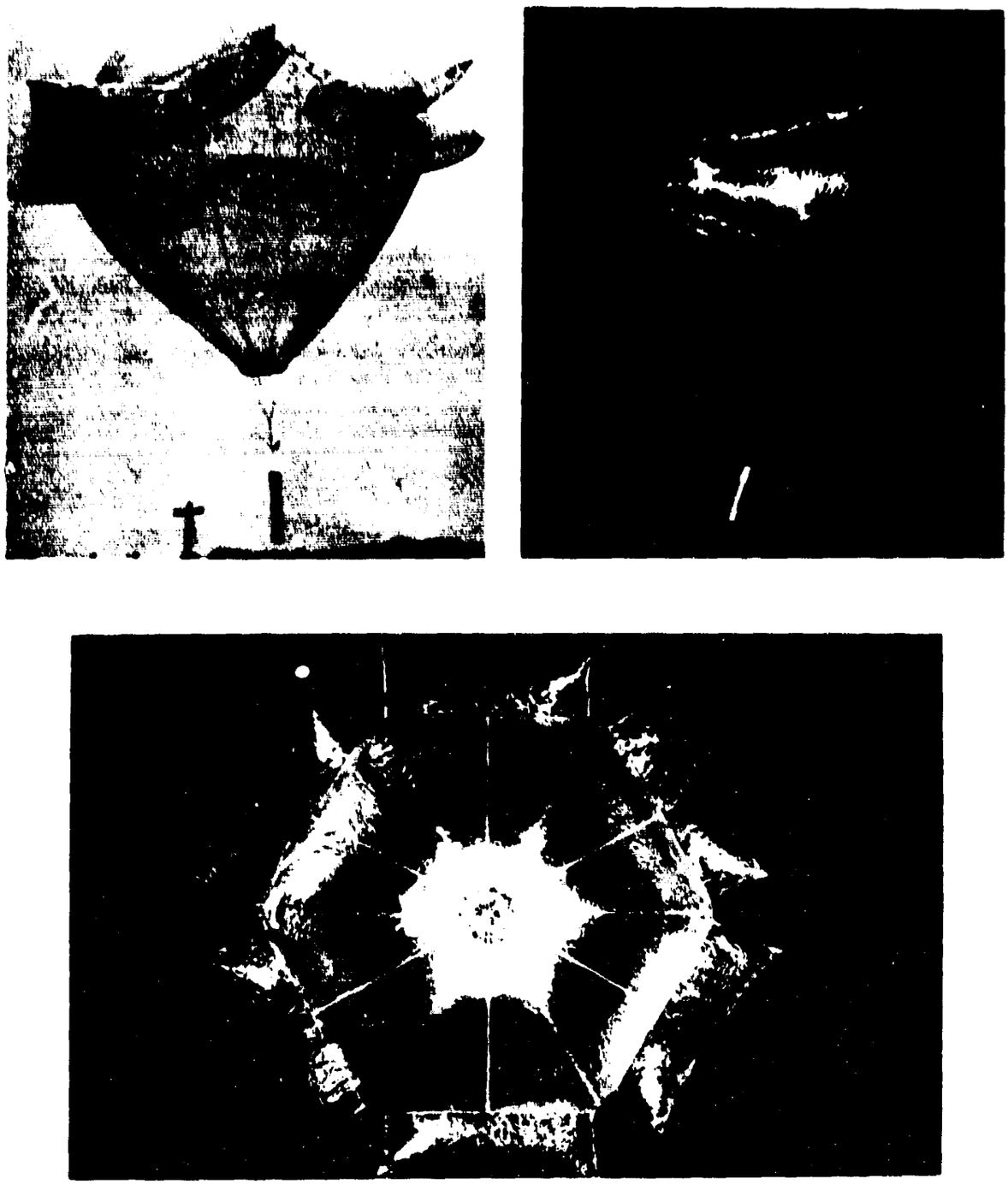

Figure 3 - Rotating BALLUTE Configuration

coupling forces being developed. Second, more repeatable performance is achieved because of the inherent "shape-retention" qualities that stem from the isotensoid designed geometry and the nonporous material. These two characteristics result in the device acting as a closed-pressure vessel, which in turn provides the shape retention of a nearly rigid-based structure.

Size and weight analyses are contained in Items 3 and 4, respectively.

d. Rotor Description

Design drawings were prepared that illustrate the various components of the rotor system. Two designs - one with the flare maneuver and one without - were examined, and the configuration differences of each were determined. Figures 4 and 5 present the anticipated design for vertical descent without flare (Configuration I) and that with flare (Configuration II), respectively. If it is assumed that both configurations have the same diameter, then with the increased disk loading to be experienced with Configuration II (higher terminal descent velocity), the hub and blade will require more structural strength to carry the larger loads. In general, the system is comprised of the blades, the air storage bottles, hub, bearing clevis attachment eye, pyrotechnic manifold release valve, and tubing required to transfer the air from the storage bottles through the manifold into the blades.

The represented system contains four blades. The reasons for this are:

1. To eliminate undesirable vibratory problems experienced with a two-bladed system[1]
2. From Reference 2, more efficient performance will be experienced with four blades for a 10-percent solidity
3. For a given diameter, air storage bottle size decreases with an increase in the number of blades, thus decreasing the system weight
4. If damage to one blade would be experienced during descent, the more remaining blades there are, the better the possibility of delivering the load undamaged

A detail of the blade cross section is shown to indicate the contour obtained with the AIRMAT[a] structure. The additional plies of material at the blade's leading edge are required to ensure that the mass axis and aerodynamic center are ahead of the forward quarter chord.

[a]TM, Goodyear Aerospace Corporation, Akron, Ohio. Citation of the registered trademark AIRMAT in this report does not constitute an official endorsement or approval by the Government of AIRMAT material.

The leading edge must be strengthened if the blade is to be aerodynamically stable. The detail of the hub assembly is shown for both Configurations I and II. A comparison of the two hubs will indicate that the hub for Configuration II contains a larger bearing and thicker structure for the spider and root attachment fittings. The reason for this is due to an increase in disk loading, which results in an increase in tip velocity. The increase in tip velocity results further in an increase in centrifugal forces, and thus an increase in the amount of material required to carry the load. With the increased disk loading, the payload weight will also increase; thus the requirement for larger bearing.

The air storage bottles required for inflation are located at the blade roots (the point where the blade attaches to the hub). Tubing is attached from each bottle to the centrally located manifold valve. A second duct of tubing connects the manifold to the blade. Although not shown in detail, a diaphragm is located inside this manifold between the inlet ports from the bottles and the outlet ports to the blades; a pyrotechnic charge punctures the diaphragm. The charge is initiated by extracting a firing pin with a lanyard attached to the blade pack. A quick-disconnect on one of the pressure bottle tubes is provided as a means of pressurizing the storage bottles.

To provide a bearing surface at the blade-root pivot, a split teflon collar is installed over the pressure bottle. The required amount of fabric then is wrapped around the teflon sleeve and attached to the upper and lower surfaces of a blade. The ends of the bottles also are designed to be the attachment points to the hub spider. This allows interchangeability of the blades if damage should result during use.

A feature required for Configuration II is the daisy chain arrangement at the blade tip. This restraint forces a predetermined amount of camber into the blade tip, so that when severed by a pyrotechnic cutter, the aerodynamic forces acting on the blade force it to a new increased angle of attack, initiating the flare maneuver. The ground proximity device required to initiate the flare is not shown on the drawing of Configuration II.

The method used in determining rotor sizes is contained in Item 3. The structural analysis required for weight determination is contained in Item 4.

3. FUNCTIONAL PERFORMANCE

a. BALLUTE Size Determination

The method used in establishing the various BALLUTE diameters required to develop the 1.5-g force is covered in this section. The generalized equation used is

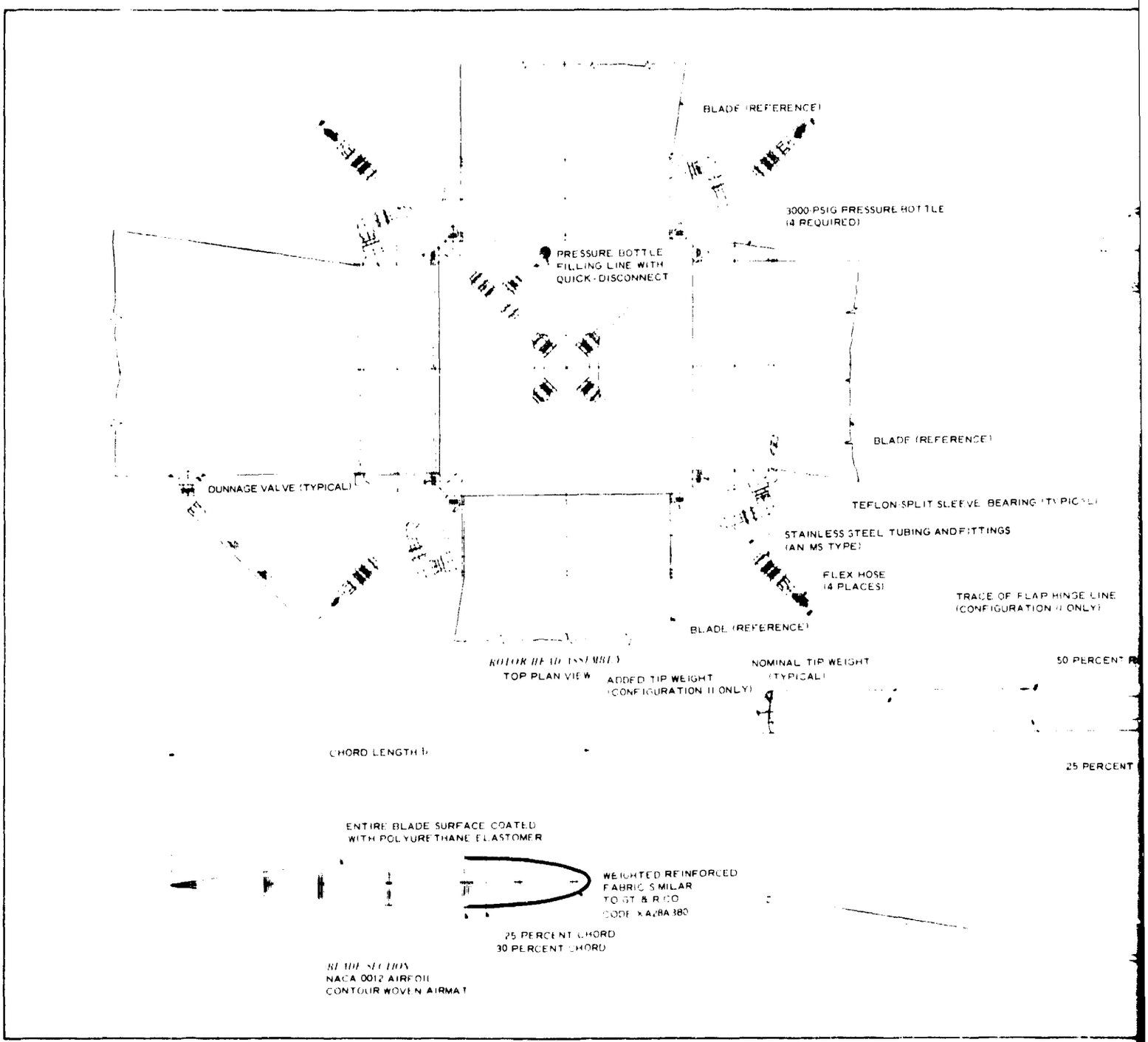
BLADE (REFERENCE)
3000-PSIG PRESSURE BOTTLE (4 REQUIRED)
PRESSURE BOTTLE FILLING LINE WITH QUICK-DISCONNECT
BLADE (REFERENCE)
DUNNAGE VALVE (TYPICAL)
TEFLON-SPLIT SLEEVE BEARING (TYPICAL)
STAINLESS STEEL TUBING AND FITTINGS (AN MS TYPE)
FLEX HOSE (4 PLACES)
TRACE OF FLAP HINGE LINE (CONFIGURATION II ONLY)
BLADE (REFERENCE)
ROTOR HEAD ASSEMBLY
TOP PLAN VIEW
ADDED TIP WEIGHT (CONFIGURATION II ONLY)
NOMINAL TIP WEIGHT (TYPICAL)
50 PERCENT
CHORD LENGTH
25 PERCENT
ENTIRE BLADE SURFACE COATED WITH POLYURETHANE ELASTOMER
WEIGHTED REINFORCED FABRIC SIMILAR TO GT & R CO. CODE XA/BA 380
25 PERCENT CHORD
30 PERCENT CHORD
BLADE SECTION
NACA 0012 AIRFOIL
CONTOUR WOVEN AIRMAT

A.

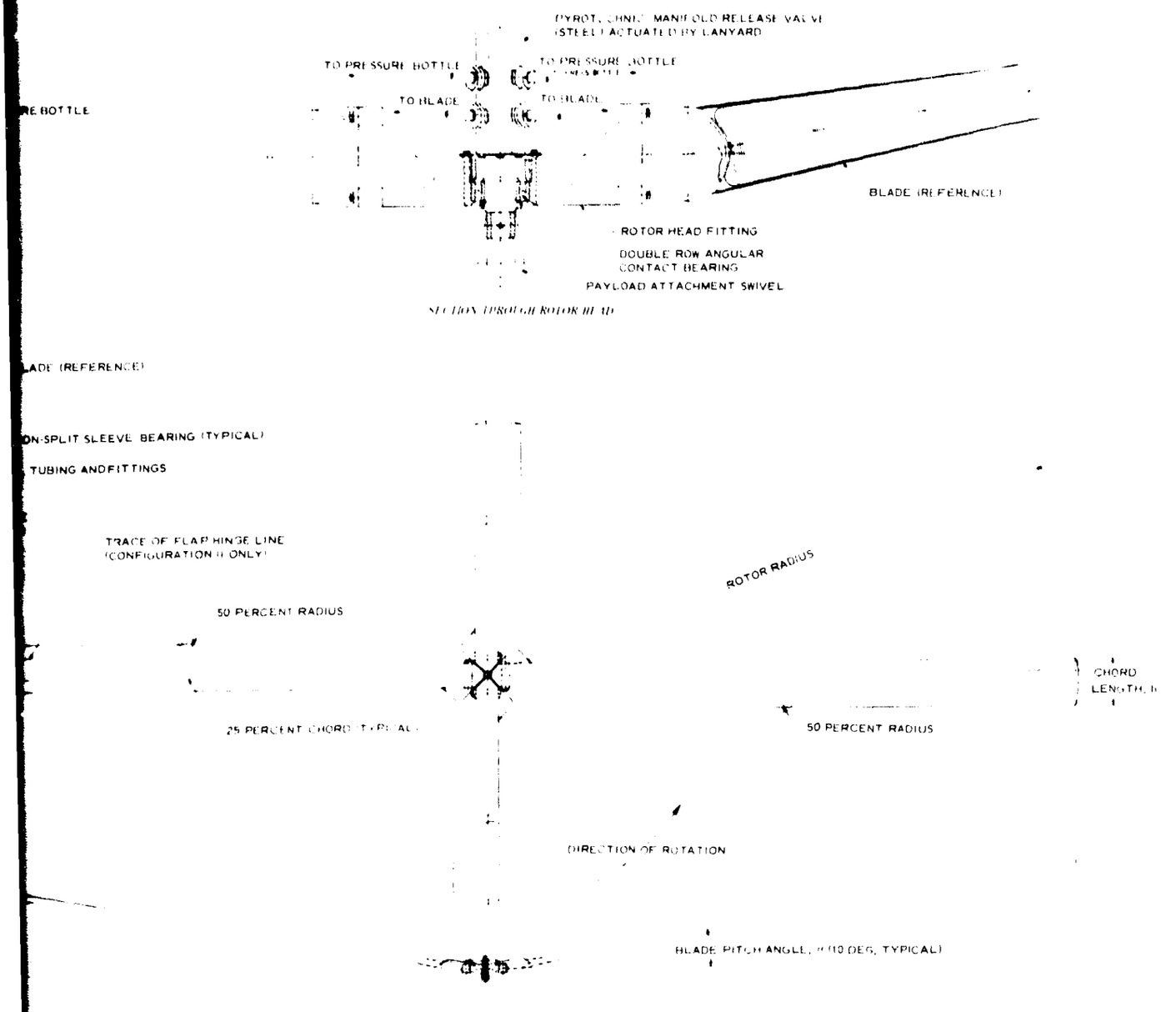

Figure 4 - Inflatable Rotor (No-Flare Version)

B.

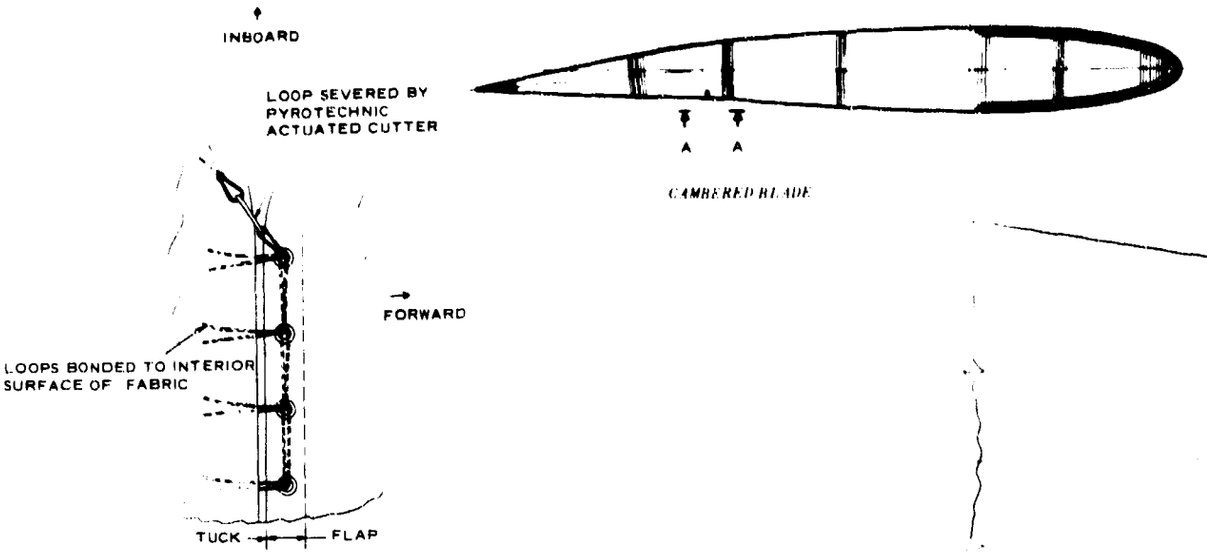

CAMBERED BLADE

DETAIL OF DAISY CHAIN BLADE COLLECTIVE CAMBER RESTRAINT

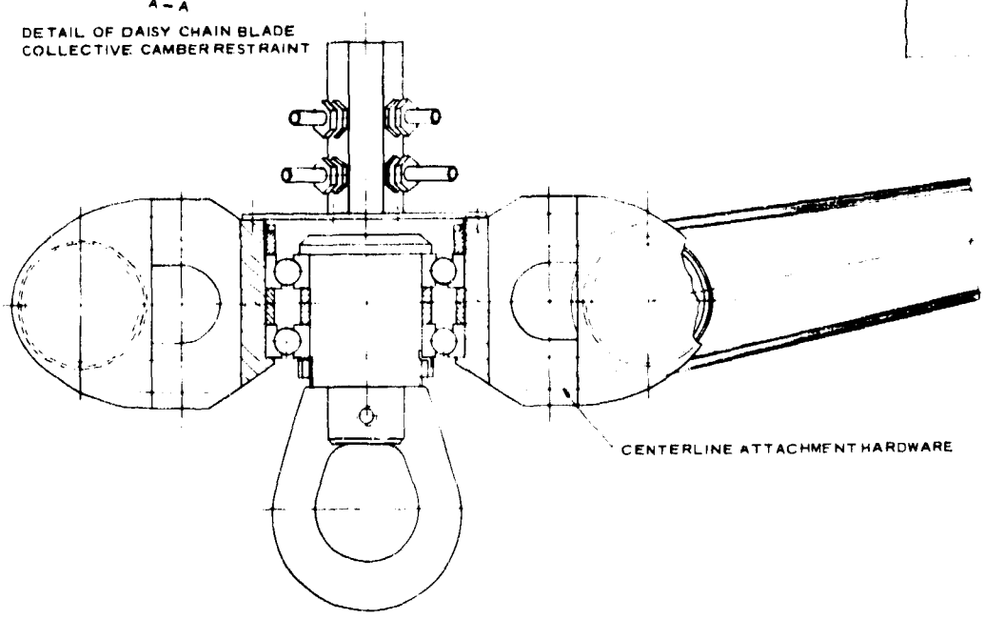

SECTION THROUGH ROTOR HEAD

A.

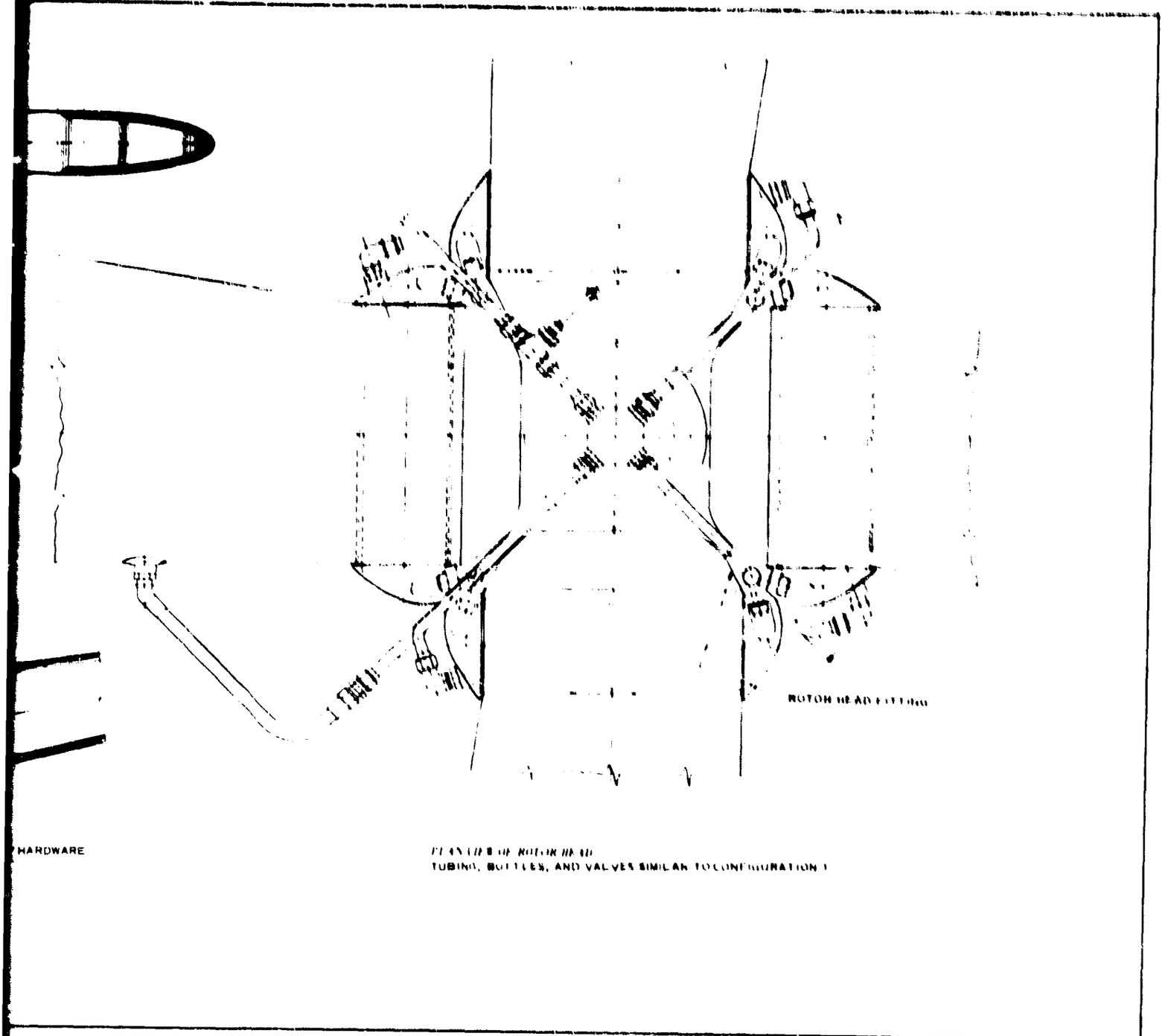

Figure 5 - Inflatable Rotor (Flare Version)

B.

$$F_E = q C_D A \quad , \tag{1}$$

where

F_E = 1.5 × W = extraction force

W = extracted load

$q = 1/2\ \rho V_I^2$

V_I = initial deployment velocity

C_{D_B} = drag coefficient relative to A

$A = \frac{\pi (D_B)^2}{4}$ = BALLUTE area where D_B is the diameter of the basic envelope at its maximum section.

From the statement of work, extraction velocity will be from 110 to 150 knots at altitudes from 500 to 5500 ft above sea level. Taking a nominal average value for design purposes of 130 knots, the dynamic pressure, q, was calculated. The density, ρ, used in determining q was that density experienced at 500 ft above sea level. With a lower density of air to be encountered at 5500 ft above sea level, the extraction force would be reduced to 1.29 g's. This difference in g load is a function of the ratio of the air densities at the two altitudes: ρ at 500 ft = 0.00234 slugs/cu ft, and at 5500 ft, ρ = 0.00201 slugs/cu ft. According to Chernowitz and DeWeese,[1] a minimum extraction force of 1 g is required to prevent toppling and instability of the cargo as it leaves the door. Since the minimum is met at 5500 ft, the extraction device is designed for 1.5 g's at 500 ft. For preliminary design, a C_{D_B} of 0.8 is used which is practical for a nonrotating BALLUTE. Experience indicates that a significant increase in C_{D_B} will be encountered for a rotating configuration. Presented in Table II are BALLUTE diameters for various extracted loads with the diameters being rounded to the nearest foot.

b. Rotor Size Criteria

The performance characteristics of an autorotating rotary wing decelerator have been established through years of extensive testing and analytical efforts. The results have formulated certain relationships between descent velocity, V_D, blade solidity, σ, pitch angle, θ, and blade tip velocity,

TABLE II - RESPECTIVE BALLUTE DIAMETERS

Load item	Load, W (lb)	Diameter, D_B (ft)
1	2,000	9
2	4,000	14
3	8,000	19
4	12,500	22
5	17,000	26
6	21,500	30
7	26,000	33
8	30,500	35
9	35,000	40

V_T. The relationship between the advance ratio, λ, (ratio of vertical descent velocity, V_D, and tip velocity, V_T) and rotor drag coefficient, C_{D_R}, is the most pertinent for preliminary rotor design. Referring to the C_{D_R} versus λ curve in Figure 6, the maximum conservative value of C_{D_R} that can be employed is 1.38 at a λ of 0.085 for a σ = 0.10.

By definition

$$\sigma = \frac{\text{Blade area}}{\text{Rotor disk area}} = \frac{NbR}{\pi R^2} \quad . \tag{2}$$

From Figure 6 for solidities greater than 10 percent, a small increase in C_{D_R} would be experienced. This small increase would not compensate for the large increase in blade weight for a larger σ.

By definition, disk loading, W_D, is

$$W_D = \frac{W}{A} = C_{D_R}\, 0.5 \rho\, V_D^2 \quad , \tag{3}$$

where ρ is air density in slugs/cu ft.

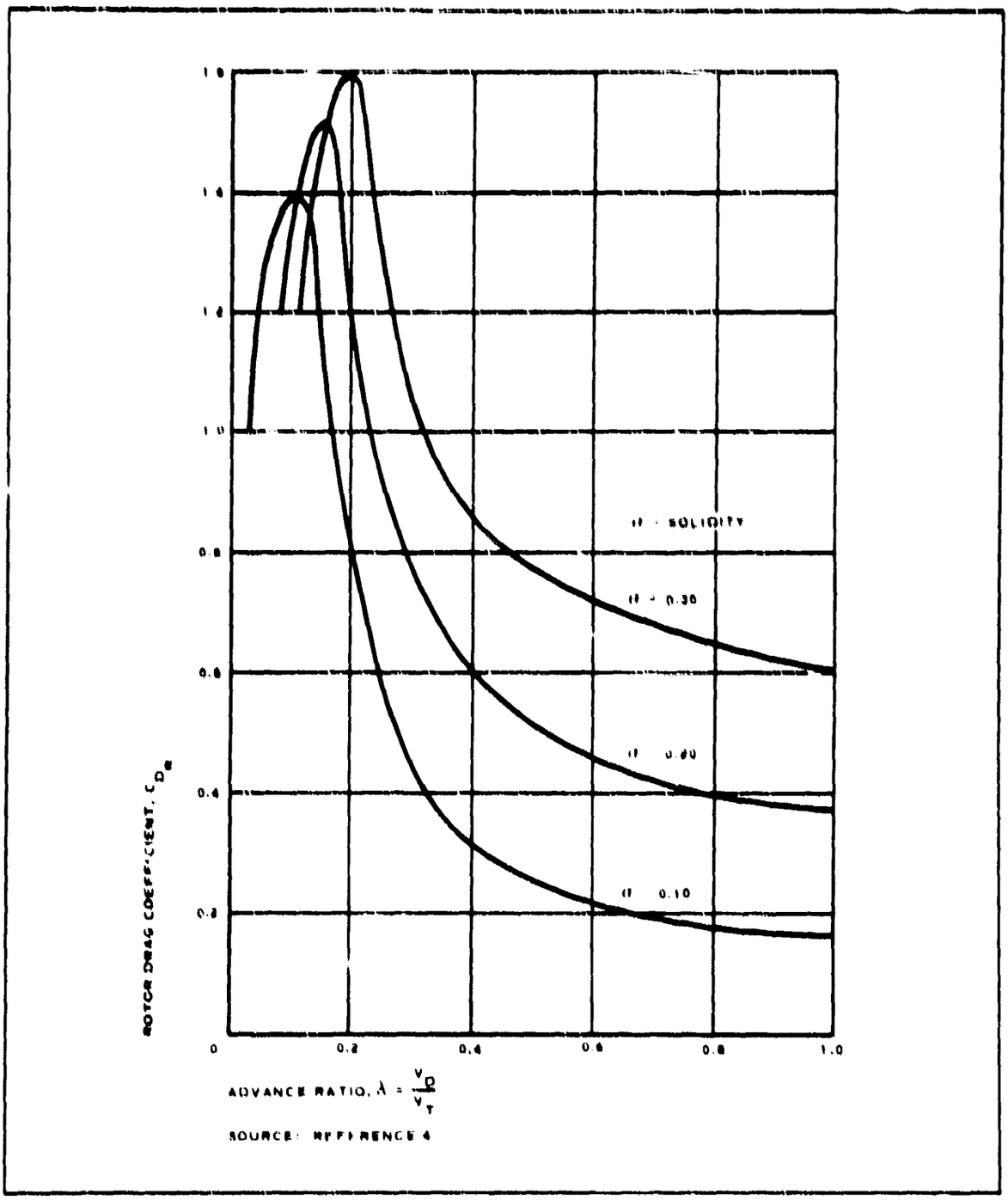

Figure 6 - Rotor Drag Coefficient versus Advance Ratio

For sea level conditions and $C_{D_R} = 1.38$,

$$W_D = 0.0016\, V_D^2 \quad . \tag{4}$$

Presented in Figure 7 is the performance curve or operating regime of an autorotating rotor system based on Equation 4. From this plot for the requirement of 22 fps impact velocity, a disk loading of 0.8 psf is stipulated. The corresponding tip velocity is 260 fps for $\lambda = 0.085$. From the definition of disk loading $W/\pi R^2$, the range of rotor radii required for the range of 2000 to 35,000-lb payload weights can be generated. Presented in Table III are the rotor diameters for nine load items. The range of loads have been chosen arbitrarily and approximate an increase of one G-11A type parachute per step. The values are established for the disk loading of 0.8 psf.

TABLE III - RESPECTIVE ROTOR DIAMETERS (NO FLARE)

Load Item	Gross weight, W (lb)	Rotor diameter (ft)
1	2,000	60
2	4,000	80
3	8,000	110
4	12,500	140
5	17,000	160
6	21,500	180
7	26,000	200
8	30,500	220
9	35,000	240

The effect of increased disk loading on blade diameter can be seen in Figure 8.

From the analysis in Item 4, below, a considerable weight savings in the rotor system for payload weights greater than 8000 lb will be experienced for disk loadings greater than 0.8 psf. Because of the design parameters effect of increasing disk loading to minimize the system weight, the performance of the system at disk loadings greater than 0.8 psf were evaluated.

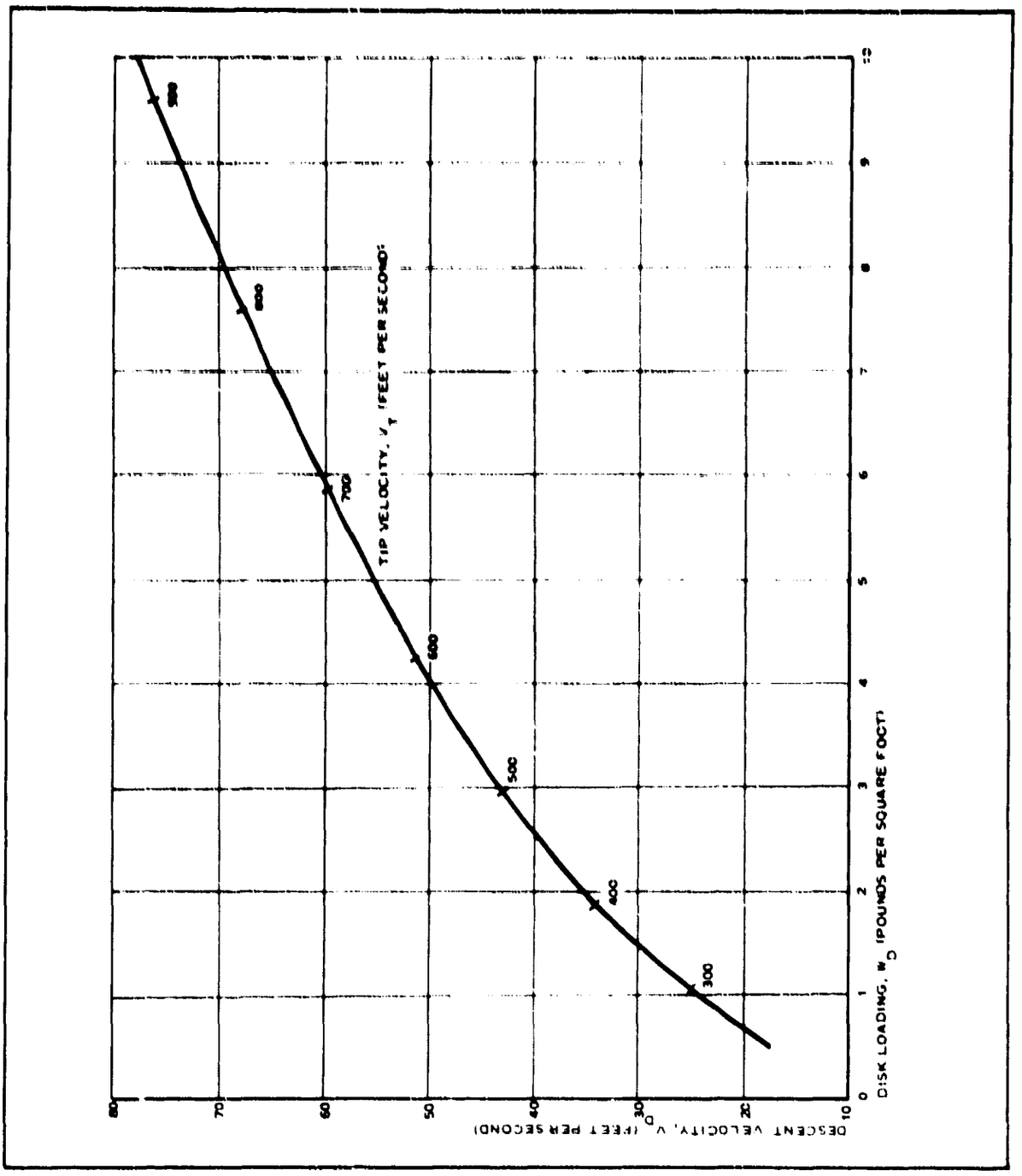

Figure 7 - Descent Velocity versus Disk Loading at Constant $\lambda\left(\frac{V_D}{V_T}\right) = 0.085$

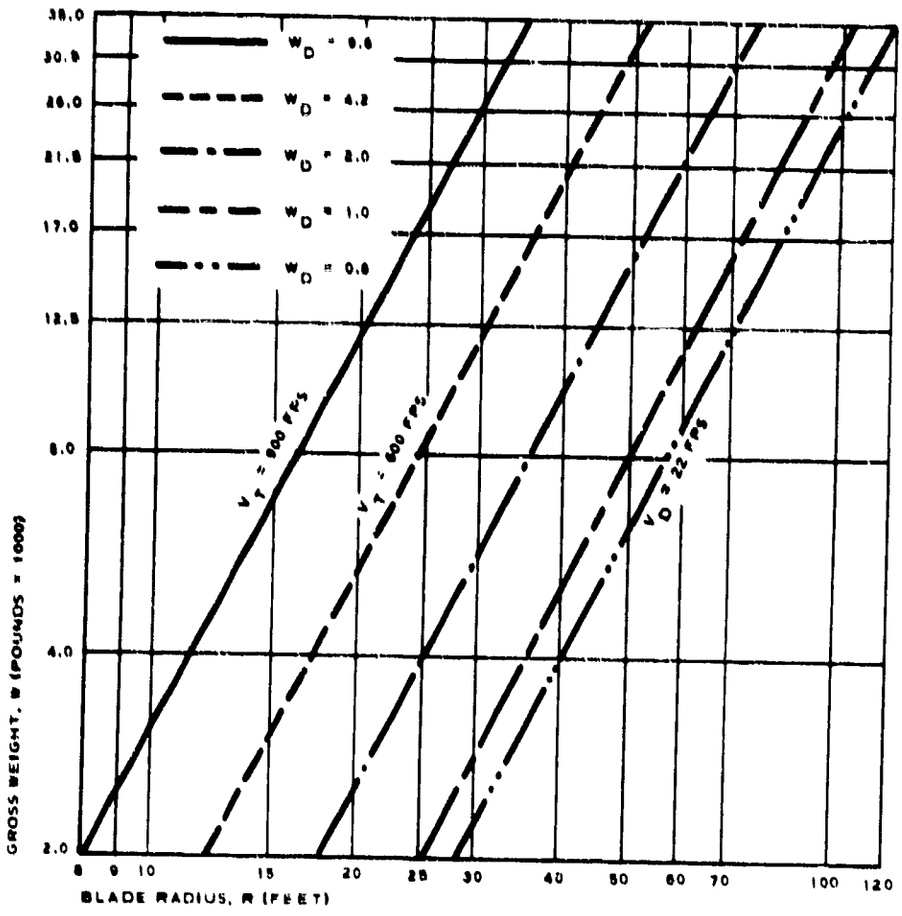

Figure 8 - Gross Weight versus Blade Radius at Selected Disk Loadings

The upper limit on disk loading is dictated by rotor tip velocity. Mansfield[2] indicates a maximum operating limit of 600 fps for tip velocity, while the experimental efforts of Goodale and Boryda[5] show a possibility of approaching blade tip velocities of 900 fps without experiencing adverse high subsonic speed compressibility effects. Point mass computer runs were made to determine the trajectories for the limiting cases of V_D = 22 fps, V_T = 600 fps, and V_T = 900 fps.

The following assumptions were used for the trajectory analysis in this report:

1. Time zero is when the cargo leaves the door
2. Deployment velocity at t = 0.0 is 220 fps (130 knots) and at an altitude of 500 ft above sea level
3. The drag force of the rotor does not begin until one second (t = 1.0) after the cargo leaves the door
4. The drag area ($C_{D_R} A_r$) increases linearly with time from zero to its maximum value
5. The transient spin-up time (drag area increase) is six seconds. This value was established from preliminary work performed by Mansfield[2]

The results of this analysis are only approximations and are presented to indicate the trend of the effect of high descent velocities. The results of the analysis are presented in Figures 9, 10, and 11 for altitude versus time, altitude versus range, and acceleration versus time, respectively.

These plots clearly indicate that terminal descent velocity has a significant effect on system performance. The most pertinent is that of descent time. This is reflected in Figure 9. Since smaller diameters are required for the higher disk loadings, the g load on the cargo during the deceleration period decreases. The magnitude and time of occurrence can be seen in Figure 11. The decrease in deceleration force also has a significant effect on the ground distance (range) covered during descent. This effect can be seen in Figure 10.

The trajectories that will be experienced for the final disk loadings established in Item 4, below, will be in the regime between V_D = 22 fps and V_T = 600 fps.

4. STRUCTURAL DESIGN ANALYSIS

a. BALLUTE Weight Determination

The principal components of the BALLUTE include fabric coverings, the

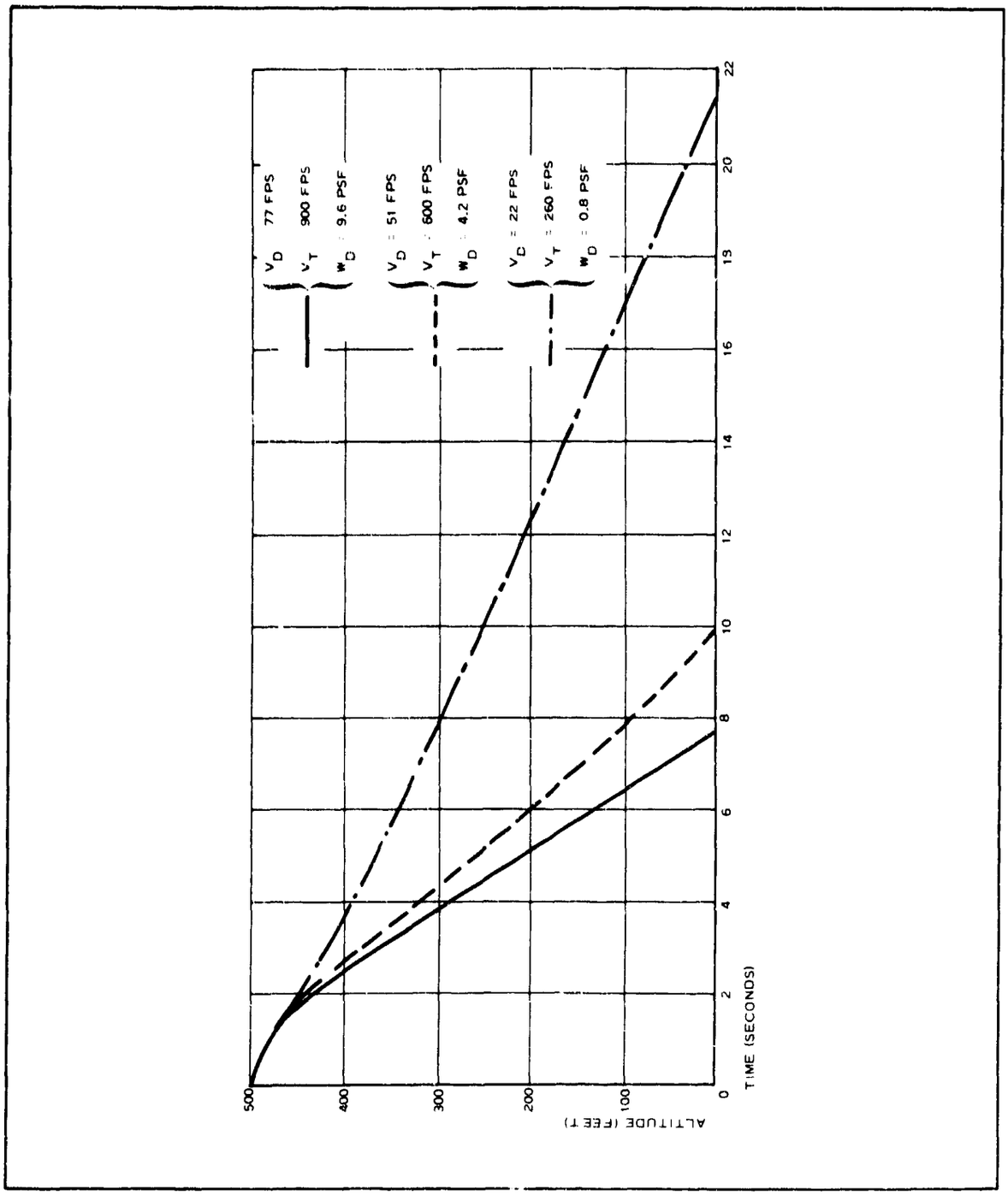

Figure 9 - Altitude versus Time

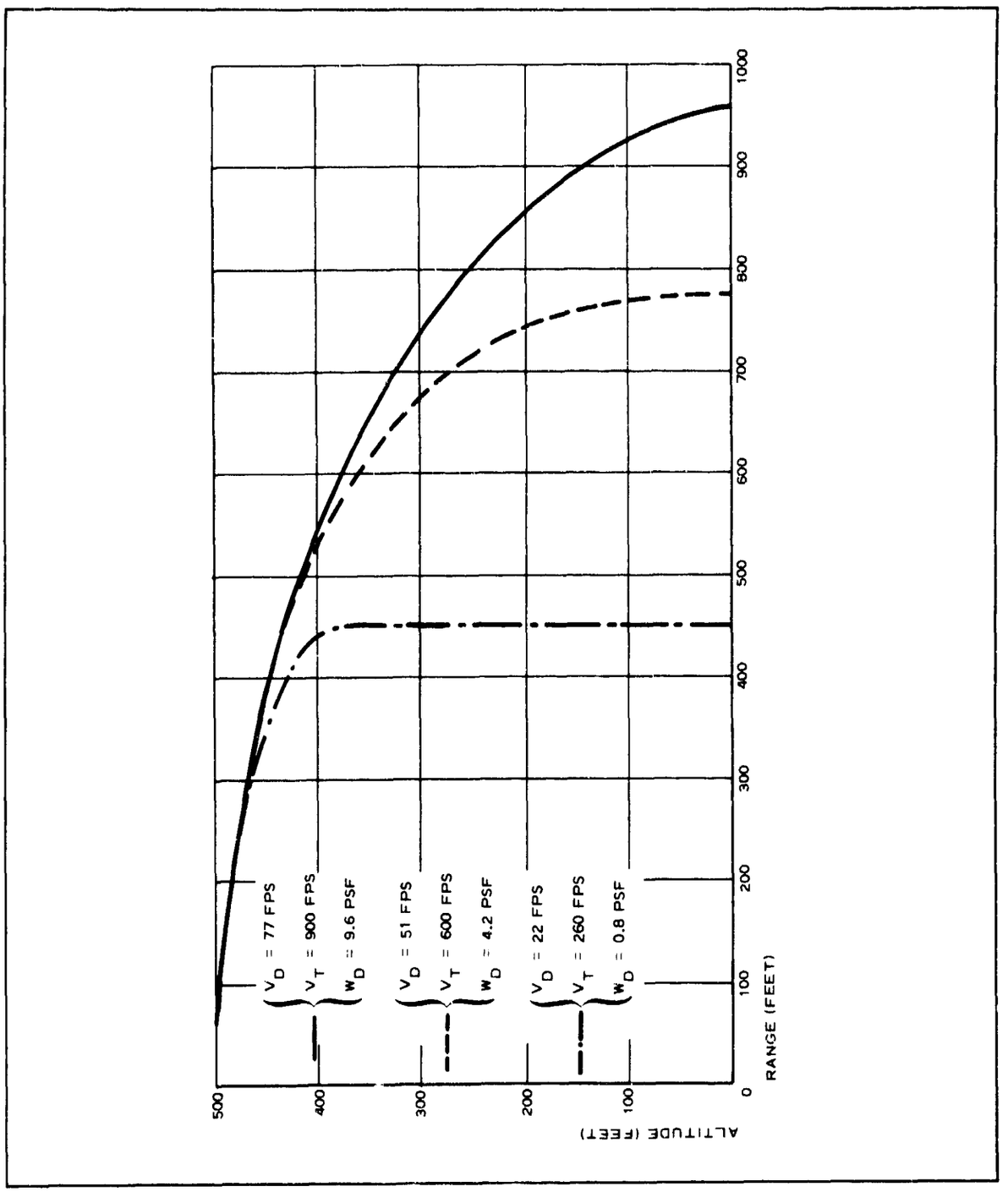

Figure 10 - Altitude versus Range

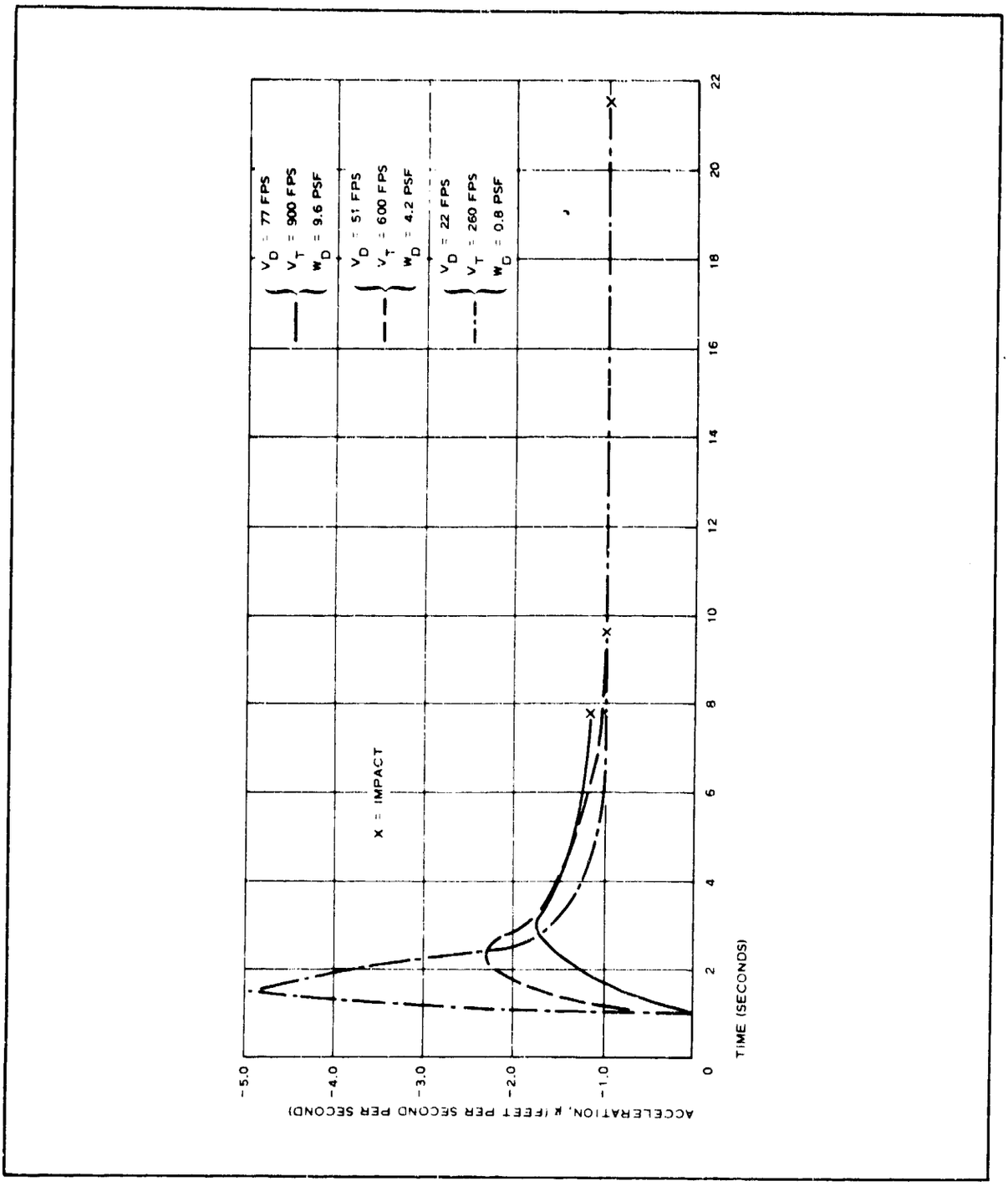

Figure 11 - Acceleration versus Time

meridional webs, and the elastomeric coating. The fabric covering is a high-strength material that forms the envelope of the structure. The meridional webs help to support the load by continuing around the structure and passing through the apex at the back. The webs may terminate on a nose fixture at the front of the model, or they may extend out to become the suspension lines. The coating applied to the envelope makes it nonporous and helps to provide protection for the fabric structure.

The weight of a BALLUTE, W_B, is the sum of the weight of its components. Therefore,

$$W_B = W_f + W_m + W_C \quad , \tag{5}$$

where

W_f = fabric weight

W_m = meridian weight

W_C = coating weight .

The weight then becomes

$$W_B = \frac{A_f f_f (D.F.')}{K_f} + \frac{HLT(D.F.')}{K_m} + A_f(C.F.) \quad , \tag{6}$$

where

A_f = surface area of decelerator (sq ft)

f_f = design stress due to the design inflation pressure and the decelerator radius

D_f = total fabric design factor, which is the product of safety factor, dynamic loading, seam efficiency, temperature, etc

K_f = envelope fabric strength-to-weight ratio (in.)

H = number of meridians (webs)

L = length of each meridian (ft)

T = meridian design tension load (lb)

$D.F.'$ = total meridian design factor

K_m = meridian strength-to-weight ratio (in.)

$C.F.$ = unit coating weight (weight/area) ,

Equation 6 uses a safety factor of two and does not include the weight of the burble fence or the riser line. The meridian length and fabric area are approximately $2\pi R_B$ and $4\pi R_B^2$, respectively. For a 10-percent fence, the fabric weight is increased by approximately 10 percent.

Table IV presents BALLUTE weight for the various required diameters and is based on the preceeding analysis for deployment q = 56.6 psf (deployment at 500 ft and 130 knots). BALLUTE stowage-volume requirements are dependent on its weight and packing density. Typical packing-density values range from 20 to 30 pcf for handpack and 30 to 40 pcf for a pressure pack.

TABLE IV - RESPECTIVE BALLUTE WEIGHTS

Item	Load, W (lb)	BALLUTE diameter (ft)	Weight, W_B (lb)	$\frac{W_B}{W}$ (percent)
1	2,000	9	5	0.25
2	4,000	14	16	0.40
3	8,000	19	36	0.45
4	12,500	22	53	0.42
5	17,000	28	100	0.59
6	21,500	30	120	0.56
7	26,000	33	155	0.59
8	30,500	35	180	0.59
9	35,000	40	250	0.72

b. Rotor Weight Determination

(1) General

Fabric rotor blades are made from AIRMAT, an inflatable type material. The AIRMAT fabric blade has two outer surfaces of fabric made pressure tight by an elastomer coating. When the AIRMAT structure is inflated, it attains the predetermined airfoil shape established by the length of the drop threads, as shown in Figure 12. The rotor blade is completed by addition of plies of cord fabric (unidirectional strength fabric) at the leading edge. These plies are arranged to properly position the mass axis and elastic axis ahead of the quarter chord for flutter stability. In addition this material provides sufficient strength to resist centrifugal forces resulting from tip and blade weights.

The structural design of the rotor system is comprised of the design of the various individual components. The rotor system weight, W_R, is equal to the summation of the weights of the fabric blades, W_{BLF}, the tip weight, Q, the air storage bottle weight, W_{PB}, and the hub weight, W_{HUB}. In equation form, this is:

$$W_R = W_{BLF} + Q + W_{PB} + W_{HUB} \qquad (7)$$

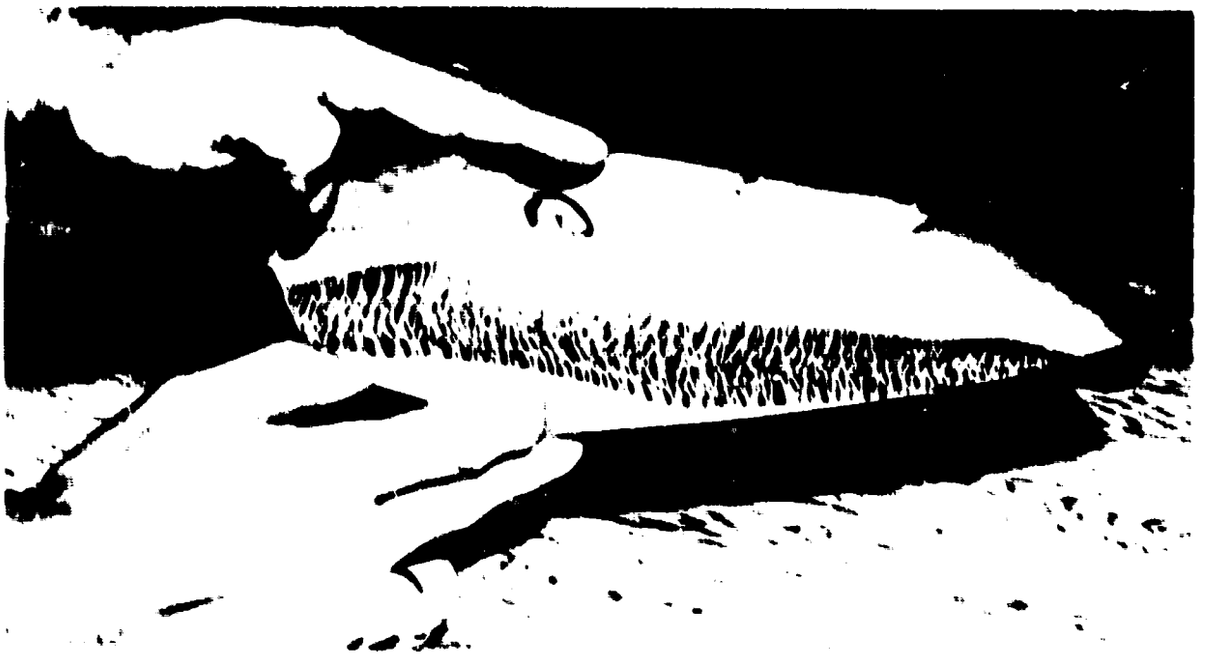

Figure 12 - Typical AIRMAT Airfoil Section

Evaluation of each of these terms is performed in the following portions of this section.

(d) Blade Weight Analysis

(a) Total Weight

The total weight of the blade portion of the rotor system is:

$$W_{BT} = W_{BP} + W_{AIR} + W_C + W_{LE} + \quad (8)$$

where

W_{BP} = weight of the AIRMAT required for pressure (lb)

W_{AIR} = weight of air in the blade (lb)

W_C = weight of elastomer coating required to eliminate the porosity in the material (lb)

W_{LE} = weight of material required for mass balance ahead of forward quarter chord (lb)

(b) Blade Weight as Pressure Vessel

Costakos[6] shows the minimum weight of a flat AIRMAT pressure vessel to be

$$W_{FA}^{MIN} = \frac{3pV_{FA}FS}{K} , \quad (9)$$

where

p = internal pressure (psi)

V_{FA} = volume of flat AIRMAT (cu ft)

FS = factor of safety, and

K = strength-to-weight ratio of face and drop yarns (in.)

The flat AIRMAT has two outer surfaces and drop yarns. Generally, the weights of each outer surface are equal and the drop-yarn weight is equal to the weight of one surface. The factor of 3 in Equation 9 represents the outer surfaces and drop yarns.

Equation 9 can be used to find a conservative weight for the airfoil blade by using the volume of a flat AIRMAT blade, V_{FA}, with the same chord and depth as the airfoil. The blade cross section is that of a NACA 0012 airfoil. Since

$$V_{FA} = bhR, \tag{10}$$

Substituting 0.12b for h in Equation 10 yields:

$$V_{FA} = 0.12\, b^2 R, \tag{11}$$

Equation 12 below then gives the AIRMAT weight from pressure alone:

$$(W_{FA})_{min} = \frac{0.10\, pb^2 R(FS)}{K}, \tag{12}$$

Looping AIRMAT drop yarns over yarns in the face cloths can reduce drop-yarn strength by as much as one half. Because of this, the weight of fabric must be increased by pV(FS)/K. This discussion assumes the face and drop-yarn materials are the same. Therefore, to account for reduced loop strength of the drop yarns, Equation 9 becomes

$$W_{BP} = (W_{FA})_{min} + \frac{pV(FS)}{K}, \tag{13}$$

Simplifying and collecting terms yield

$$W_{BP} = \frac{4pV_{FA}(FS)}{K}. \tag{14}$$

Equation 14 should be used instead of Equation 9 to account for reduced loop strength. Equation 14 gives the structural weight without elastomers. The analysis used in obtaining Equation 14 showed that the face-material weight is 60 percent and the drop-yarn weight is 40 percent of the total AIRMAT weight. The coating weight required is explained further in Item (e) below.

(c) Blade Weight Calculations - Pressure (W_{BP})

To calculate the weight of the blade when pressurized, let

$$V_{FA} = 0.12\, b^2 R$$

$$FS = 4$$

$$K = 2 \times 10^6 \text{ in.}$$

Then Equation 14 becomes

$$W_{BP} = 14.4 \times 10^{-6} pb^2 R, \tag{15}$$

where b and R are in feet and p is in pounds per square inch.

The chord dimension is found by using the solidity, σ, as 10 percent and the number of blades, N, in Equation 2.

Equations 2 and 15 yield

$$W_{BP} = \frac{(1.421 \times 10^{-6}) R^3 p}{N^2}; \tag{16}$$

for p = 1440 psf (10 psi),

$$W_{BP} = \frac{(2.046 \times 10^{-3}) R^3}{N^2} . \tag{17}$$

Table V presents AIRMAT weight, W_{BP}, required to retain a pressure of 10 psi for respective rotor radius, R, with the number of blades being being four and disk loading equal to 0.8 psf.

(d) Weight of Air in the Blade (W_{air})

The volume of an NACA 0012 airfoil is

$$V_{AF} = 0.082 b^2 R . \tag{18}$$

Air density, ρ, at standard conditions is 0.07651 pcf. The weight of air in one blade at p psf is given by:

$$W_{air} = \frac{\rho p \ V_{AF}}{p_o} . \tag{19}$$

Using the following values

$$p_o = 14.7 \text{ psia} = 2116 \text{ psf}$$

TABLE V - WEIGHT PERCENTAGE OF BLADE COMPONENTS FOR VARYING ROTOR RADII

Item	Gross weight W (lb)	Rotor radius, R (lb)	AIRMAT weight, W_{BP} (lb)	Weight of air, W_{air} (lb)	Weight of coating, W_C (lb)	Weight of leading edge, W_{LE} (lb)	Total, weight, W_{BT} (lb)	W_{BT}/W (percent)
1	2,000	10	16	1.8	9.6	55	82.5	4.12
2	4,000	40	33	16.8	19.8	139	208.6	5.2
3	8,000	55	85	43.0	51.0	358	537.0	6.6
4	12,500	70	180	90.0	108.0	756	1134.0	9.1
5	17,000	80	265	132.0	159.0	1112	1668.0	9.8
6	21,500	90	375	188.0	225.0	1576	2364.0	11.0
7	26,000	100	520	260.0	312.0	2184	3276.0	12.6
8	30,500	110	680	344.0	398.0	2844	4266.0	13.9
9	35,000	120	900	440.0	540.0	3760	5640.0	16.1

$$p = 10 \text{ psig}$$
$$= 24.7 \text{ psia}$$
$$= 3556 \text{ psfa}$$
$$\rho = 0.07651 \text{ pcf}$$

and substituting Equation 18 into 19 gives

$$W_{air} = \frac{(1.03 \times 10^{-3}) R^3}{N2} . \qquad (20)$$

Table V presents the weight of air, W_{air}, for respective rotor radii for four blades and $\frac{W}{A} = 0.8$ psf.

(e) Weight of Coating (W_C)

The weight of the required coating equals approximately 0.6 of the AIRMAT weight. Coating generally equals the weight of the parent farbic, which for AIRMAT surfaces is equal to 0.6 of the total weight. Table V presents the coating weight for respective radii.

(f) Mass Balance (W_{LE})

Because the aerodynamic center and the center of mass must coincide if an airfoil section is to be aerodynamically stable the center of mass must be located at the forward chord (one-fourth of the chord length from the leading edge).

The weight required at the blade's leading edge includes the weight of the AIRMAT, air, and coating. To this weight, material must be added to bring the amount to W_1 (see Figure 13).

Generally, the added material is tire cord made with uniaxial yarns placed in the radial direction because it will carry only centrifugal loads.

The following analysis was used to find W_{LE} based on the mass balance requirement.

From Figure 13

$$W_1 = 3W_2, \tag{21}$$

where

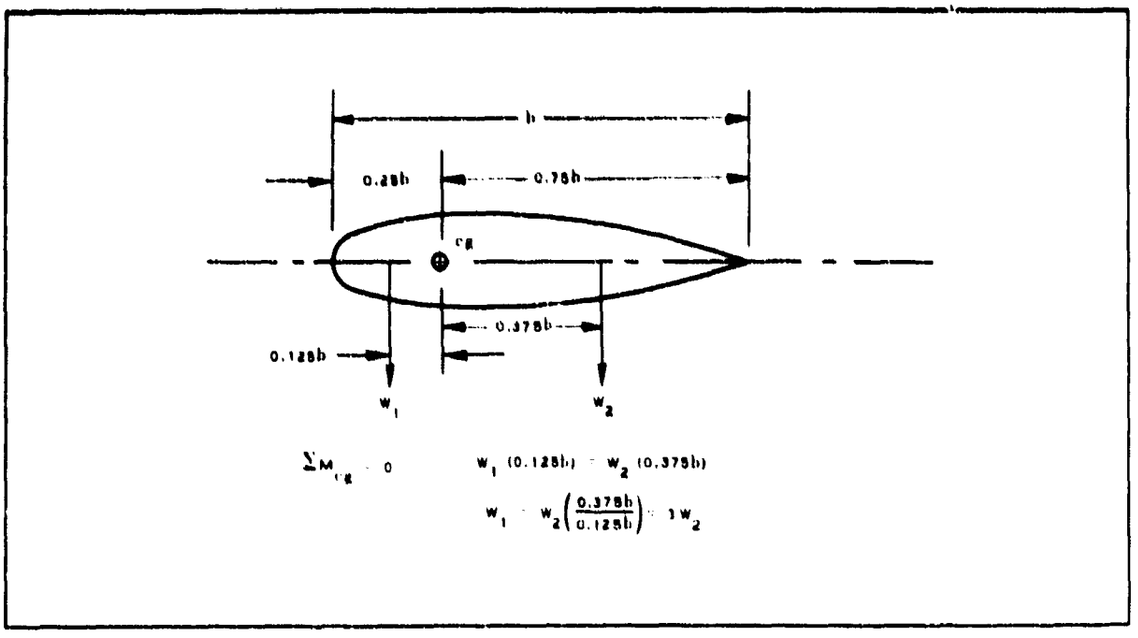

Figure 13 - Airfoil Center of Mass

$$W_2 = \frac{3}{4} W_{BP} + \frac{3}{4} W_{air} + \frac{3}{4} W_C \quad (22)$$

Substituting into Equation 21 yields

$$W_1 = \frac{9}{4} W_{BP} + \frac{9}{4} W_{air} + \frac{9}{4} W_C \quad (23)$$

by definition

$$W_{LE} = W_1 - \left(\frac{1}{4} W_{BP} + \frac{1}{4} W_{air} + \frac{1}{4} W_C\right). \quad (24)$$

Substituting for W_1 from Equation 23 yields

$$W_{LE} = 2 W_{BP} + 2 W_{air} + 2 W_C \quad (25)$$

presented in Table V is W_{LE} for respective values of W_{BP}, W_{air}, and W_C.

(g) Total Blade Weight (W_{BT})

The total blade weight, W_{BT}, was established by substituting respective values of W_{BP}, W_{air}, W_C, and W_{LE} into Equation 8. Presented in Table V are the values for W_{BT}.

(3) Inflation System Weight (W_{PB})

Design of the inflation system for this application has been directed toward the high-pressure storage bottle type. Although other types of systems exist; for example, cool gas generator, hot gas generator, and ram air, the steel bottle system has been selected from a basis of cost and complexity tradeoff. For a preliminary estimate of the weight of the bottle system, the following method was used. The weight of a pressure bottle is dependent upon the energy that it contains. This energy, E, is defined as

$$E = PV \quad (26)$$

where

P = absolute pressure (psi)

V = volume of air, (cu ft)

The volume of air can be shown to be

$$V = \frac{W_{air}}{\rho_{air}} , \tag{27}$$

where

W_{air} = weight of air

ρ_{air} = density of the air at the pressure p.

Substituting for V in Equation 26 yields

$$E = P\left(\frac{W_{air}}{\rho_{air}}\right) . \tag{28}$$

The energy at the storage bottle or the blade to give

$$E = 3000 \text{ psia } \left(\frac{W_{air}}{\rho_{air \text{ at } 3000 \text{ psi}}}\right); \tag{29}$$

also

$$E = 24.7 \text{ psia } \left(\frac{W_{air}}{\rho_{air \text{ to } 10 \text{ psig}}}\right) . \tag{30}$$

From Table V the weight of air required to inflate four blades to 10 psig is presented. The density of air at 3000 psi is 0.478 slugs per cu ft. The energy term, PV, therefore can be evaluated for various blade radii. Figure 14 presents bottle weight versus energy, PV, and was taken from Figure 118 of Reference 7 for a steel bottle.

Substituting for ρ and W_{air} for one blade for each load item into Equation 30 will result in the storage energy requirement. The resultant bottle weight per blade then can be obtained from Figure 14, at each energy level. The total bottle weight with four blades for each load item is presented in Table VI for a disk loading of 0.8 psf.

(4) Tip Weight Determination

(a) General

The calculation of tip weight has been left as the last step of the design

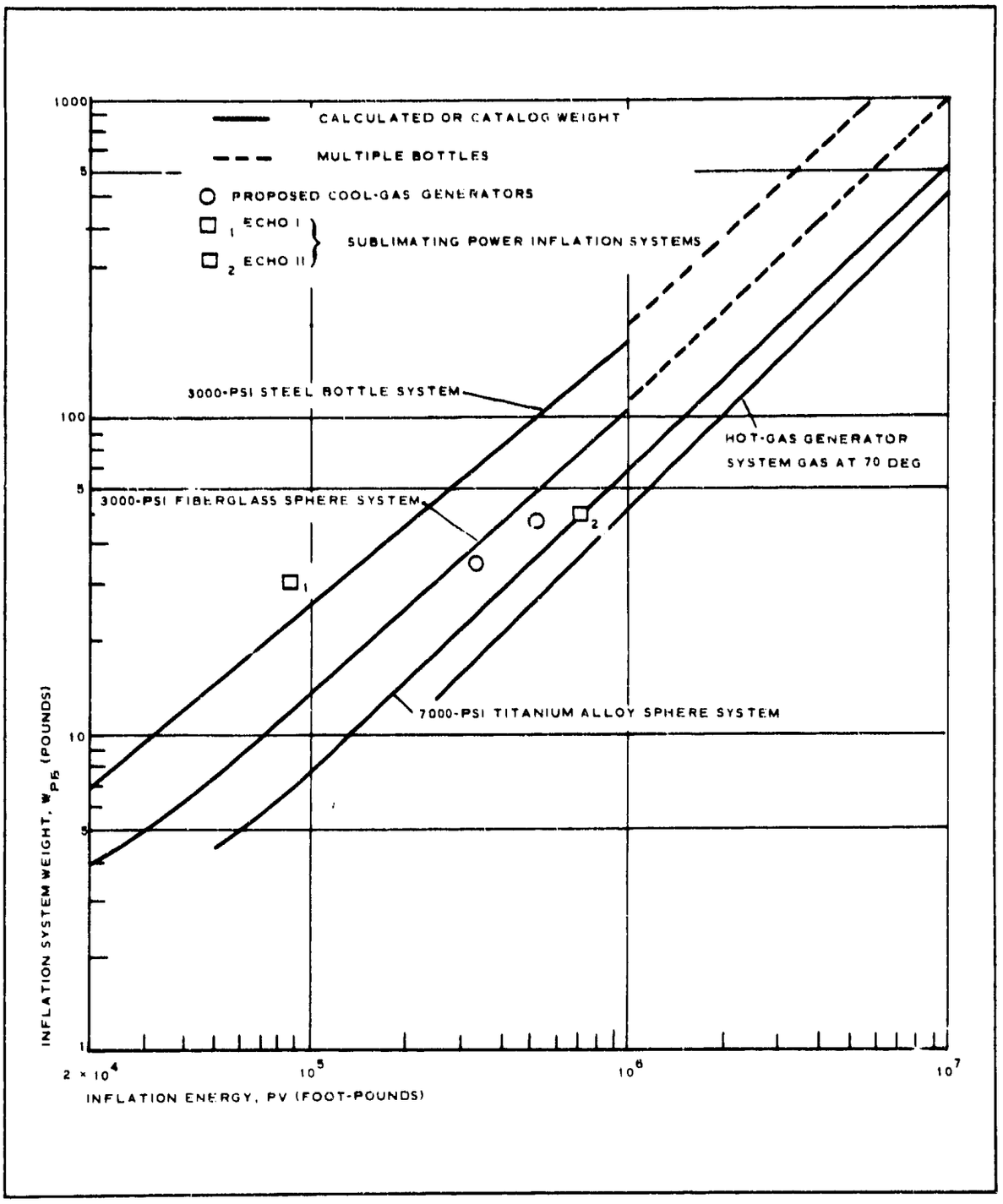

Figure 14 - Inflation System Weights for Various Energy Levels

TABLE VI - PRESSURE BOTTLE AND TIP WEIGHT VALUES (NO FLARE)

Load item	Gross weight, W (lb)	Rotor radius, R (ft)	W_{PB} (lb)	Q (lb)
1	2,000	30	34	42
2	4,000	40	94	120
3	8,000	55	256	360
4	12,500	70	488	770
5	17,000	80	765	1190
6	21,500	90	1075	1760
7	26,000	100	1420	2500
8	30,500	110	1800	3350
9	35,000	120	2170	4300

analysis due to the fact that it is a dependent variable whose magnitude is determined when a balance of forces is evaluated. For given values of lift, blade weight, tip speed, and coning angle, a moment through the axis of rotation gives the magnitude of the tip weight. Based on the following assumptions, three equations or statics can be written for the forces acting on the blade shown schematically in Figure 15.

1. A blade is subjected to lift, weight, and centrifugal forces distributed along the length
2. There is no spiral twisting along the blade
3. A blade is hinged at the hub
4. The hub is at the axis of rotation.
5. The airfoil shape is maintained by pressure in an AIRMAT structure
6. Although a blade is flexible, it is assumed to be rigid because of large centrifugal tensions in a blade
7. The solidity is 10 percent

(b) Forces Acting on a Rotor Blade

Lift Forces - Figure 16 shows an airload distribution for an NACA 0012

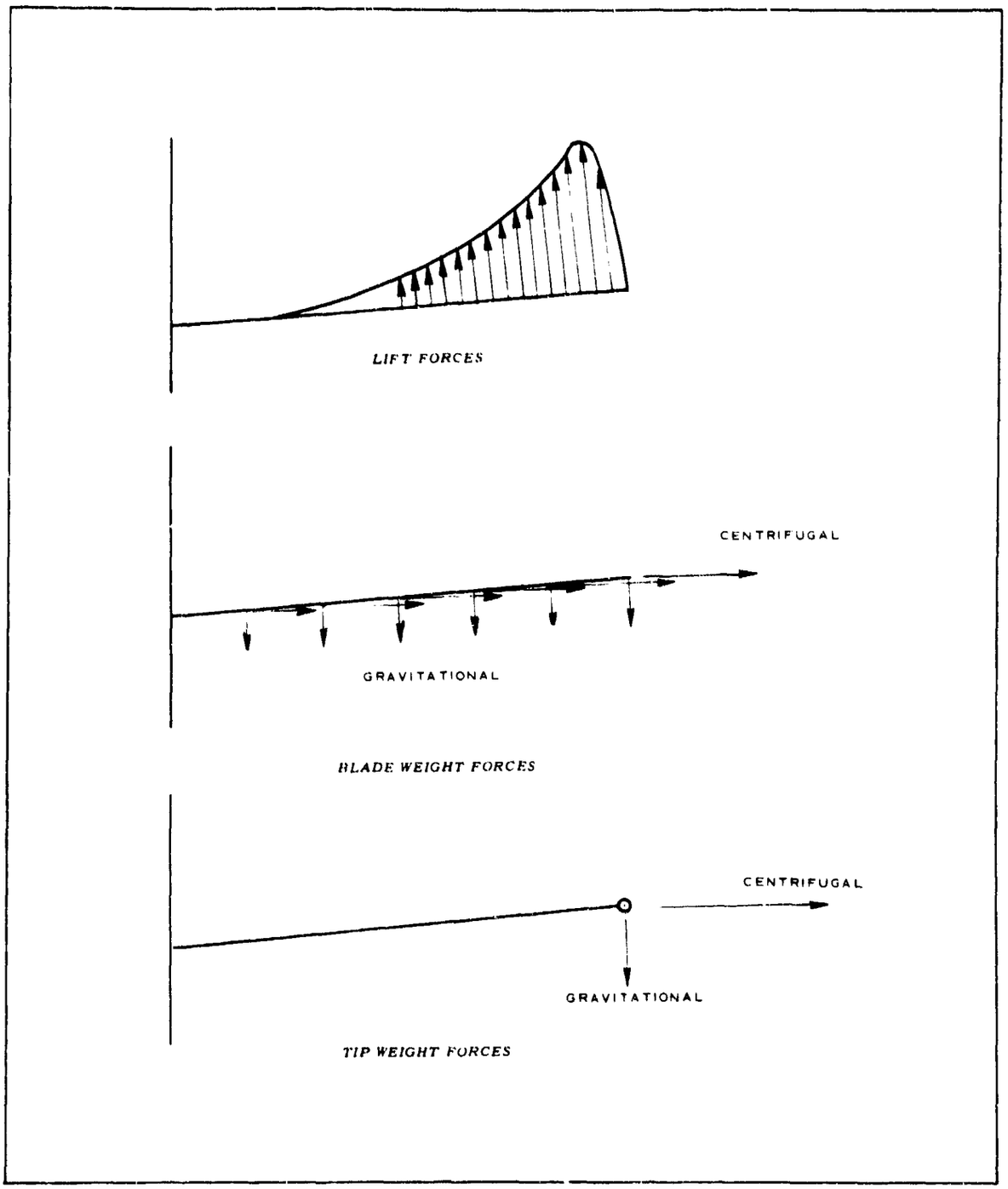

Figure 15 - Forces Acting on a Rotor Blade

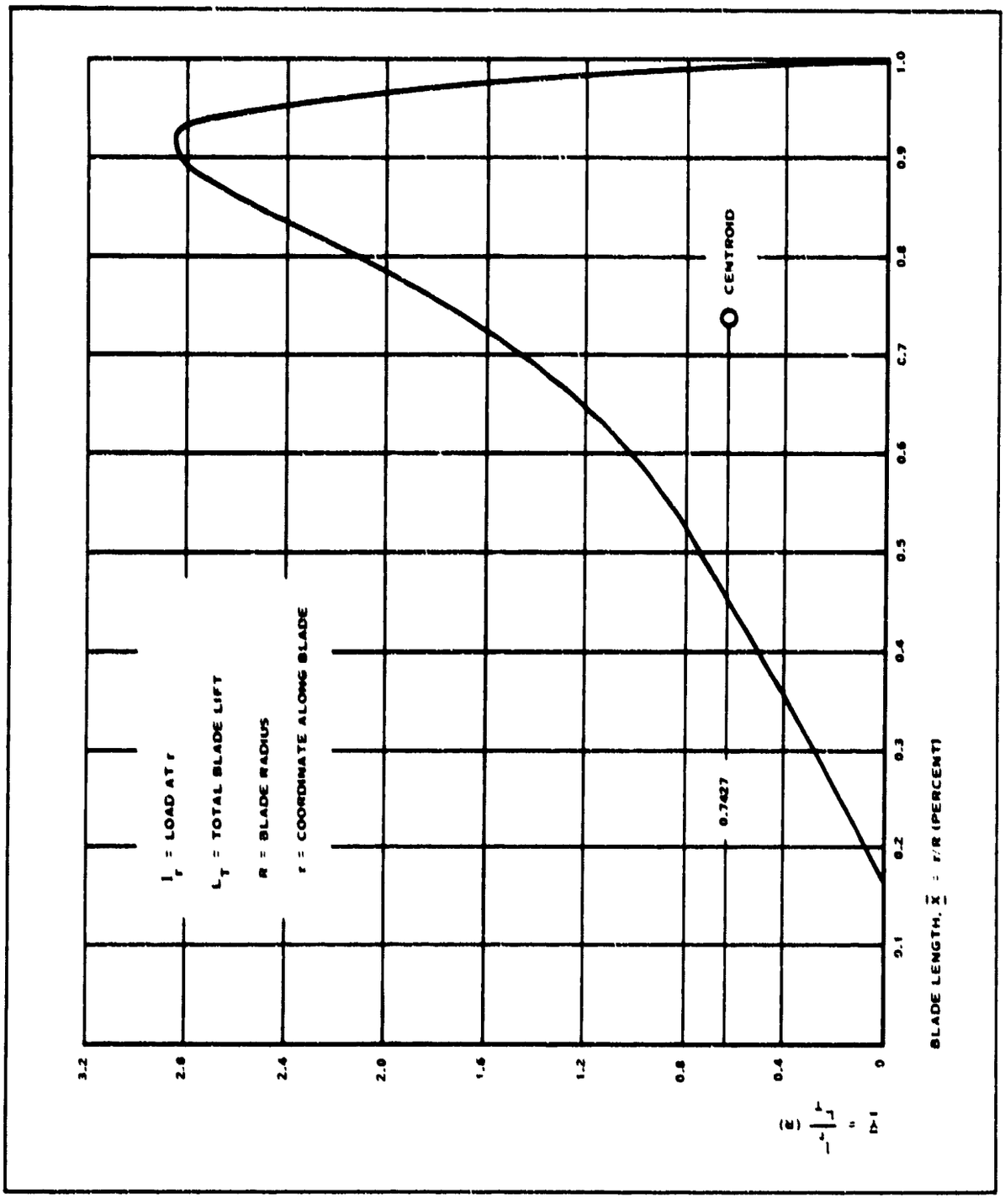

Figure 16- Rotor Airload Distribution (NACA 0012 Airfoil)

airfoil. The loading and coordinates are given as a dimensionless parameter. The dimensionless coordinates are

$$\overline{X} = r/R \text{ and } \overline{Y} = l_r R/L_T,$$

where

r = any radius along the blade

R = blade radius

l_r = lift at point of radius r

L_T = total blade lift

The location of the centroid of the lift distribution is shown to be at 74.27 percent of the blade radius as measured from the hub.

Forces Due to Blade Weight and Tip Weight - Figure 15 shows a rotor blade assumed to be uniform in weight distribution along its length with centrifugal forces increasing uniformly outward along the blade.

If

w = weight per unit length (ppf)

x = horizontal coordinate = $r \cos \theta_o$

Ω = rotor angular velocity (radians per second)

V_T = tip speed (fps) at $X_T = R \cos \theta_o$ (ft/sec)

W_{BT} = total weight of blade = Rw, (lb)

$\overline{X}$ = centroidal distance (ft)

g = acceleration of gravity (ft/sec^2)

CF = centrifugal force (lb)

X_T = tip horizontal coordinate = $R \cos \theta_0$, (ft)

Then the centrifugal force created by the blade weight is

$$CF = \int_0^R w \times \Omega^2 \frac{dr}{g} = \frac{w \Omega^2 R^2}{2 g} \cos \theta_o \, . \qquad (31)$$

Substituting $\Omega = V_T / R \cos \theta_o$ into Equation 31 yields

$$CF = \frac{W_{BT} V_T^2}{2 Rg \cos \theta_o} \, . \qquad (32)$$

The resultant force (see Figure 17) acts at

$$\overline{X} = \frac{2 R}{3} \cos \theta_o \, . \qquad (33)$$

The tip weight, Q, and its centrifugal force also are shown in Figure 15.

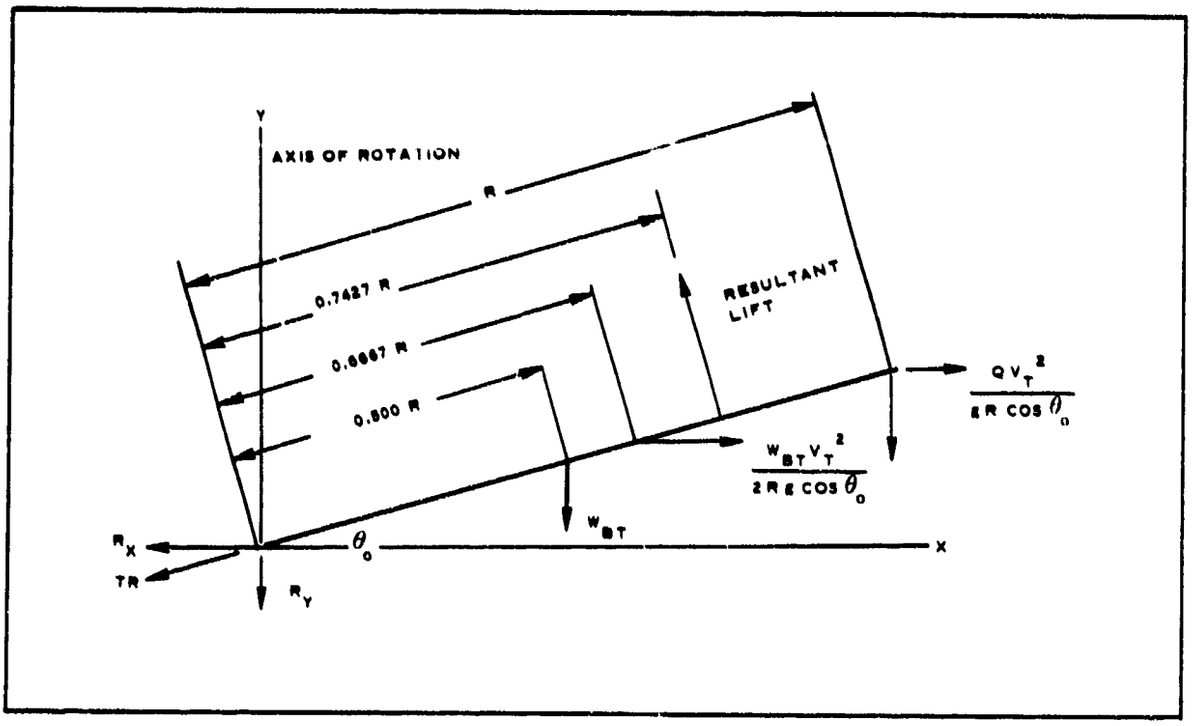

Figure 17 - Equivalent Concentrated Forces Acting on Rotor Blades

(c) Static Equations of Equilibrium

Figure 17 shows a rigid blade with each distributed force system replaced by an equivalent concentrated force. The static equations consist of a moment about the hub and summation of forces in the x and y direction. Summations in x and y directions yield

$$R_X = \frac{(0.5\ W_{BT} + Q)\ V_T^2}{R\ g \cos \theta_o} - (L_T) \sin \theta_o \qquad (34)$$

and

$$R_Y = (L_T) \cos \theta_o - W_{BT} - Q\ . \qquad (35)$$

From a moment about the hub,

$$Q = \frac{0.7427(L_T) - W_{BT}\left[0.5 \cos \theta_o + \frac{V_T^2 \tan \theta_o}{3\ Rg}\right]}{\cos \theta_o + \frac{V_T \tan \theta_o}{R\ g}}\ . \qquad (36)$$

The resultant blade tension is

$$T_R = \sqrt{R_X^2 + R_Y^2}\ , \qquad (37)$$

and the angle θ_o is defined as

$$\theta_o = \tan - 1\ \frac{R_X}{R_Y}\ . \qquad (38)$$

From Equation 36 with values of lift, blade radius, and tip velocity (dictated by disk loading, blade weight, and coning angle), the tip weight, Q, can be calculated. Table VI shows the Q for each load item at a disk loading of 0.8 psf.

(5) Rotor System Total Weight Without Flare

The total rotor system case without flare now can be established. From Equation 7 the total system weight is equal to the weights of the four components. Values for all of these components except W_{HUB} have been

established in the preceeding subsections. The hub weight analysis is contained in Item 7 below. Knowing the value for W_{HUB}, the total weight can be found for the nine load items at a disk loading of 0.8 psf. Table VII presents a summary of the component weights as a percentage of the gross weight. The trend of the resulting total rotor system weight (as a percentage of the gross weight) is clearly an increase with an increase in gross weight.

TABLE VII - COMPONENT AND TOTAL WEIGHTS FOR CONFIGURATION I

Load item	Gross weight, W (lb)	Rotor radius, R (in.)	W_{BT}/W (percent)	Q/W (percent)	W_{PB}/W (percent)	W_{HUB}/W (percent)	W_{R}/W (percent)
1	2,000	30	4.12	2.1	1.7	5	12.9
2	4,000	40	5.2	3.0	2.35	5	15.5
3	8,000	55	6.6	4.5	3.20	5	19.3
4	12,500	70	9.1	4.7	3.90	5	22.8
5	17,000	80	9.8	6.9	4.5	5	26.2
6	21,500	90	11.0	8.0	5.0	5	29.0
7	26,000	100	12.6	9.1	5.4	5	32.1
8	30,500	110	13.9	10.6	5.9	5	35.4
9	35,000	120	16.1	11.5	6.2	5	38.8

Since the rotor concept does have the ability to transform rotational energy into a form that will result in a transient deceleration force to the cargo, a study was conducted to determine if descending at a velocity greater than 22 fps (which would permit a smaller diameter rotor) and then flare to a 22-fps impact velocity would provide an overall savings in rotor system weight.

(6) Flare Maneuver Weight Requirements

Utilizing a sudden collective pitch change as the descending autorotating rotor nears the ground to provide the desired lower touchdown velocity, which is being reduced from a higher sustained descent velocity, promises certain rewards. The kinetic energy of the rotating blades can be exploited to obtain an additional decelerating force for reducing the

descent velocity. The analytical mechanics[5] of this maneuver were obtained and modified to suit the conditions of this problem. It is assumed, as in Reference 5, that the initial load factor, LF, in this maneuver is 2.0 and decreases linearly with time to the end of the maneuver to become 1.0. At any time, t,

$$LF = LF_o - (LF_o - 1)\, t/t_f \,. \tag{39}$$

The difference in the initial descent velocity, V_D, and the final velocity, V_f, is

$$V_D - V_f = \int_o^{t_f} a\,dt \tag{40}$$

$$= \tfrac{1}{2} (LF_o - 1)\, g\, t_f \tag{41}$$

$$t_f = \frac{2(V_D - V_f)}{(LF_o - 1)\, g} \,. \tag{42}$$

At any instant during the vertical flare, the power required per pound of vehicle as reported in Reference 5 is

$$F_P/W = \left(\frac{14.5}{M}\right) (LF)^{3/2} \left(\frac{W}{A}\right)^{1/2}, \text{(M is figure of merit)} \,. \tag{43}$$

The kinetic energy, KE, required for the flare per pound of vehicle is

$$\frac{KE}{W} = \int_o^{t_f} \frac{F_P}{W}\, dt \tag{44}$$

$$= \int_o^{t_f} \frac{14.5}{M}\, LF^{3/2} \left(\frac{W}{A}\right)^{1/2} dt \tag{45}$$

$$= \frac{14.5}{M} \left(\frac{W}{A}\right)^{1/2} \int_o^{t_f} \left[LF_o - (LF_o - 1)\, \frac{t}{t_f}\right]^{3/2} dt \,. \tag{46}$$

Based on the solution of the standard form integral

$$\int (a + bx)^n dx = \frac{(a + bx)^{n+1}}{(n+1)(b)} , \tag{47}$$

where $a = LF_o$ and $b = -\left(LF_o - 1/t_f\right)$:

$$\frac{KE}{W} = \frac{14.5}{W}\left(\frac{W}{A}\right)^{1/2} \frac{\left(LF_o^{5/2} - 1\right)}{\frac{5}{2}\left(\frac{LF_o - 1}{t_f}\right)} . \tag{48}$$

With the assumption that the figure of merit, M, is 0.7 and $LF_o = 2.0$,

$$t_f = \frac{2}{g}(V_D - V_f) , \tag{49}$$

and

$$\left(\frac{KE}{W}\right)_{Reqd} = 2.40\left(\frac{W}{A}\right)^{1/2}(V_D - V_f) . \tag{50}$$

The kinetic energy must be possessed by the rotor at the time the flare commences. If the rotor blade's mass is uniformly distributed and a two-bladed rotor is assumed and as well as assuming only 2/3 of the energy is available for the flare before stalling occurs, then

$$KE_{rotor} = \frac{1}{9}\left(\frac{W_{RS}}{g}\right)(R\Omega)^2 , \tag{51}$$

where

W_{RS} = the weight of the rotor system that contributes to the rotational kinetic energy, i.e., W_{BT} and Q

Ω = blade rotation speed

R = blade radius.

The rotor blades then must possess a weight ratio relative to the gross weight of the system through the substitution of the KE_{rotor} in the $(KE/W)_{reqd}$ equation:

$$\frac{W_{RS}}{W} = 695\left(\frac{W}{A}\right)^{1/2}\frac{(V_D - V_f)}{(R\Omega)^2} \quad . \tag{52}$$

The rotor tip velocity, V_T, is

$$V_T = R\,\Omega \tag{53}$$

or

$$\frac{W_{RS}}{W} = 695\left(\frac{W}{A}\right)^{1/2}\frac{(V_D - V_f)}{(V_T)^2} \quad . \tag{54}$$

Rotor blades in autorotational descent have the drag coefficient, C_{D_R} related to the ratio V_D/V_T from Reference 5. A solidity ratio, σ, of 0.10 was assumed for minimum weight in this study since increasing the solidity by a factor of two and three only increases the drag coefficient between 7 and 14 percent. In Reference 5 the aerodynamic design criteria for the descent condition prior to execution of the flare in order to ensure against rotor stall occurring during the flare, the thrust coefficient, C_T, and solidity, σ, should be related as

$$\frac{C_T}{\sigma} \leq 0.10 \quad . \tag{55}$$

The thrust coefficient and the drag coefficient are related as

$$\frac{C_T}{C_D} = \left(\frac{V_D}{V_T}\right)^2 \quad . \tag{56}$$

The descent speed, V_D, the tip speed, V_T, disk loading, W/A, and the blade's weight ratio, W_{RS}/W, requirement are related by the above mathematical expressions. This is expressed by Figure 18 for standard sea level conditions (ρ = 0.002378 slugs/cu ft) and for a final touchdown velocity of 22.0 fps. The plot represents the minimum weight requirements. The parts of the rotor system that contribute to kinetic energy required to accomplish flare are the mass of the blade and mass of the tip. Values for blade weight at all disk loadings can be found from the analysis in Item (2) above. Values for tip weight at disk loadings greater than 0.8 psf now must be developed. Calculation of tip

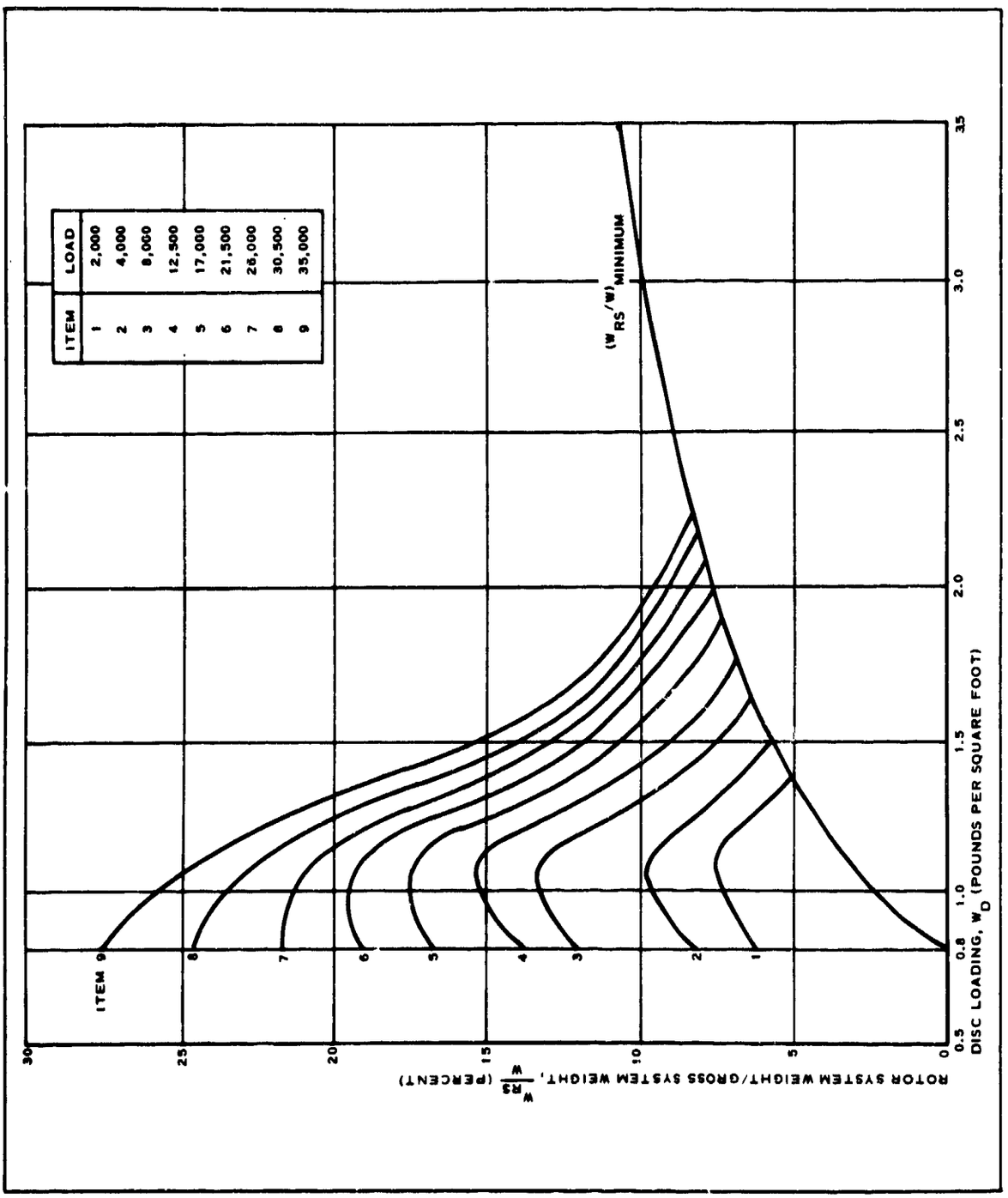

Figure 18 - Flare Weight Requirements

weight for the cases when the rotor will flare is performed in a slightly different manner as for the case without flare. The difference lies with the values for lift to be used in Equation 36. Since a load factor of two is to be experienced at the initiation of the flare maneuver, the total lift, L_T, will be twice the value experienced at steady-state descent conditions. Therefore to balance this increased lift force, larger centrifugal loads must be imposed on the blades during the steady-state condition. Based on this fact, values for tip weight, Q, were calculated at various disk loadings for each load item. The sum of the values for W_{BT}/W and Q/W are plotted on Figure 18 for each of the load items at the particular disk loadings. The minimum weight system is the point where the load item curves and the theoretical minimum weight curves intersect. The end points for the disk loading of 0.8 psf were taken from Figure 7.

Since a considerable weight savings can be seen for the load Items 4 through 9, it is advantageous to consider them further in an attempt to minimize the number of rotor diameters required.

From Table III, the diameters required for load Items 1, 2, and 3 are 60, 80, and 110 ft, respectively. If the diameters are referenced to the loads 4 through 9, then load Item 4 would be delivered with an 80-ft diameter rotor; loads 5 and 6 can be dropped with a 110-ft diameter unit; and for loads 7, 8, and 9, a 140-ft diameter system must be employed. For each of these items (4 through 9) the appropriate blade weight, W_{BT}, was taken from Table V. Tip weights, Q, then were calculated for each respective disk loading. These two values along with their sum, W_{RS}, and ratio to the load items $(W_{RS}/W)_{calc}$ can be found in Table VII.

The minimum requirement for $(W_{RS}/S)_{min}$ was obtained for each load item at its respective disk loading from Figure 18 and is presented in Table VIII. Any value of $(W_{RS}/W)_{min}$ that is greater than $(W_{RS}/W)_{calc}$ must be used for final weight determination. The $(W_{RS}/W)_{actual}$ is the resulting significant value and is presented in Table VIII. Evaluation of the hub weight now can be made.

(7) Hub Weight (W_{HUB})

Presented in Figure 5 is the preliminary design concept for the rotor hub as would be required for this application. From Figure 3-19 found in Reference 3, the hub weight for a conventional helicopter system is approximately equal to the weight of the rotor blades (this includes tip weight). Included in this value for W_{HUB} is the weight of the linkages

TABLE VIII - ACTUAL VALUES FOR BLADE WEIGHTS AND TIP WEIGHTS

Load item	Gross weight, W (lb)	Blade radius, R (ft)	Disk loading, W/A (psf)	Total blade weight, W_{BT} (lb)	Tip weight, Q (lb)	W_{RS} (lb)	$\left(\frac{W_{RS}}{W}\right)_{calc}$ (percent)	$\left(\frac{W_{RS}}{W}\right)_{min}$* (percent)	$\left(\frac{W_{RS}}{W}\right)_{actual}$+
4	12,500	40	2.49	208	331	539	4.3	9.0	9.0
5	17,000	55	1.79	537	885	1422	8.4	6.9	8.4
6	21,500	55	2.26	537	913	1450	6.7	8.4	8.4
7	26,000	70	1.69	1134	1810	2944	11.3	6.6	11.3
8	30,500	70	1.98	1134	1790	2924	9.6	7.6	9.6
9	35,000	70	2.27	1134	1920	3054	8.7	8.4	8.7

*Values taken from Figure 18 for respective disk loading.

+Values of $(W_{RS}/W)_{min}$ greater than $(W_{RS}/W)_{calc}$ have precedence.

and mechanism required for both cyclic and collective pitch control. It is assumed that the control linkage comprises 50 percent of the hub weight. Therefore since the design as presented in Figure 5 does not require any control mechanism, the hub weight will be assumed to be approximately 1/2 of the sum of W_{RT} and Q. From Figure 18, for an optimum design system that will employ the flare maneuver and therefore approach a powered rotor, W_{RS}, the minimum weight required will be between 8 and 12 percent of the gross weight. From the preceeding assumptions, the hub weight would be from 4 to 6 percent of the gross weight. For preliminary design, a nominal value for W_{HUB} will be 5 percent.

(8) Final Size and Weight Evaluation

To obtain the total system weight for each load item, the appropriate pressure bottle weight, W_{PB}, from Table VI along with the value for hub weight (W_{HUB}) must be added to $\left(W_{RS}/W\right)_{actual}$ of Table VIII. Presented in Table IX are the resulting values of W_{PB}/W, W_{HUB}/W, and W_{RS}/W and their sum W_R/W. (See Figure 19 for final weight ratio data).

TABLE IX - FINAL SYSTEM WEIGHT (WITH AND WITHOUT FLARE)

Load item	Gross weight, W (lb)	$\left(W_{RS}/W\right)_{actual}$ (percent)	W_{PB} (lb)	W_{PB}/W (percent)	W_{HUB}/W (percent)	$\left(W_R/W\right)_F$ (with flare)	W_R/W^* (without flare)
1	2,000	. . .	. . .	. . .	. . .	. . .	12.9
2	4,000	. . .	. . .	. . .	. . .	. . .	15.5
3	8,000	. . .	. . .	. . .	. . .	. . .	19.3
4	12,500	9.0	94	0.75	5.0	14.8	22.8
5	17,000	8.4	256	1.5	5.0	14.9	26.2
6	21,500	8.4	256	1.2	5.0	14.6	29.0
7	26,000	11.3	488	1.8	5.0	18.1	32.1
8	30,500	9.6	488	1.6	5.0	16.2	35.4
9	35,000	8.7	488	1.4	5.0	15.1	38.8

*Values taken from Table VII.

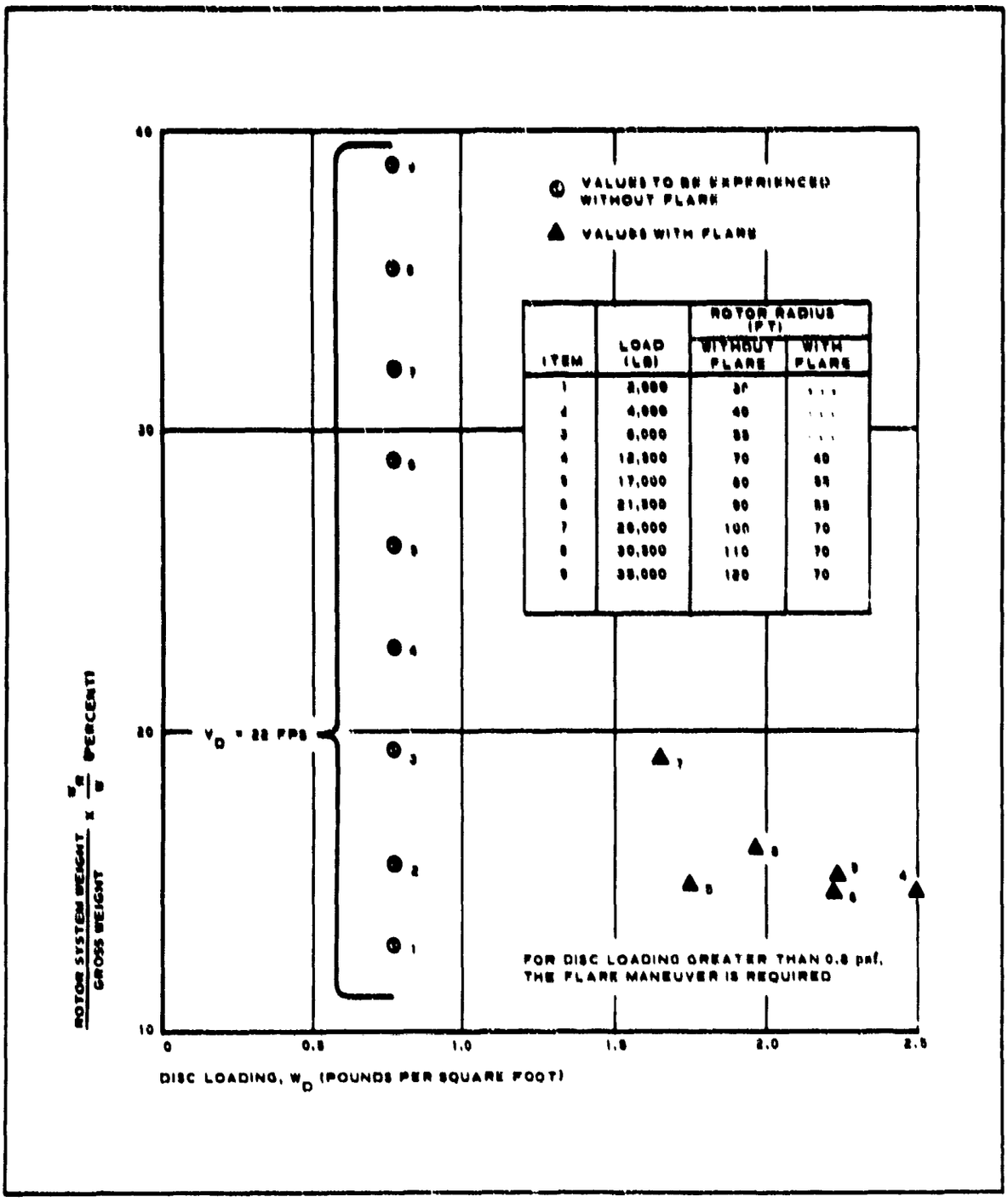

Figure 19 - Rotor System Weight Ratios

SECTION III - OPERATIONAL ANALYSIS

1. GENERAL

The BALLUTE-flexible rotor system as applied to the U.S. Army low-altitude airdrop mission must meet, along with the functional performance goals, certain operational requirements. Compatibility with U.S. Army and U.S. Air Force rear-loading cargo aircraft flying in mass formations is of utmost importance. Other operational requirements are making only minor alterations to the aircraft and also meeting the allowable volume envelope for each cargo item. The factor for major consideration is the complexity of the rigging, loading, derigging, and drop zone clearance operations. For the system to be desirable, a minimum requirement for special and additional training must be met. Reliability consideration is an additional factor that determines the usefulness of the system for this operation.

An indication of the system complexity can be realized if the steps required for preparation are known. A description of the packing and rigging operations and maintenance of the BALLUTE and rotor system follows.

Data concerning reliability estimates are contained in Item 4 below.

2. PACKING AND RIGGING

a. Method

The method for packaging the BALLUTE and flexible rotor system would be very similar to that presently experienced with standard parachute systems. The anticipated technique will be outlined below with discreet check points established.

b. Steps for Packaging BALLUTE

The BALLUTE is packaged as follows:

1. Inspect for areas that may have been overstressed during previous use. If necessary, inflate with a suitable blower to check questionable areas. Then make necessary repairs

2. Check geodetic suspension line arrangement to make certain there is no entanglement and proper attachment orientation
3. Elongate system on table
4. Compress inlets and restrain in loaded position with suitable fabric lines. These lines will be removed at a later step during the packing. The number of lines removed will be recorded on the sign-off sheets
5. Pleat BALLUTE by placing gore on gore, similar to present parachute folding techniques. After the pleating is complete, the packaged width of the BALLUTE is approximately one gore wide
6. Divide gore length into a predetermined number of segments for final folding. These segments then are accordion-folded on top of each other
7. Remove restraints on the inlets and make the proper record
8. Attach a breakline between the BALLUTE crown and the deployment bag
9. Place BALLUTE in the deployment bag, then install and tighten the proper lacing
10. Attach geodesic riser to the rotor pack
11. Make proper BALLUTE deployment bag closing restraints and install proper passive cutter knives

c. Step for Packaging Rotor

The rotor is packaged as follows:

1. Stretch out, inflate, and inspect blades for any damage that might have been received during a previous drop. It is assumed at this point that any damaged blades would be sent to a special area and necessary repairs made
2. Attach appropriate blades to the hub assembly. Install proper tip weight
3. Replace pyrotechnic manifold release valve with rebuilt unit. Rebuilding the unit requires replacing a diaphragm. Install two pyrotechnic charges. For clarification, the pyrotechnic charges, which are

lanyard initiated, puncture the diaphragm and permit the air in the storage bottles to pass through the manifold and into the blades

4. Make respective inflation tubing attachments. The blade is deflated at the beginning of this operation

5. For the version of the rotor that will utilize the flare maneuver to obtain the required 22-fps impact velocity, an additional step must be performed before the blades can be folded. This additional packaging step will require:
   a. Assembly of a daisy chain
   b. Attachment of two pyrotechnic (reefing line type) cutters per blade for release of the restraint to permit terminal flare. Two cutters are required at this time to provide a redundance
   c. Suitable attachment to each cutter through which the flare command signal is transmitted

6. Fold blades to the desired size dictated by the deployment bag. Depending on the blade size, it might be necessary to fold the blade before attaching to the hub assembly

7. Place folded rotors into the deployment bag

8. As the blades are being positioned into the bag, a lanyard that was previously attached to the bag is attached to the firing pin at the manifold release valve

9. Place remainder of the blades in the bag and make a suitable tie through two large reefing line type cutters at the bag inlet

10. Inflate storage bottles to the required pressure through the quick-disconnect extension. Perform leak-rate check to insure no leakage. This step could be performed after Step 4 to ease tightening of tubing fittings if required, but final inflation should be performed as a final step in an attempt to eliminate handling of the high-pressure system

11. A lanyard that previously has been attached to the suspension riser is left to be attached, but final attachment will be made after the package is placed in the aircraft to prevent premature release from handling

12. Attach rotor system to cargo

3. MAINTENANCE

a. General

Maintenance of the BALLUTE-rotor system as applied to cargo airdrop operation can be divided into two sections - one for the BALLUTE and the other for the rotor assembly. This separation results from the two different fabrication techniques for each item.

b. BALLUTE Maintenance

Maintenance of the BALLUTE will be required only if damage is experienced during a drop mission. Presently, it is anticipated that the BALLUTE be fabricated using a sewing procedure. All repairs could, therefore, be made using conventional sewing equipment. Repair of this type is practical because of the equipment available to make sewing repairs. The equipment referenced here consists of sewing machines and their related components.

An alternative to the sewn repairs would be a cementing process. The steps that would be followed if a cementing procedure were to be used are outlined in Item c, (3). Repair of the BALLUTE using a cementing technique could be done only if the BALLUTE previously had been coated. For this application the BALLUTE probably would not be coated unless the need arose to decrease its porosity for aerodynamic performance reasons.

c. Rotor Maintenance

(1) General Maintenance

The term general maintenance can be defined as any operation required by all rotor systems in preparation for the airdrop mission. Any function required by all of the rotor systems can be considered as part of the rigging operation. A complete description of rigging and packing requirements of the rotor portion of the recovery system can be found in Item 2, above.

(2) Repair Maintenance

Repair to the rotor system would be required only if damage to the rotor were encountered during the airdrop operation. The repair can be [illegible]oken into two sections - hardware and fabrics. The hardware portions are the hub, bearing, pressure bottles, manifold, tubing, and tip weight and cannot be repaired easily. The reason lies with the design of each component and their critical strength requirements. Emergency repairs could be made for use during one drop, but repeated use of a repaired part would not be recommended. Of major consideration would

be all pressure-carrying components such as air storage bottles, manifold, and tubing. The reasoning here lies with the large storage pressure requirements that dictate high and critical strength.

Repair to the fabric rotor blades will be quite different from repairs to cloth of the parachutes presently being used. By definition, a fabric is a cloth which is impregnated (coated) with an elastomer. Depending on the cloth, the type and amount of elastomer, and type of structure, the repair technique of either sealing or cementing is dictated. For the fabric rotor blades, a cementing technique is the only suitable repair procedure.

(3) Repair Procedure

(a) General

An outline of the procedure to make cemented repairs to fabrics follows.

(b) Size of Patches

(c) Surface Preparation

Remove all dust and lint from surfaces to be cemented with rag dampened with toluene or 1, 1, 1-trichloroethane.

(d) Cement Mixing Instructions

When cementing seams, apply a cement mixture consisting in a ratio of 128 cc of activator to one gallon of cement. Use only thoroughly mixed and freshly made cement. Discard when they begin to jell or after eight hours, whichever occurs first.

(e) Application

For all cement coats, a brush with an effective length bristle of 2-1/2 in. shall be used to flow the cement on as uniformly as possible. Brushes shall be washed free of set-up cement with toluene or 1, 1, 1-trichloroethane at least once every eight hours to maintain this effective 2-1/2 in. bristle length. If the effective length of the brush falls below 2-1/4 in. it shall be replaced with a new brush.

(f) Number of Coats

Apply the following minimum cement buildup to both surfaces that will be bonded:

1. Three heavy coats 1497-C (plus activator)
2. One heavy lay coat 1473-C (plus activator)

The cement, as received without any dilution, shall constitute a heavy coat.

(g) Drying

Allow each coat of cement to dry past the tack-free stage before applying the next coat. Normally this takes 15 to 30 min. Last coat should dry to the "laying tack" point. In the event that the cement becomes too dry for seaming, apply a new coat of cement.

(h) Seaming Procedures

Judgment and drying conditions determine the length of time after the last coat of cement is applied before seaming. Do not swab the cement if it becomes too dry; but apply a new coat as specified in the drying step. Lay the cemented seam or tape when the tack point is reached. Do not try to lay more seam or tape than can be put together before the cement becomes too dry. Roll down immediately. Avoid stress on tape or seams while laying.

Allow cemented seams to air dry for 24 hr before placing under any undue strain such as flexing or moving in a manner that would tend to loosen or distort a fresh seam.

(i) Curing

Allow the repair to age for a minimum of seven days before folding or boxing if possible. As an alternate, it is permissible to cure the repair with infrared heat lamps set at a distance so as to provide 140- to 160-F heat. Curing time shall be one hour; provide accurate heat control measure. Heat shall not be applied until cement has dried a minimum of eight hours.

Allow a minimum of 14 days room temperature curing before placing seams under any tension, such as test inflating.

As an alternate, seams may be cured for eight hours minimum at 200 F in circulating hot air. Seams must be aged 24 hr minimum before curing.

4. RELIABILITY

a. General

Reliability information applicable to the rotor blade delivery concept is

presented below. The method of approach is to present anticipated rotor blade system reliability and compare it to present parachute system data since the prepared system utilizes similar sequencing methods.

b. Mechanical

Presented in Table X are the pertinent data relative to mechanical reliability of parachute systems.

c. Human Error

(1) BALLUTE

Presented in Table XI are data concerning preparation of the BALLUTE for the airdrop system.

(2) Rotor

Table XII presents the data for preparing the rotor system for the airdrop operation.

TABLE X - MECHANICAL RELIABILIT

No.	Failure source	Reliability figure	Rational or calculation basis of reliability figure
1	Passive cutters at BAL-LUTE bag-closing re-straint	100	When a proper load is applied, sive cutters used for release o BALLUTE deployment bag seve textile line passing through the ter. Cutter reliability is depe upon proper application and ma tude of the force. Through pro development, the two factors w be completely defined and the s tem design and packing data es blished accordingly.
2	Time-delay cutters on rotor deployment bag	Seven out of 29 malfunc-tions that were experi-enced during 1679 drops in October, November, and December 1965 were contributed to reefing line cutters[8]	Exact reliability figures for tim delay cutter cannot be establish now due to the new application reefing line cutter and no defin of the exact type. Documented in WADDTR 60-2009[9] are relia figures for a particular type re line cutter. An estimate of rel bility at various confidence lev is provided. In general, a reli bility of 0.985 at a 99 percent fidence level has been establish for the M2AI reefing line cutte
3	Inflation system pyro valve	N/A	A pyrotechnic device will be a velopment item and reliability only be established during a de ment program. The method to used in establishing these figur is documented in Navord Repor 2101[10]
4	Ground-sensing probe system	. . .	Same as No. 3
5	Pyro cutters at blade tips (for flare)	N/A	Same as No. 3

A.

ELIABILITY OF PARACHUTE SYSTEMS

l or basis y figure	Consequence of failure	Visibility or detectability of incipient feature	Comments
is applied, pas- r release of the nt bag sever a through the cut- ity is dependent tion and magni- through proper o factors would d and the sys- ing data estab-	Inability to deliver load	Proper rigging determined only by visual inspection	. . .
ures for time e established pplication of the nd no definition ocumented in 9 are reliability lar type reefing mate of relia- idence levels ral, a relia- 9 percent con- n established line cutter.	Damage to load to a degree affecting its usefulness in combat or increased probability of such damage (due to increased rate of descent).	A visual inspection is the only means to determine that the arming lanyard attachment was properly made. This prevents an initiation failure of the cutters.	Although one device will perform the required task, two devices are incorporated for redundancy.
will be a de- reliability can uring a develop- method to be these figures ord Report	Same as No. 2	Same as No. 2	Same as No. 2
	Same as No. 2	Same as No. 2	Same as No. 2
	Same as No. 2	Same as No. 2	Same as No. 2

B.

TABLE XI - BALLUTE PREPARATION FAILUR

Error source*	Estimated frequency of occurrence	Consequence of error	Times inspected	Redun and fai featu
1	N/A	Inability to deliver load	1	Visual inspec sign-off
2	N/A	Inability to deliver load. Damage to load to a degree affecting its usefulness in combat or increased probability of such damage (due to increased rate of descent, for example)	1	Visual inspec sign-off
4	N/A	. . .	1	Visual inspec sign-off
7	N/A	Inability to deliver load	1	Visual inspec sign-off
8	N/A	. . .	1	Visual inspec sign-off
9	N/A	. . .	1	Visual inspec sign-off
10	N/A	Damage to load to a degree affecting its usefulness in combat or increased probability of such damage (due to increased rate of descent, for example)	1	Visual inspec sign-off
11	N/A	Inability to deliver load. Damage to load to a degree affecting its usefulness in combat or increased probability of such damage (due to increased rate of descent, for example)	1	Visual inspec sign-off

*Numbers in this column correspond to BALLUTE packing steps in Item 2, b of this section.

A.

PARATION FAILURES DUE TO HUMAN ERROR

	Redundancy and failsafe features	Comments
	Visual inspection and/or sign-off	BALLUTE inspection similar to present parachute inspection
	Visual inspection and/or sign-off	Improper attachment of BALLUTE to rotor pack could result in BALLUTE separating from rotor pack at BALLUTE deployment, resulting in a lack of force to strip off rotor deployment bag. Visual inspection is only means of preventing this
	Visual inspection and/or sign-off	. . .
	Visual inspection and/or sign-off	If inlets are restrained and not permitted to spring into airflow, BALLUTE will not inflate and cargo cannot be extracted from aircraft. Even though this could exist, there still would be sufficient drag provided to strip the rotor deployment bag and perhaps allow the drag of the trailing rotor to extract cargo
	Visual inspection and/or sign-off	Failure to make this attachment would reduce the inflation time of the BALLUTE slightly but would not have a significant effect on the performance
	Visual inspection and/or sign-off	Improper installation of the BALLUTE into the deployment bag would affect repeatability but would not hinder system performance
	Visual inspection and/or sign-off	Improper attachment of BALLUTE to rotor pack could result in BALLUTE separating from rotor pack at BALLUTE deployment, resulting in a lack of force to strip off rotor deployment bag. Visual inspection is only means of preventing this
	Visual inspection and/or sign-off	Improper attachment of the BALLUTE deployment bag could result in no deployment of the BALLUTE and no (1) direct removal of cargo from the aircraft, (2) strip-off of the rotor deployment bag, and (3) transmittal of torque to the rotor to assist the transient spin-up

b of this section.

B.

TABLE XII - ROTOR PREPARATION FAILU

Error source*	Estimated frequency of occurrence	Consequence of error	Times inspected	Redundan and failse features
1	N/A	Damage to load to a degree affecting its usefulness in combat or increased probability of such damage (due to increased rate of descent, for example)	1	Inspection records w sign-off by proper pe suing steps could not without signature on
2	N/A	Damage to load to a degree affecting its usefulness in combat or increased probability of such damage (due to increased rate of descent, for example)	1	Attachment of blade t weight to blade is ma of bolts. The failsafe fiber locknut assembl
3	N/A	Damage to load to a degree affecting its usefulness in combat or increased probability of such damage (due to increased rate of descent, for example). Error in assembly would be detected in pressure checks	1	Leakage tests on asse would indicate impro Although one charge c ficient to perform the be employed for redu
4	N/A	Error in assembly would be detected in pressure checks	1	Leakage tests on asse would indicate improp
5	N/A	Damage to load to a degree affecting its usefulness in combat or increased probability of such damage (due to increased rate of descent, for example)	1	Although one charge c ficient to perform the be employed for redu
6	N/A	. . .	. . .	. . .
7	N/A	. . .	. . .	. . .

*Numbers in this column correspond to rotor packing steps in Item 2, c of this section.

A.

RATION FAILURES DUE TO HUMAN ERROR

Redundancy and failsafe features	Comments
tion records would require a ff by proper personnel. En- steps could not be performed t signature on components	The pressure test would be performed to verify a certain leakage rate (psi drop per minute). If within limits, the blade needs no repair; structural components would be inspected. Usable blades would be tagged and transferred to a packing and rigging area. Damaged blades would be transferred to a repair area
ment of blade to hub and tip to blade is made with a group s. The failsafe would be by ocknut assembly	Inspector would check the torque on the attachment blade. Visual inspection would determine whether or not the proper tip weight is being used
e tests on assembled system ndicate improper installation. h one charge or cutter is suf- to perform the task, two will loyed for redundancy	Failure to puncture the diaphragm is reflected under "consequence of error". After development, the only anticipated reason for failure of the charge to fire would be a failure in the removal of the firing pin during deployment. A direct cause would be no attachment of required lanyard.
e tests on assembled system ndicate improper installation	. . .
h one charge or cutter is suf- to perform the task, two will loyed for redundancy	Visual inspection would indicate improper assembly. Sign-off of the packing record would be required before further steps could be performed. The flare maneuver would not be required for the drop of all systems
	Improper folding and installation of the blades into the bag should not affect the performance of the system
	Improper folding and installation of the blades into the bag should not affect the performance of the system

section.

B.

TABLE XII - ROTOR PREPARATION FAILURES

Error source*	Estimated frequency of occurrence	Consequence of error	Times inspected	Redundancy and failsafe features
8	N/A	Damage to load to a degree affecting its usefulness in combat or increased probability of such damage (due to increased rate of descent, for exan ple)	1	. . .
9	N/A	Damage to load to a degree affecting its usefulness in combat or increased probability of such damage (due to increased rate of descent, for example)	1	Although one charge or ficient to perform the t be employed for redund
10	N/A	Damage to load to a degree affecting its usefulness in combat or increased probability of such damage (due to increased rate of descent, for example)	1	. . .
11	N/A	Damage to load to a degree affecting its usefulness in combat or increased probability of such damage (due to increased rate of descent, for example)	1	Although one charge or ficient to perform the t be employed for redund
12	N/A	Damage to load to a degree affecting its usefulness in combat or increased probability of such damage (due to increased rate of descent, for example)	1	Cargo would not be per craft without proper si ing record

*Numbers in this column correspond to rotor packing steps in Item 2, c of this section.

A.

N FAILURES DUE TO HUMAN ERROR (Continued)

Redundancy and failsafe features	Comments
	Visual inspection and proper sign-off would be the only means of ensuring proper assembly
one charge or cutter is sufficient to perform the task, two will be employed for redundancy	Failure to properly attach the cutter and restraint line could result in a premature deployment of the blades or no deployment of the blades
	Proper sign-off would indicate completed step
one charge or cutter is sufficient to perform the task, two will be employed for redundancy	Failure to install lanyard would result in no deployment of the blades
ould not be permitted on aircraft without proper sign-off on packard	Final attachment of the rotor system to the cargo would be indicated by proper sign-off

ection.

B.

SECTION IV - FEASIBILITY DEMONSTRATION

1. GENERAL

Autorotating inflatable rotory wing decelerators for the recovery of descending payloads has been previously demonstrated analytically as a sound concept for a recovery device. To demonstrate that the concept also is functional, a model inflatable rotor was designed, fabricated, and tested. Goodyear Aerospace has concluded from tests that an inflatable flexible fabric rotor will assume a steady autorotating state and decelerate a payload to the desired touchdown velocity.

2. MODEL DESIGN

a. Size:

To design a system that would adequately perform as required and yet be fabricated within a reasonable time period, existing and readily available components were utilized where possible. The critical part of the system relative to size determination was that of an inflation system. Since simplicity was of major concern, a standard CO_2 cartridge pressure bottle system was incorporated into the design. The pressure-volume relationships for CO_2 are known to be at one atmosphere of pressure; there are 34.56 cu in. of CO_2 per gram of CO_2 and the volume is in direct inverse relationship with absolute pressure. The rotor size now is determined from Equation 18 for a NASA 0012 airfoil:

$$V_{AF} = 0.082\, b^2\, RN \quad . \tag{57}$$

If we substitute $b = 0.314\, R/N$ (from the definition of solidity), Equation 18 reduces to:

$$V_{AF} = 0.00404\, R^3/N \quad . \tag{58}$$

Assuming that a 5-psig pressure would be sufficient to provide the necessary steady-state performance characteristics, the available volumes of CO_2 for a 4-, 8-, and 12-gm cartridge and resulting rotor radii for N = 2 blades is presented in Table XIII.

TABLE XIII - ROTOR DIAMETER AND CO_2 BOTTLE SIZE

Size (gm)	Volume at 5 psig (cu in.)	R (in.)
4	104	29.5
8	208	37.2
12	312	42.6

Since steady-state experimental data are in existence for a five-foot diameter system, the final system design diameter for this model was chosen to be five feet so that, if possible, a performance comparison and evaluation could be made. Table XIII designates that the four-gram CO_2 bottle will be required. Solving for chord length, b, from above for a radius of 30 in. and N = 2 yields:

$$b = 0.314\ (30)/(2)$$

$$b = 4.75 \text{ in.}$$

The selected rotor size will be the following:

$$R = 30 \text{ in.}$$

$$b = 4.75 \text{ in.}$$

$$N = 2 \ .$$

The similitude of this system to the full-scale configuration will be that of a terminal descent velocity of 22 fps. The disk loading to be experienced at this descent velocity will be 0.8 psf and is obtained from Figure 7. The area swept by the blades will be equal to πR^2 and is 19.6 sq ft. The thrust produced will be

$$W = W_D A$$

$$W = (0.8)(19.6)$$

$$W = 15.68 \text{ lb} \ .$$

b. Material

The blade design configuration is shown in Figure 20. As can be seen, the blade is comprised of a base cloth, and cover ply (1.30 oz/sq yd Dacron pattern number 3598). The basic cloth strength is 45 pounds per inch in the warp direction and 52 pounds per inch in the fill direction. A special material comprised of tire cord and a leaded elastomer[a] was used at the forward blade's leading edge to achieve mass balance ahead of the forward quarter chord. An additional layer of Dacron material[b] was placed over the tire cord cap so that a relatively smooth leading edge could be obtained. Design weights of various components can be found in Table XIV.

TABLE XIV - MODEL BLADE WEIGHT DETERMINATION

Description	Base material weight (oz/sq yd)	Approximate coating and elastomer weight (oz/sq yd)	Component weight (lb)
Base cloth	1.30	1.20	0.03285
Cover	1.30	1.20	0.03285
Cap (leaded)	70.00	. . .	0.20250
Cap (outer)	3.32	1.68	0.01300
Tube	. . .	. . .	0.00840
		Total per blade =	0.28960

c. Tip Weight

The tip weight was determined from Equation 36. If total thrust, T, and total system blade weight are used, then the system total tip weight can be determined by

$$Q_{TOT} = \frac{0.7427(W) - W_{B_{TOT}} \left[.5 \cos \theta_o + \frac{(V_T)^2 \tan \theta_o}{3gR} \right]}{\cos \theta_o + \frac{(V_T)^2 \tan \theta_o}{R\, g}} \qquad (59)$$

[a] Goodyear Tire & Rubber Pattern XZ 28A263

[b] Goodyear Tire & Rubber Pattern 15268/1

By substituting numerical values for the symbols as follows:

$$T = 15.68 \text{ lb}$$

$$W_{B_{TOT}} = 0.576 \text{ lb}$$

$$\theta_o = 3 \text{ deg}$$

$$R = 2.5 \text{ ft}$$

$$V_T = \text{fps} = 260 \text{ fps}$$

$$Q_{TOT} = 0.064 \text{ lb} \quad ,$$

the tip weight per blade therefore will be

$$Q = Q_{TOT}/N = 0.064/2 = 0.032 \text{ lb} \quad .$$

The tip weight design can be found in Figure 21.

3. FABRICATION

Resulting from the relatively small size of this model the most economical means of fabrication of the AIRMAT portions was to handsew the drop yarns. Figure 22 depicts the tooling required to handsew the AIRMAT to the NACA-0012 contour. The general fabrication consisted of first fitting the base cloth around the tool. Prior to this, the material was cross hatched to form a pattern to ensure systematic stitch spacing. The drop yarns then were sewn continuously in the radial or longitudinal direction. Once the sewing was complete, the outer cover was applied with the proper cementing technique. After curing, the root and tip fittings were installed and then the leaded cover and outer cover applied. The root fitting design can be found in Figure 21. After leakage checks the blade was ready for preliminary testing. Figure 23 is a platform view of the blade. An end view looking at the blade tip can be seen in Figure 24. The symmetrical airfoil shape can be seen in this view. The sewing pattern can be seen as the dark straight parallel lines running longitudinally on the blade surface. Figure 25 is a view sighting along the trailing edge and indicates the straight contour of the blade.

4. TESTING

After fabrication of the blades was completed, a series of preliminary

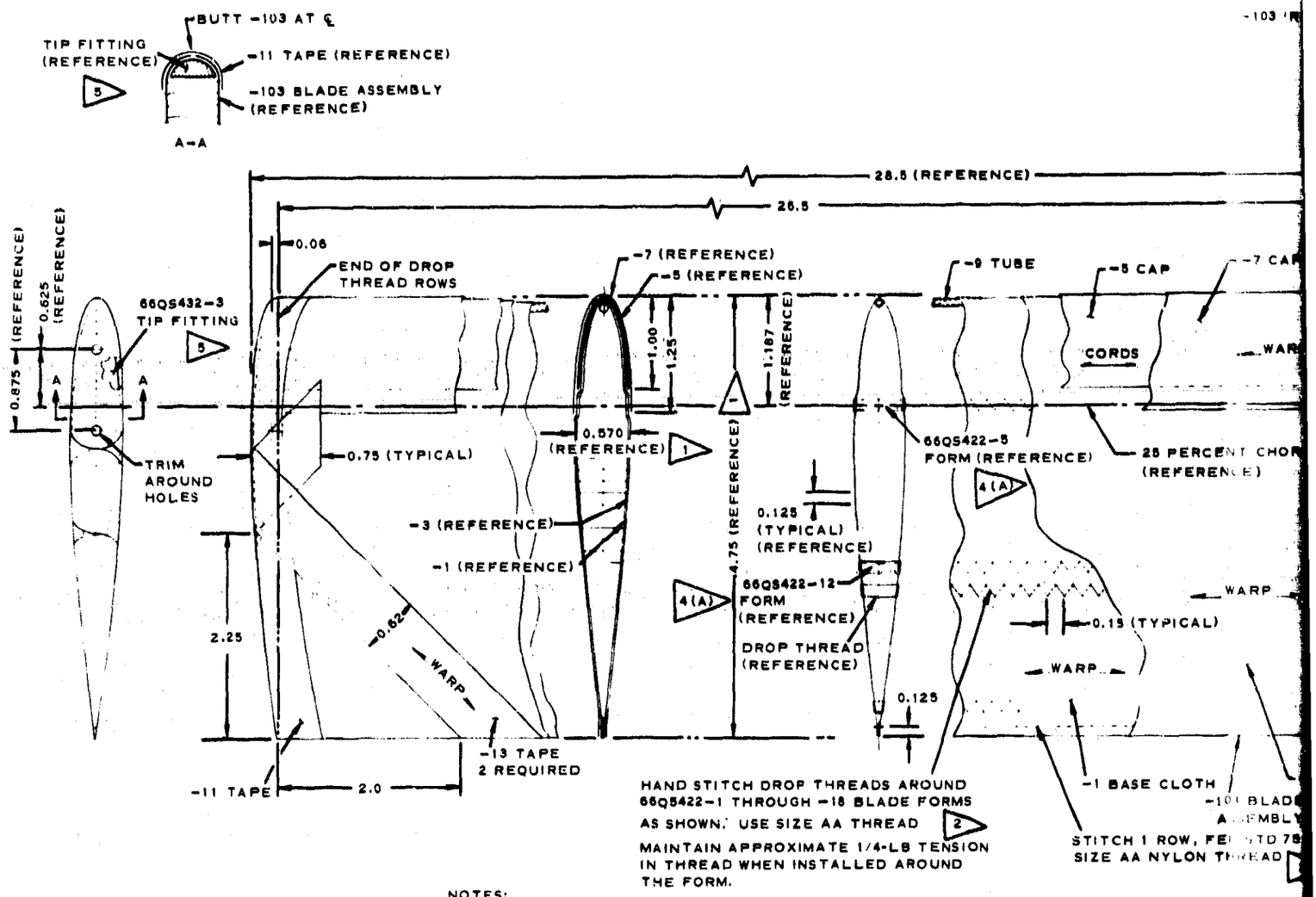

NOTES:

UNLESS OTHERWISE SPECIFIED, ALL DIMENSIONS ARE IN INCHES AND

1. FINISHED CONTOUR SHALL CONFORM TO 66QS422-19 TEMPLATE
2. NYLON THREAD, FED SPEC V-T-295, TYPE I
3. AFTER INSTALLING DROP THREADS AND BEFORE REMOVING BLADE FORMS, CEMENT -1 CLOTH AND EXPOSED DROP THREADS AS FOLLOWS:
   - A. CLEAN WITH MEK
   - B. APPLY ONE THIN COAT POLYURETHANE (GT & R CODE D-1569-F838) CUT TO 2 PARTS POLYURETHANE / 1 PART MEK
   - C. APPLY ONE FULL COAT D-1569-F838 AND CURE

A.

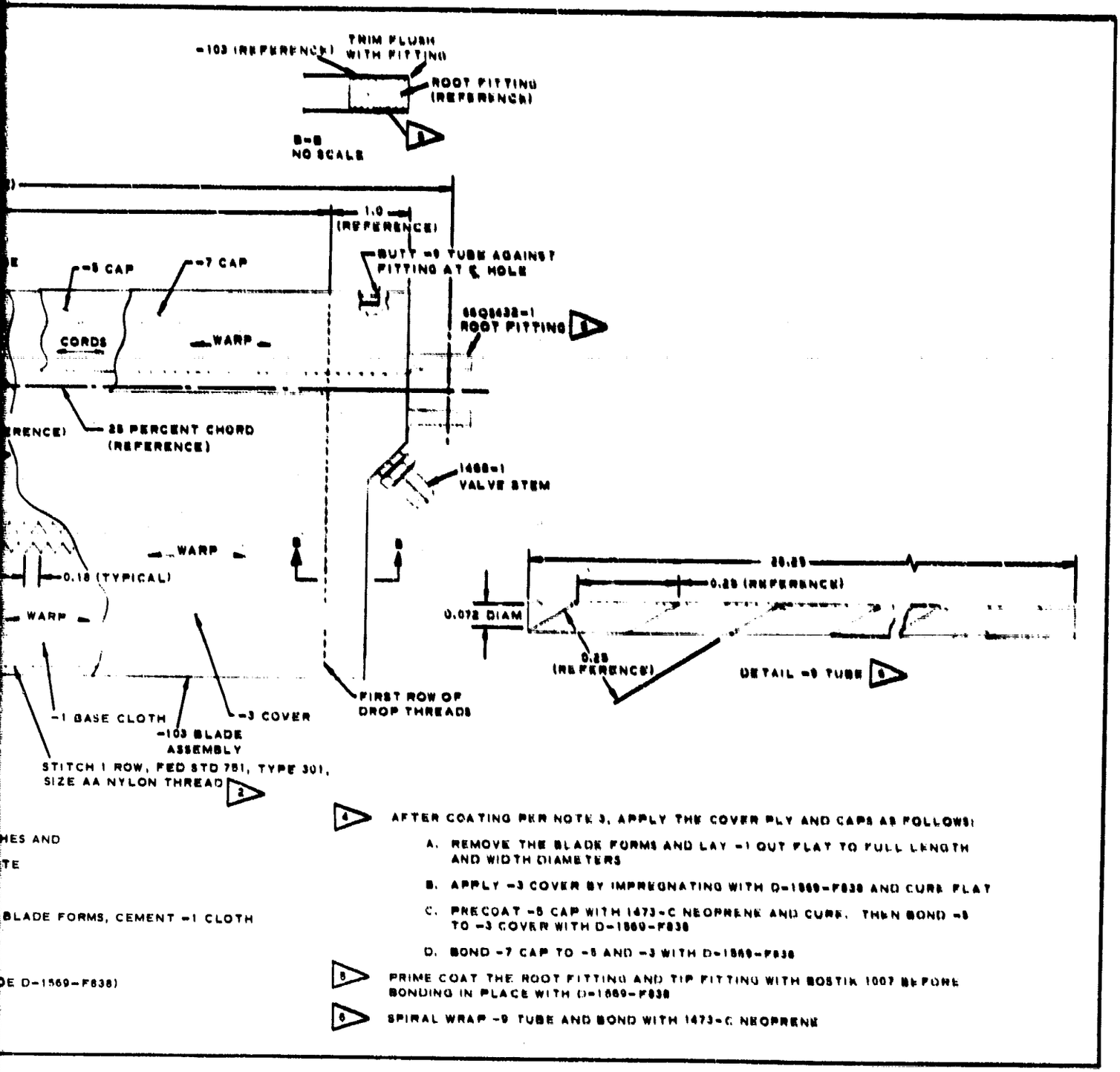

Figure 20 - Model Blade Design

B.

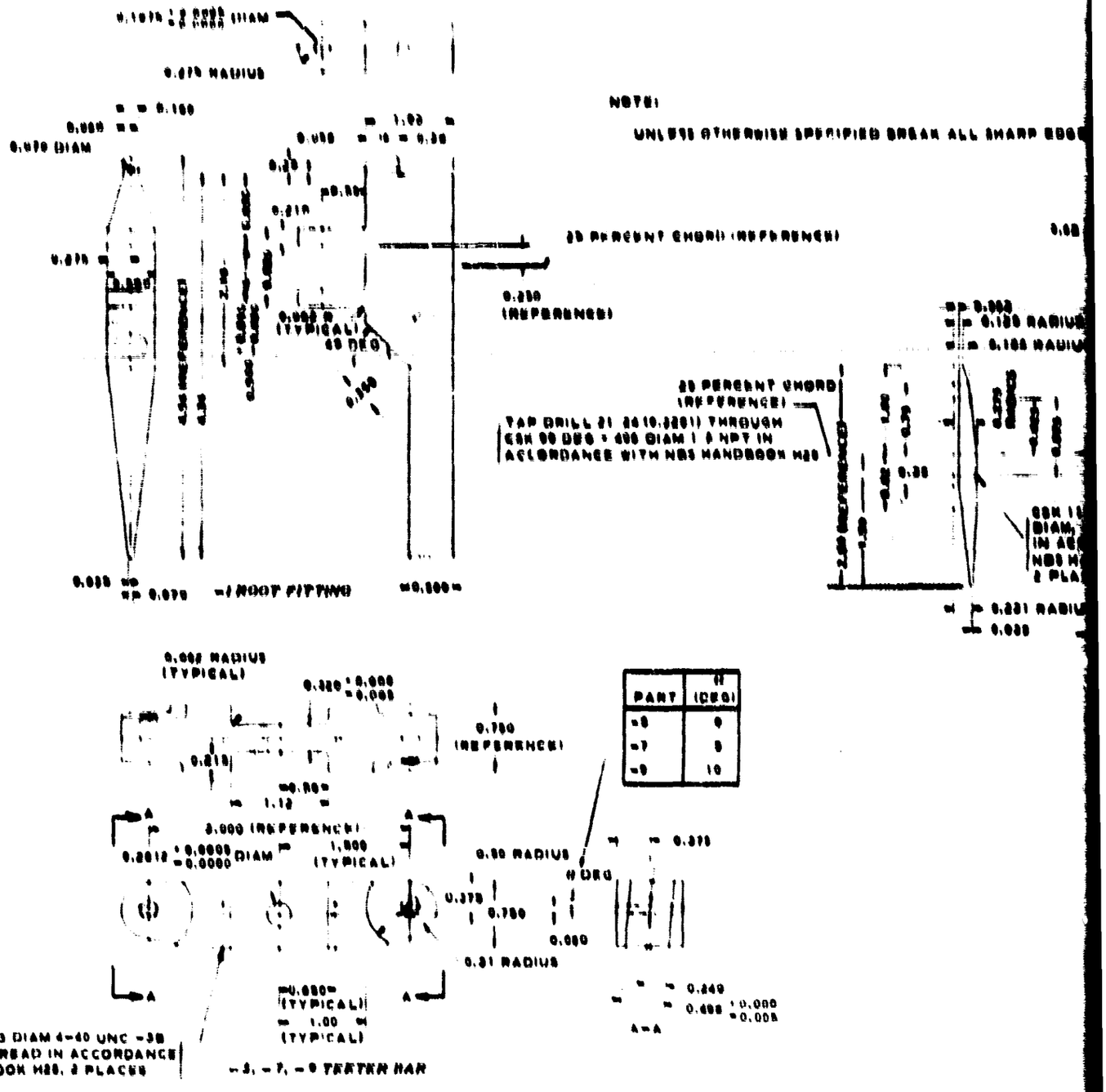

Figure 21 - Model

A.

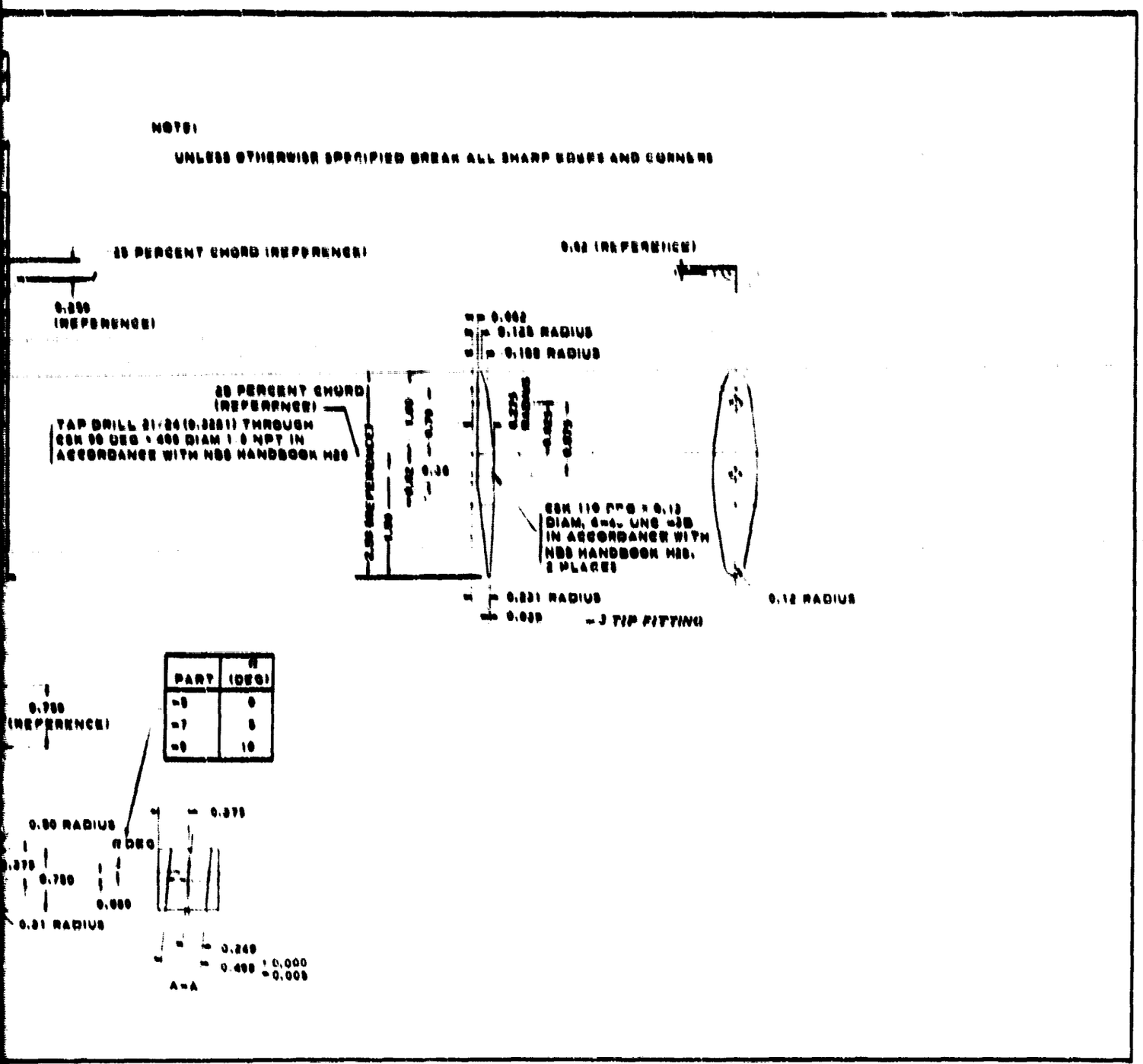

Figure 21 - Model Tip Weight and Root Fitting Design

B.

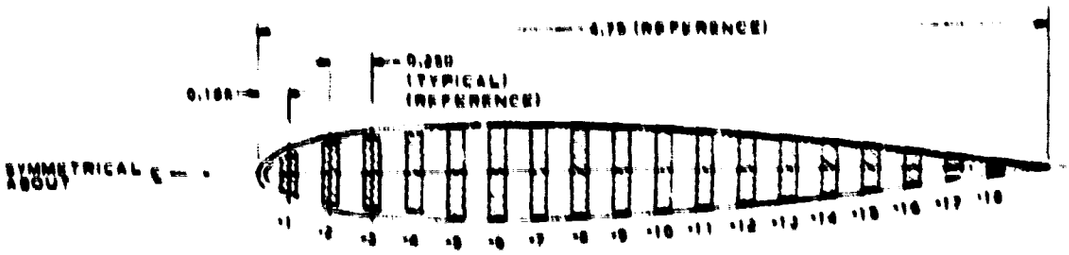

BLADE FORMARRANGEMENT (REFERENCE)
NACA 0018

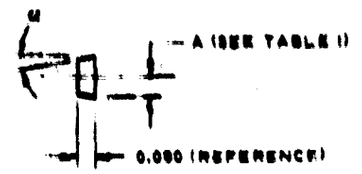

B - B
NO SCALE

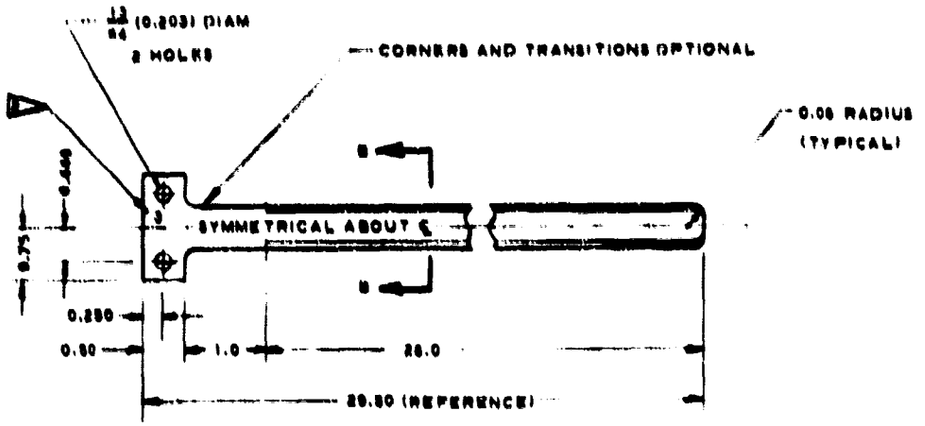

DETAIL -1 THROUGH -18 BLADE FORM
NO SCALE

NOTES: UNLESS OTHERWISE SPECIFIED

1. BREAK ALL SHARP EDGES
2. METAL STAMP DASH PART NUMBER AT APPROXIMATE LOCATION SHOWN

A.

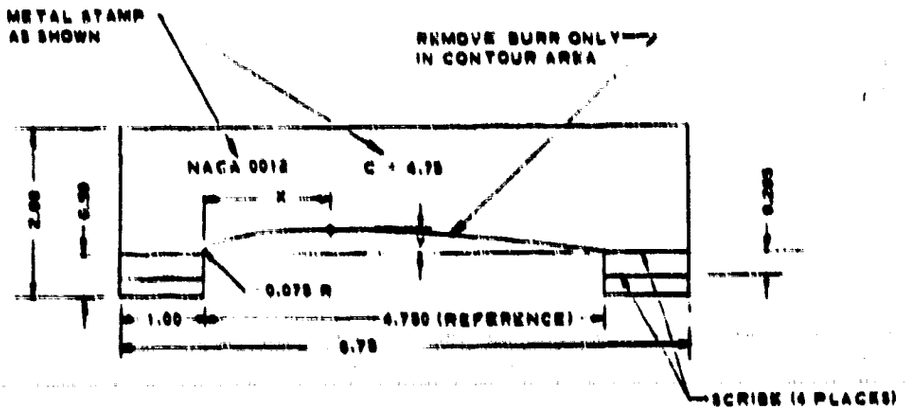

DETAIL -19 TEMPLATE
SEE TABLE II FOR X AND Y COORDINATES

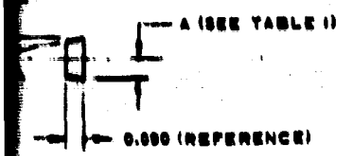

B - B
NO SCALE

TABLE I

PART NO.	α (DEG)	A ± 0.005	B = A (REF)
-1	20	0.130	0.260
-2	10	0.191	0.382
-3	5	0.220	0.440
-4	0	0.237	0.474
-5	0	0.270	0.540
-6	0	0.278	0.556
-7	0	0.276	0.552
-8	0	0.268	0.536
-9	0	0.258	0.516
-10	↑	0.246	0.492
-11	|	0.228	0.456
-12	|	0.208	0.416
-13	|	0.186	0.372
-14	|	0.158	0.316
-15	|	0.133	0.266
-16	|	0.103	0.206
-17	↓	0.073	0.146
-18	5	0.041	0.082

TABLE II

X	Y
0.119	0.124
0.356	0.200
0.713	0.284
1.188	0.282
1.424	0.268
1.900	0.276
2.850	0.217
3.800	0.128
4.750	0.006

NOTES: UNLESS OTHERWISE SPECIFIED

1. BREAK ALL SHARP EDGES
2. METAL STAMP DASH PART NUMBER ONLY AT APPROXIMATE LOCATION SHOWN

Figure 22 - Tooling Required for Model Fabrication

B,

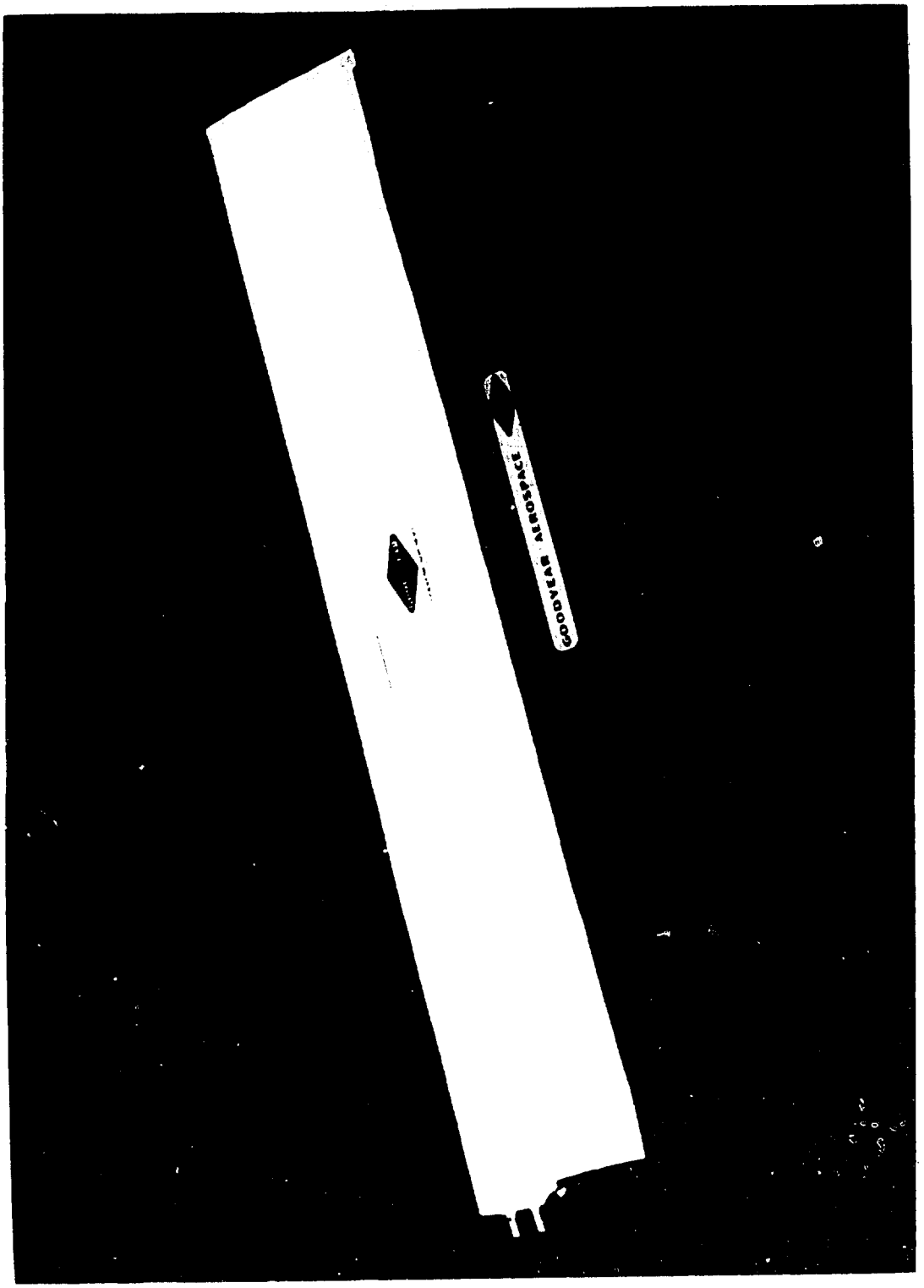

Figure 23 - Blade Planform View

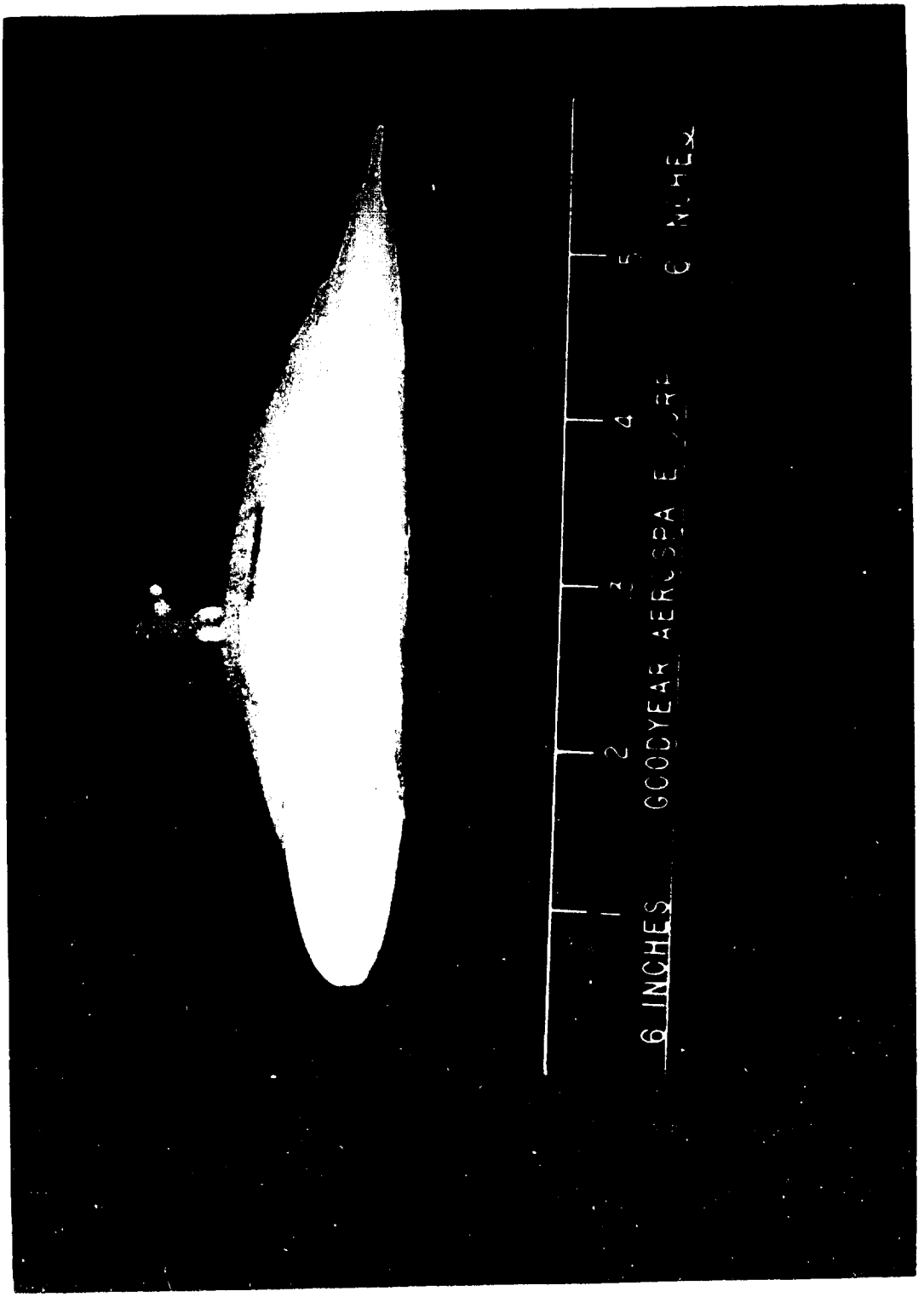

Figure 24 - Blade End View

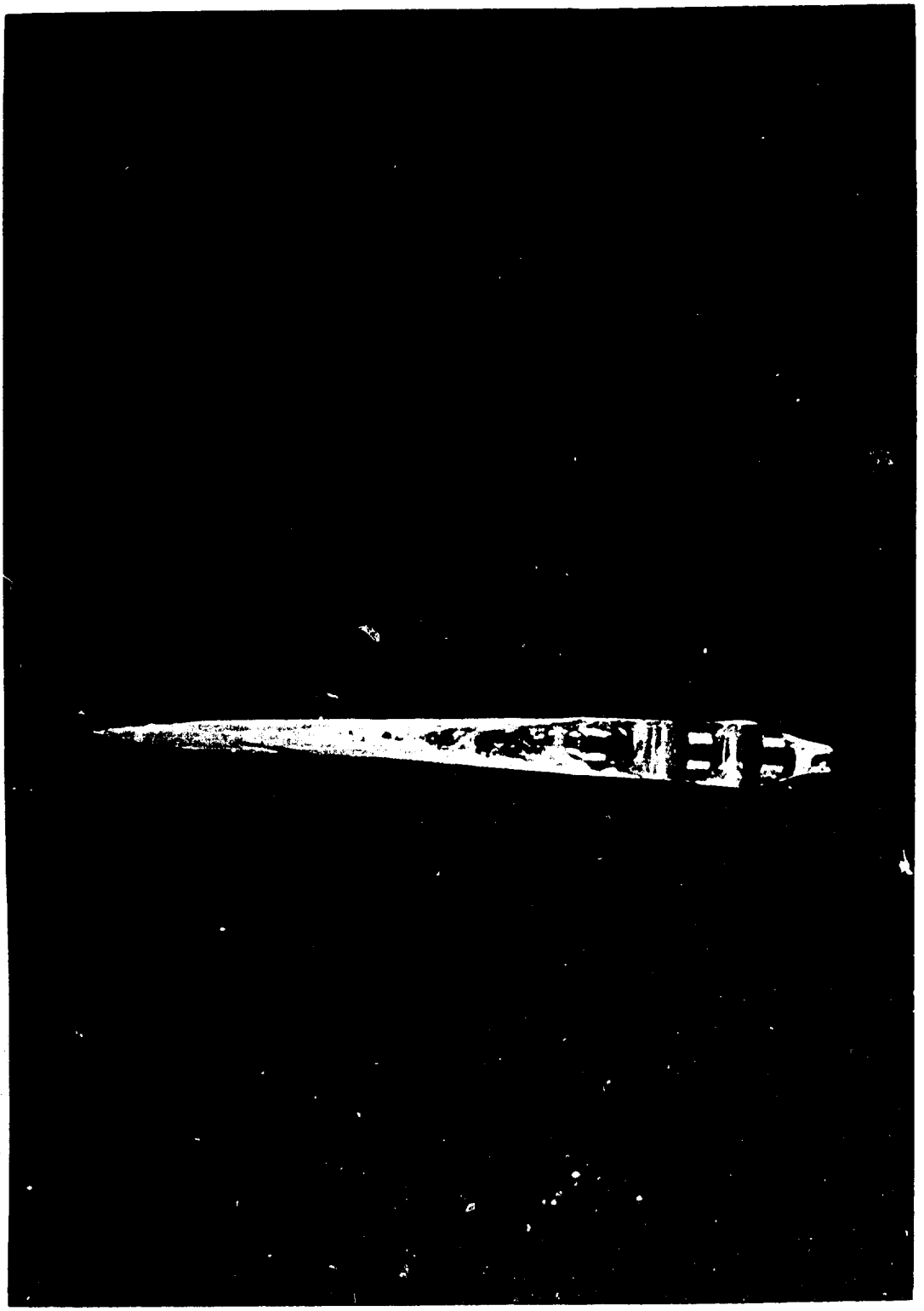

Figure 25 - Trailing Edge Contour

tests were conducted in order that an estimate of the performance characteristics could be obtained. Testing was conducted in such a manner that, if necessary, possible detrimental problem areas could be relieved before damage to the system was encountered.

The first area of testing was that of a proof test on internal pressure to ensure that any possible overpressure experienced during bottle inflation would not be harmful. The system functioned safely at 10 psig, which was adequate for the pressure test.

Dynamic balance during steady-state rotation was considered next. To evaluate this condition a test fixture was assembled and a series of rotational velocities induced into the rotor system. These angular velocities were obtained by a controlled-rpm motor. The tests had very favorable results up to an anticipated 300-rpm limit. An increase in weight of eight grams at the tip of one blade was required to bring the blades into the same rotational plane. Once the unit was considered to be dynamically and structurally continuous, a series of preliminary tests were made with the system mounted on an automobile. With the blades preinflated and initially in a trailing position, a series of runs were made to evaluate transient spin-up characteristics. For all of the five tests, the blades assumed an autorotative state when an inflow velocity of approximately 20 mph was attained. At an inflow velocity of approximately 35 mph, the test fixture was bent due to excessive thrust produced by the blades. All tests were performed with the blades at a negative 5-deg pitch angle, θ.

Following the preliminary spin-up tests, a series of bottle inflation tests were performed to evaluate the effect of rapid inflation. Figure 26 depicts the actuator mechanism and its attachment to the swivel and teeter bar. Figure 27 shows the adapter required to connect the swivel and actuator. As can be seen in Figure 28, the blades are then attached to the teeter bar and although not shown in the picture, rubber tubing from a Tee fitting at the actuator to the fitting at the blade root provides the necessary inflation duct. Along with Figure 28, Figures 29 and 30 indicate how the blades appear in a packaged state. The accordion type pleating as shown appears to be more advantageous than a radial roll. This also provides a systematic unfolding of the blade during deployment.

The inflation tests consisted of first inflating the blades in their normal elongated condition. Since the pressure-volume relationship for this model is very sensitive to small volume changes, it first was necessary to remove all residual ambient air from the blades. The internal pressure was checked on a manometer and determined to be 6.5 psig, which even though slightly greater than design pressure was still below the proof test pressure of 10 psig. Following this initial test, the blades were folded and restrained into shape with a suitable strength cord. When the CO_2 bottle was released, the internal pressure increase within

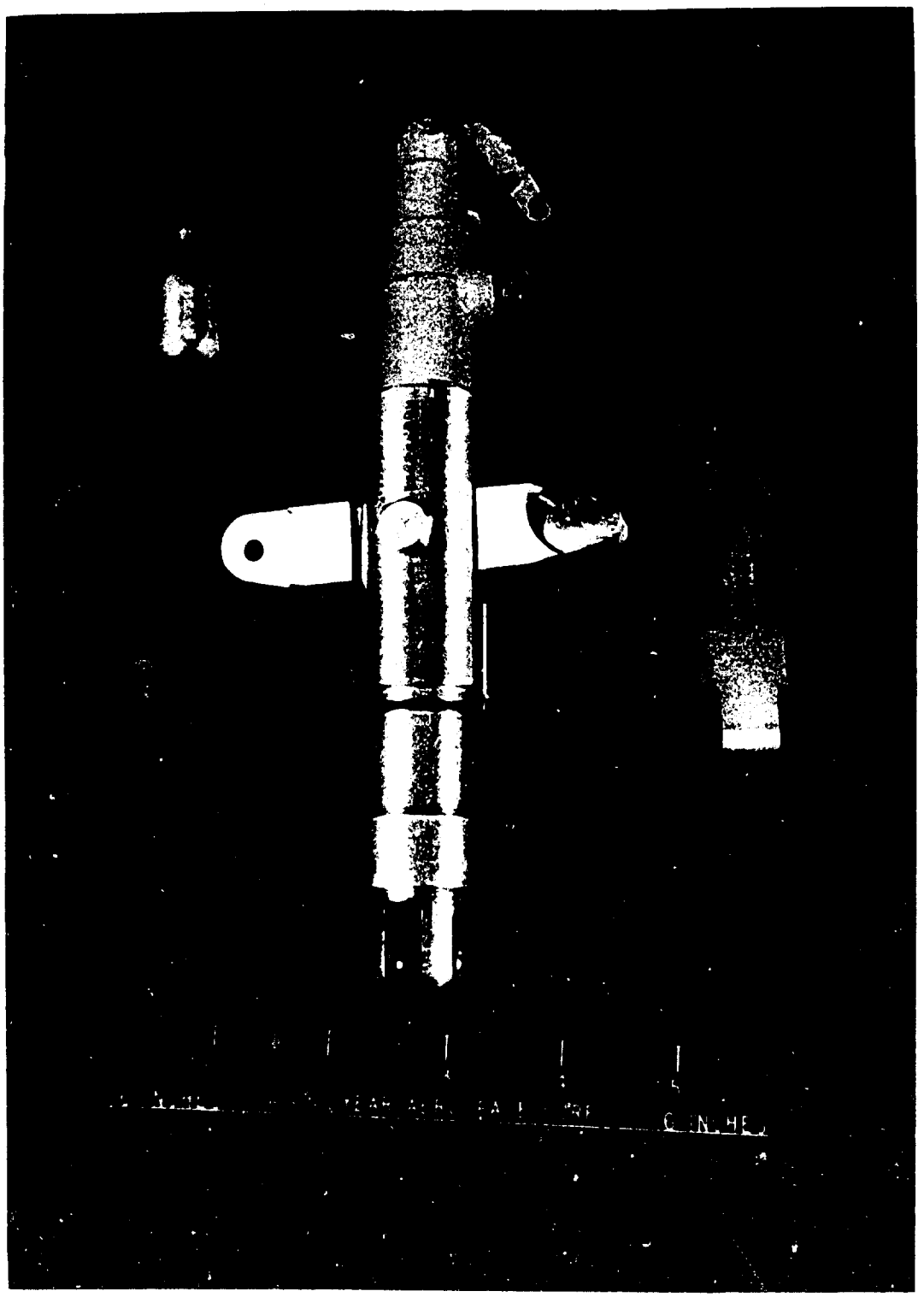

Figure 26 - Inflation Actuator and Hub Assembly

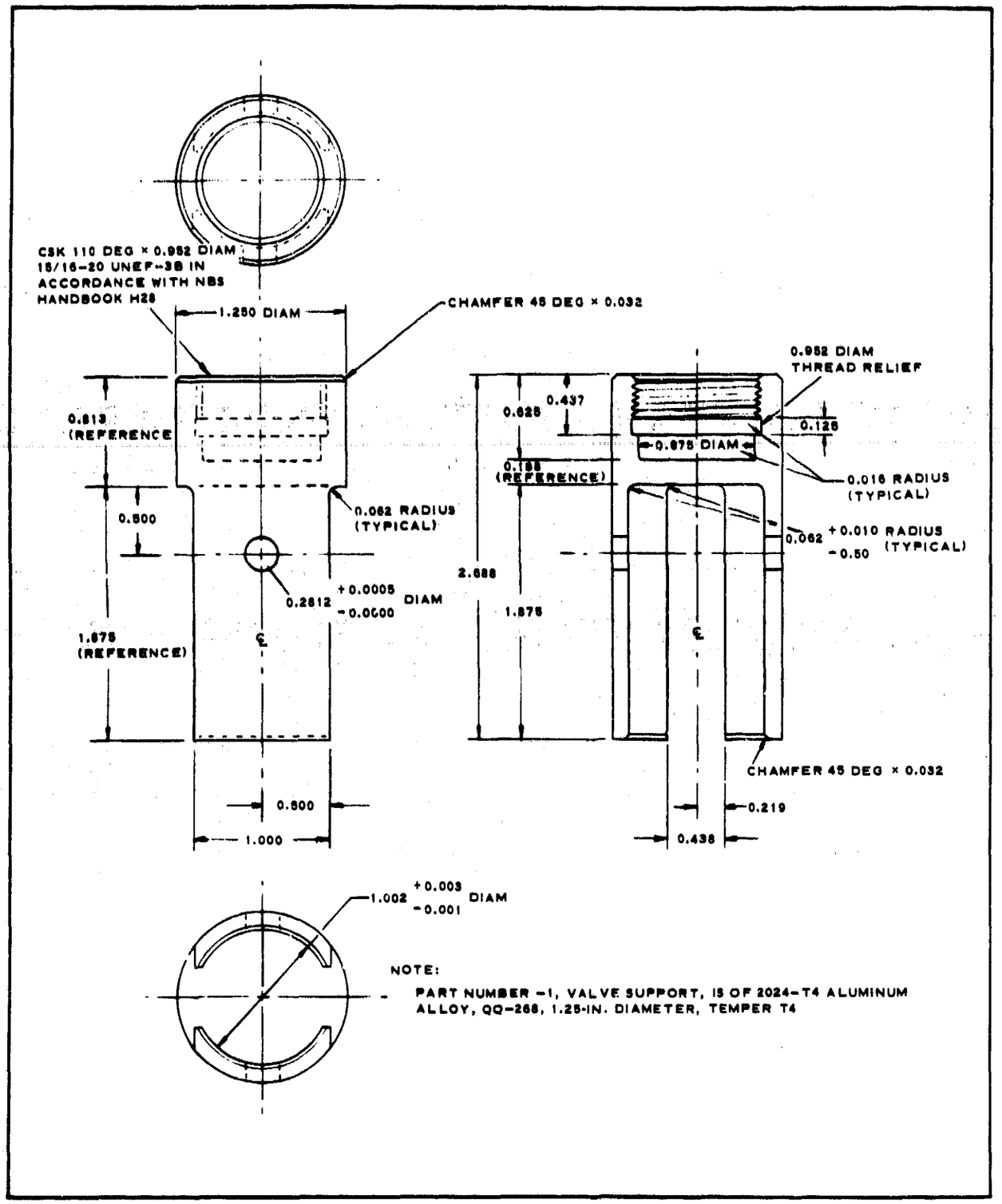

Figure 27 - Inflation Actuator, Swivel Attachment

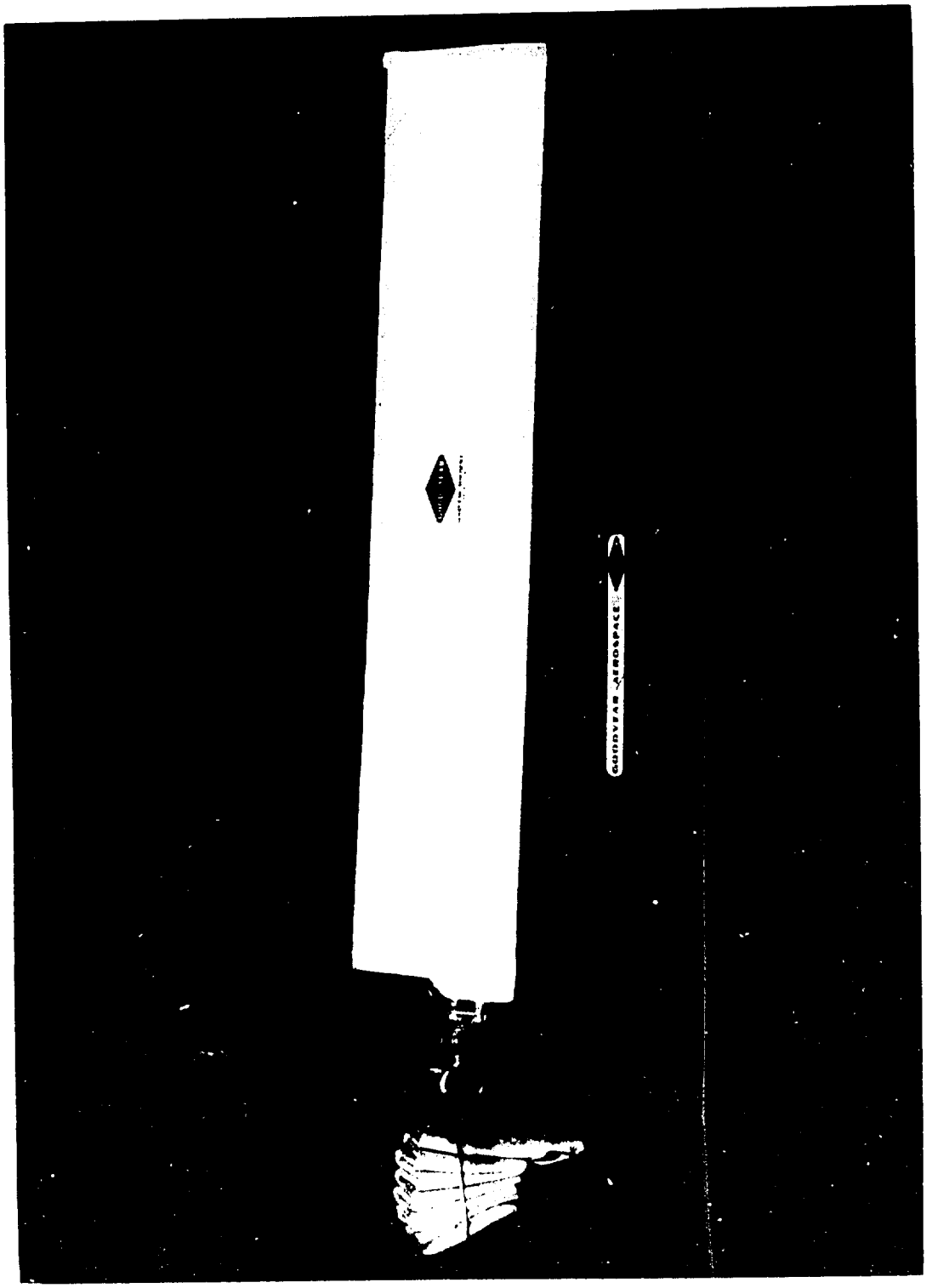

Figure 28 - Model Rotor Assembly

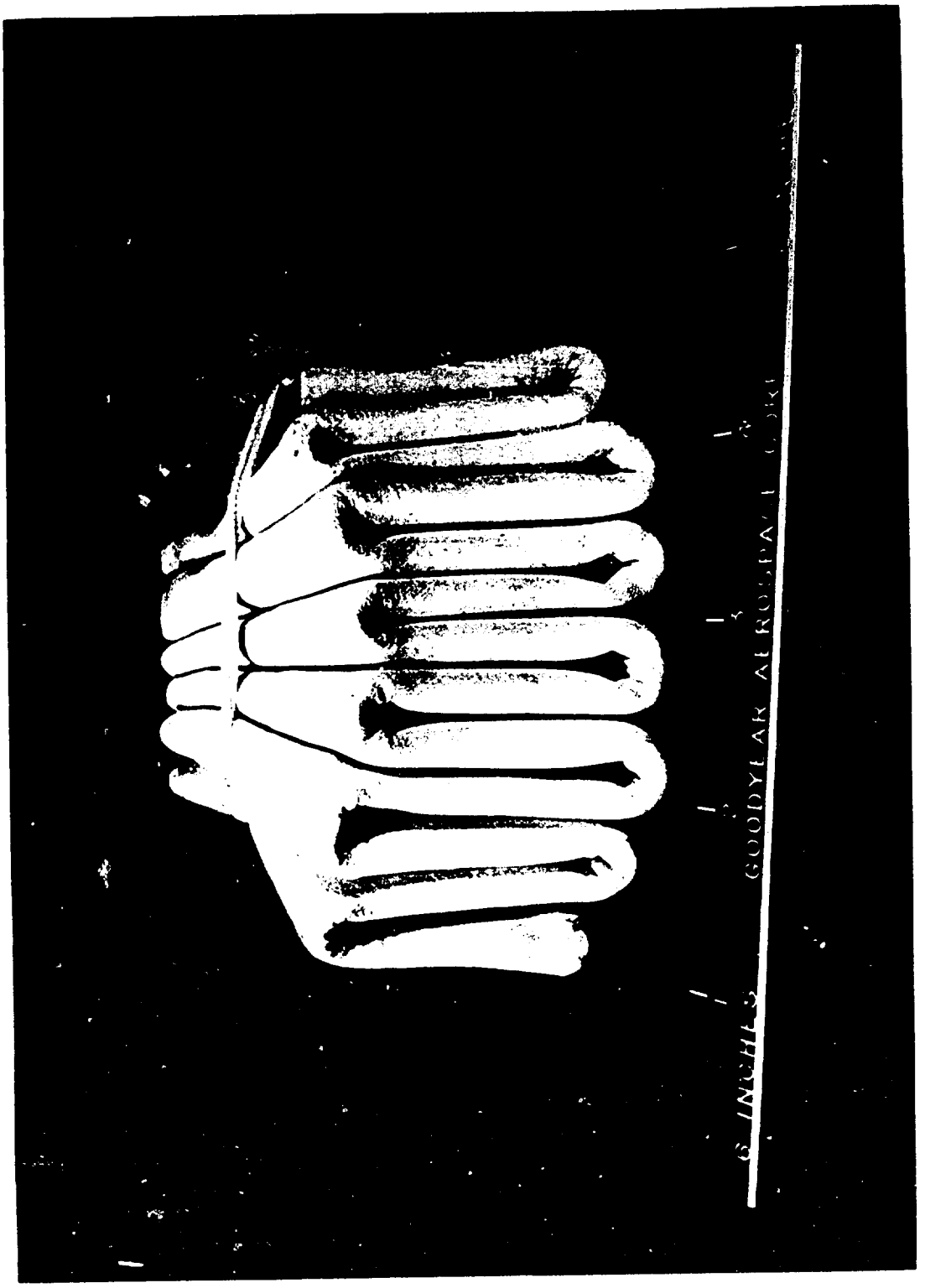

Figure 29 - Packaged Blade (Front View)

Figure 30 - Packaged Blade (Top View)

the blades was great enough to break the restraint cords and permitted the blade to elongate and inflate to their operating pressure of 6.5 psig.

5. FREE-FLIGHT TESTING

A series of five drop tests were conducted to demonstrate the free-flight capability of the inflatable rotor system. Testing consisted of releasing the rotor system from a helicopter hovering at altitude. For these tests, the blades initially were inflated to 6.0 psig and were in a trailing state. Shown in Figures 31 and 32 are pictures of the autogyro during two successful tests. Due to the downwash of the hovering helicopter, three of the five drops resulted in failure of the rotor to spin up. The lack of spin-up experienced during the three tests resulted from one of the two blades entangling in the payload. During the fifth test, one of the blades was damaged and therefore the entire test program could not be completed.

The two successful tests were sufficient to indicate that the inflatable rotor system would assume an autorotative state. The fact that autorotation began without any auxiliary device was significant. The results of this testing have demonstrated therefore that an inflatable rotor system has the capability of autorotating and decelerating a payload to a low descent velocity as required by the Army's airdrop mission.

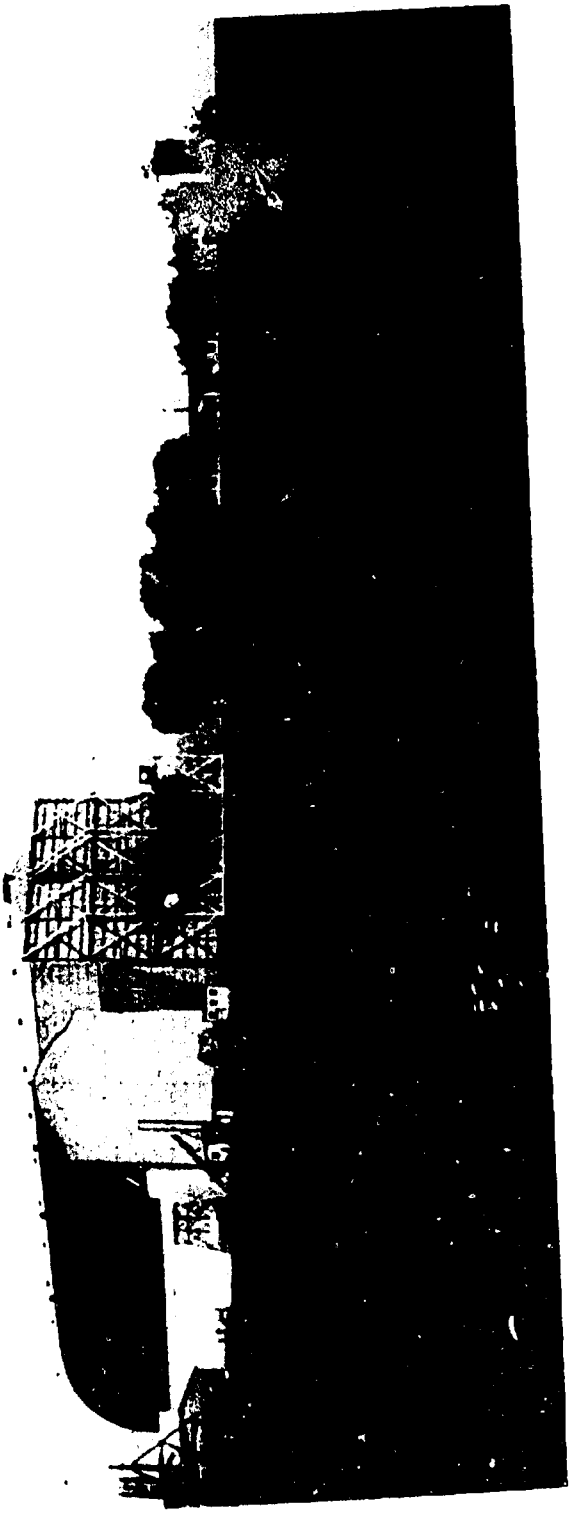

Figure 31 - Free-Flight Test

Figure 32 - Free-Flight Test (Closeup View)

LIST OF REFERENCES

1. Barada, J.J.: "Rotors for Recovery," Journal of Spacecraft. Vol 3, No. 1, January 1966, pp 104-109.

2. Mansfield, D.L.: Investigation of Ballute-Flexible Rotor Concept for Low Altitude Cargo Airdrop; March 31, 1966 to November 30, 1966, GER-12665. Akron, Ohio, Goodyear Aerospace Corporation.

3. Chernowitz, G.; and DeWeese, J.: Performance of and Design Criteria for Deployable Aerodynamic Decelerators. ASD-TR-61-579, Dayton, Ohio. Wright-Patterson Air Force Base. 1963.

4. Rabbot, J.R., Jr.; and Churchill, B.G.: Experimental Investigation of the Aerodynamic Loading on a Helicopter Rotor Blade in Forward Flight, RM L56I07. Washington, D.C., NACA 1956.

5. Goodale, B.A.; Boryda, J.J.: Investigation of Stored Energy Rotors for Recovery. ASD-TDR-63-745. Dayton, Ohio. Wright-Patterson Air Force Base. 1963.

6. Costakos, N.C.: Basic and Secondary Structural Weight of Expandable Space Structures. SAWE 456. Paper presented in Dallas, Texas to the Society of Aeronautical Weight Engineers. San Diego, Calif., 1964.

7. Alexander, W.C.: Investigation to Determine the Feasibility of Using Inflatable Balloon Type Drag Devices for Recovery Applications in the Transonic, Supersonic, and Hypersonic Flight Regime Part II. ASD-TDR-62-702. Dayton, Ohio, Wright-Patterson Air Force Base. October 1962.

8. Unpublished experimental data of Goodyear Aerospace Corporation, Akron, Ohio.

9. Jailer, R.W.; and Freilich, G.; and Norden, M.L.: Analysis of Heavy-Duty Parachute Reliability. WADDTR 60-200. Dayton, Ohio, Wright-Patterson Air Force Base. June 1960.

10. NAVORD Report 2101: Statistical Methods Appropriate for Evaluation of Fuze Explosive-Train Safety and Reliability. U.S. Naval Ordnance Laboratory, Maryland. October 1953.

BIBLIOGRAPHY

Abbot, I. A.; von Doenhoff, A. E.; and Strivers, L. S., Jr.: Summary of Airfoil Data. AGR L5C05. Washington, D. C., NACA. 1945.

Gessow, A.; and Myers, G. C.: Aerodynamics of the Helicopter. New York, N. Y., MacMillan Company. 1952.

Loewy, R. G.; Smyers, D. J.; and Gobel, R.: A Review of Theoretical and Experimental Investigations of the Rotor Aerodynamic Problem. R-217. Seattle, Wash., Boeing Company. 1960.

Meyers, J. R., Jr.; and Falabella, G., Jr.: An Investigation of the Experimental Aerodynamic Loading on a Model Helicopter Rotor. TN 2953. Washington, D. C., NACA. 1953.

Nielsen, J. N.; and Burnell, J. N.: Wind Tunnel Tests of Model Flexirotor Recovery System: Design and Construction of Drop-Test Model. Vidya Report No. 70. Palo Alto, Calif., Vidya, Inc. 1962.

Rabbot, J. P., Jr.: Static Thrust Measurements of the Aerodynamic Loading on a Helicopter Rotor Blade. TN 3688. Washington, D. C., NACA. 1956.

Vorachek, J.; and McFarland, L.: Final Report on Foam Fabric Rotor Blade Development. GER-10948. Akron, Ohio, Goodyear Aerospace Corporation. 1963.

Vorachek, J.: Progress Report on Flexible Fabric Rotor Blade Program Planning Budget for 1963. GER-10970. Akron, Ohio, Goodyear Aerospace Corporation. 1964.

Vorachek, J.: Final Report on Flexible Fabric Rotor Research for 1965. GER-12461. Akron, Ohio, Goodyear Aerospace Corporation. 1965.

FTC-TDR-64-12: Symposium on Parachute Technology and Evaluation - Proceeding. Vol I. El Centro, Calif., Flight Test Center, Edwards Air Force Base. 12 September 1964.

APPENDIX A - TRANSIENT SPIN-UP ANALYSIS

1. INTRODUCTION

Contained in this Appendix is a theoretical analysis covering the transient spin-up portion of the rotor blade deployment.

2. SUMMARY

An initial mathematical analysis of rotor deployment has been accomplished. Aside from the derived analytic relations which enable the system to be properly sized, an analytic procedure has been developed for determining to a first approximation, the variation of the rotor deployment angle and rotational speed with time for any particular design. By way of general results, it has been found that the rotor deployment angle increases linearly with time for a large initial range of angles. The rotational spin-up is accomplished primarily during the first 10 to 20 deg of rotor deployment.

3. ANALYSIS

The three equations governing the motion of the rotor during deployment have been derived to be

$$\dot{\phi}' \int_o^R \frac{dm}{dR} R1^2 dR = g \sin \phi \int_o^R \frac{dm}{dR} R1 dR + \Omega^2 \cos \phi \int_o^R \frac{dm}{dR} (r + X) R1 dR -$$

$$\int_o^R \left[(r + X)^2 \Omega^2 + (R1\dot{\phi} \sin \phi + \dot{d})^2 + R^2 1\ \dot{\phi}^2 \cos^2 \phi\right] \frac{dK_L}{dR}\ R1 dR, \quad (A\text{-}1)$$

$$\dot{\Omega} \int_o^R \frac{dm}{dR} (r + X)^2\, dR = Q_c - \int_o^R \left[(r + X)^2 \Omega^2 + (R1\dot{\phi} \sin \phi + \dot{d})^2 +\right.$$

$$\left. R1^2 \dot{\phi}^2 \cos \phi\right] \frac{dK_d}{dR} (r + X)\, dR\ , \quad (A\text{-}2)$$

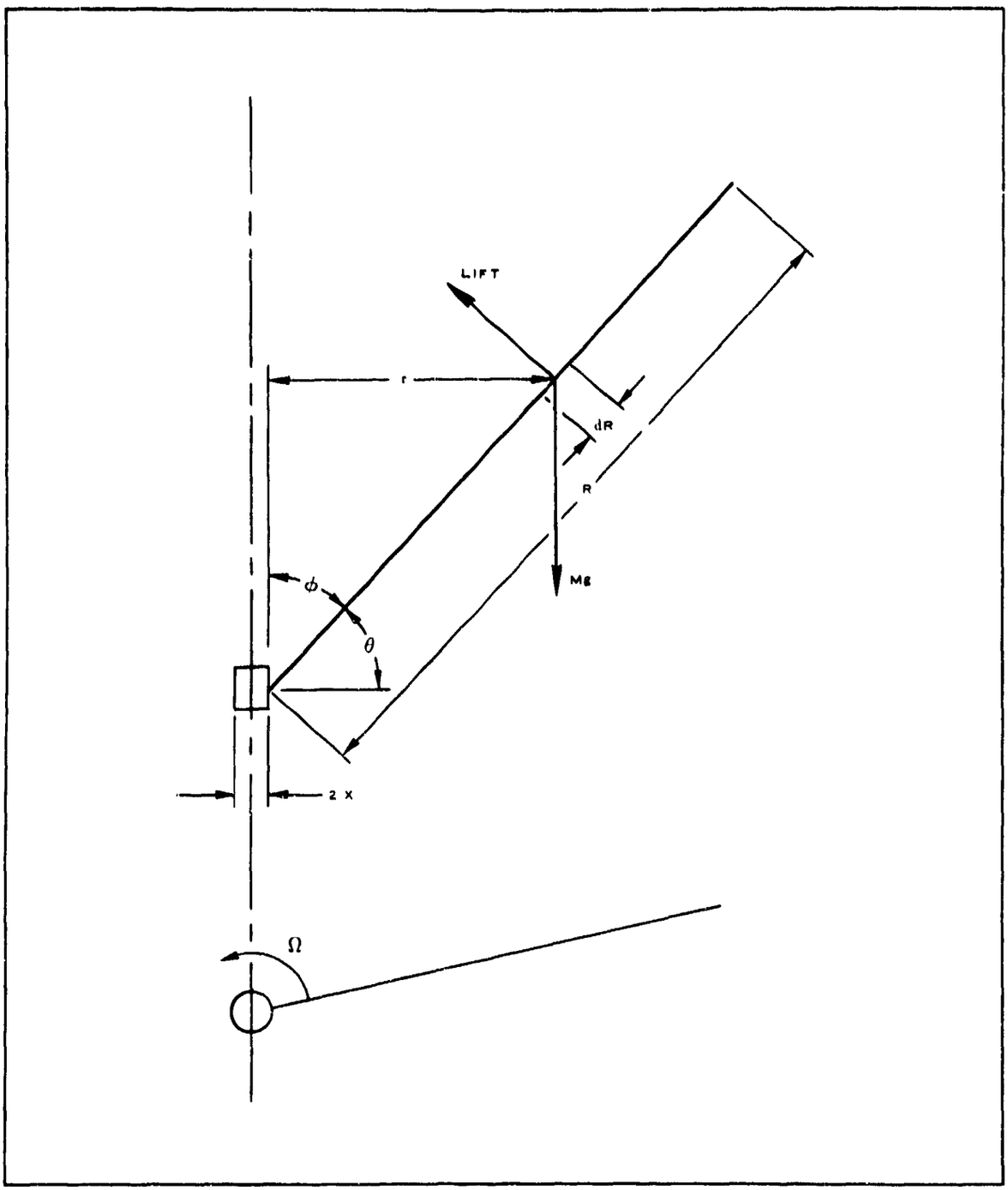

Figure A-1 - Reference for Rotor Deployment

APPENDIX A

$$\ddot{M}d = Mg - \sin\phi \int_0^R \left[(r + X)^2 \Omega^2 + (R1\dot{\phi} \sin\phi + \dot{d})^2 + R1^2 \dot{\phi}^2 \cos^2\phi\right] \frac{dK_L}{dR}\, dR. \tag{A-3}$$

Because the lift and drag forces and moments become significant only after a large amount of spin-up has occurred, the effective blade velocity may be taken as just the $(r + X)\,\Omega$ component throughout the present analysis. A major benefit realized is the decoupling of Equation A-3 from Equations A-1 and A-2. In addition, because $X/R << 1$, the effective blade velocity may be further reduced by good approximation simply to $r\Omega$.

Because of the complexity of these equations, the general analytical solution is expected to be both complex and extremely difficult to develop. It was found efficient therefore to concentrate on obtaining approximate solutions for the initial and final stages of rotor deployment.

The initial solution for Ω is:

$$\Omega = \frac{C_1 K_2}{1 - (K_2X)^2} \left\{ \frac{\sin\phi + (1 - \cos\phi)\, K_2X}{K_2X\,(\sin\phi + K_2X)} + \frac{K_2X}{\sqrt{1 - (K_2X)^2}} \right.$$

$$\left. \log \left[\frac{1 + K_2X - \sqrt{1 - (K_2X)^2}}{1 + K_2X + \sqrt{1 - (K_2X)^2}} + \frac{1 + K_2X \tan(\phi/2) + \sqrt{1 - (K_2X)^2}}{1 + K_2X \tan(\phi/2) - \sqrt{1 - (K_2X^2}} \right] \right\}. \tag{A-4}$$

Since K_2X is very small relative to unity (e.g., 5 or 6 percent), second-order terms involving $(K_2X)^2$ may be neglected. It follows that the second term in the braces does not contribute significantly over the range of interest, $0 \le \phi \le \pi/2$. Accordingly, the initial solution for Ω may be taken more simply as

$$\Omega = C_1 \frac{\sin\phi + (1 - \cos\phi)\, K_2X}{X\,(\sin\phi + K_2X)} . \tag{A-5}$$

Note that Ω approaches its indicated final value very rapidly relative to ϕ. For example, when $K_2X = 0.05$, Ω is up to 87 percent of its ultimate

value, when ϕ has increased to only 15 deg, and up to 92 percent and 95 percent of the indicated ultimate when ϕ is 30 deg and 45 deg, respectively. But according to Equation A-2, when Ω becomes zero, Ω and ϕ are related according to Equation A-6:

$$\Omega_f = \sqrt{\overline{Q}/\overline{K_D} \sin^3 \phi_f} \tag{A-6}$$

Equating Ω_f to the indicated final value of Equation A-5, the constant of integration, C_1, is evaluated as

$$C_1 = X (\sin \phi_f + K_2 X)\sqrt{\overline{Q}/\overline{K_D} \sin^3 \phi_f} \left[\sin \phi_f + (1 - \cos \phi_f) K_2 X\right]$$

or

$$C_1 \approx X\sqrt{\overline{Q}/\overline{K_D} \sin^3 \phi_f} \ . \tag{A-7}$$

The corresponding initial solution for $\dot{\phi}$ is given by

$$\dot{\phi} = (\overline{Q} - \Omega^2 \overline{K_D} \sin^3 \phi)/C_1 \ . \tag{A-8}$$

Note that ϕ increases linearly with time for a large initial range of the angle, ϕ. Furthermore, the ultimate value of ϕ, indicated by $\dot{\phi}$ going to zero, is reached simultaneously with the ultimate rotor speed, Ω_f, i.e., Ω goes to zero simultaneously. Thus, these solution(s) for the initial stages of rotor deployment have the required characteristics of the complete deployment process.

In the terminal phase of deployment, Equation A-1 may be approximated by the following equation which is more tractable:

$$K_1 \ddot{\phi} = g \sin \phi + \Omega_f^2 \left[K_1 \sin \phi (\cos \phi) - \overline{K_L} \sin^2 \phi\right] \ . \tag{A-9}$$

The corresponding solution for $\dot{\phi}$ is

$$\dot{\phi} = \left\{-2g \cos \phi/K_1 + \Omega_f^2 \left[\sin^2 \phi + (\overline{K_L}/K_L) (\sin \phi \cos \phi - \phi)\right] + C_2\right\}^{1/2} \ . \tag{A-10}$$

4. APPLICATION

The complete solutions for Ω and $\dot{\phi}$ pass from the initial solutions, Equations A-5 and A-8, to the final solutions, Equations A-6 and A-10, respectively, along smooth transition curves. Such a smooth transition already has been effected for Ω with the evaluation of the constant of integration, C_1, as in Equation A-7. A comparable transition is somewhat more difficult to achieve in the case of ϕ.

Requiring that both $\ddot{\phi}$ and $\dot{\phi}$ be zero at the end of deployment yields the two following relations:

$$g = \Omega_f^2 \left(\overline{K_L} \sin \phi_f - K_1 \cos \phi_f\right) , \tag{A-11}$$

$$2g \cos \phi_f = \Omega_f^2 \left[K_1 \sin^2 \phi_f + \overline{K_L} \left(\sin \phi_f \cos \phi_f - \phi_f\right) + C_2 K_1\right] . \tag{A-12}$$

In addition, for landing to be effected without vertical acceleration, we have according to Equation A-3:

$$Mg = \Omega_f^2 \sin^3 \phi_f \int_0^{R_L} \left(dK_L/dR\right) R^2 dR . \tag{A-13}$$

Equations A-11, -12, and -13 enable self-consistent values of Ω_f, ϕ_f, and C_2 to be chosen for any given design. The required applied torque, Q_c, then is specified by Equation A-6. As for the smooth transition for $\dot{\phi}$ from the values given by Equation A-8 to those available from Equation A-10 (C_2 having been evaluated as above), a simple initial choice at this time in the absence of additional information is for linear weighting to be used, i.e.,

$$\dot{\phi}_{\text{overall}} = \left(1 - \frac{\phi}{\phi_f}\right)\left(\overline{Q} - \Omega^2 \overline{K_D} \sin^3 \phi / C_1\right) + \frac{\phi}{\phi_f} \left\{- 2g \cos \phi / K_1 + \Omega_f^2 \left[\sin^2 \phi + \left(\overline{K}_L / K_1\right)\left(\sin \phi \cos \phi - \phi\right)\right] + C_2\right\}^{1/2} \tag{A-14}$$

APPENDIX A

Regardless of the weighting choice, Equation A-14 or its equivalent may be solved for ϕ as a function of time for any particular design isoclinically, analogically, digitally, or numerically using difference equations. It is anticipated that the dependence of the results obtained upon the weighting choice, if reasonable, will prove nominal.

Unclassified
Security Classification

DOCUMENT CONTROL DATA - R & D

(Security classification of title, body of abstract and indexing annotation must be entered when the overall report is classified)

1. ORIGINATING ACTIVITY *(Corporate author)*

Goodyear Aerospace Corp.
Akron, Ohio

2a. REPORT SECURITY CLASSIFICATION

Unclassified

2b. GROUP

3. REPORT TITLE

Preliminary Investigation of Ballute-Flexible Rotor Concept for Low Altitude Cargo Airdrop.

4. DESCRIPTIVE NOTES *(Type of report and inclusive dates)*

5. AUTHOR(S) *(First name, middle initial, last name)*

D.L. Mansfield

6. REPORT DATE	7a. TOTAL NO. OF PAGES	7b. NO. OF REFS
August 1966	102	10

8a. CONTRACT OR GRANT NO.	9a. ORIGINATOR'S REPORT NUMBER(S)
DA19-129-AMC-857(N)	
b. PROJECT NO.	
1M121401D195	GER-12970
c.	9b. OTHER REPORT NO(S) *(Any other numbers that may be assigned this report)*
d.	68-70-AD

10. DISTRIBUTION STATEMENT

This document has been approved for public release and sale; its distribution is unlimited.

11. SUPPLEMENTARY NOTES	12. SPONSORING MILITARY ACTIVITY
	US Army Natick Laboratories Natick, Mass. 01760

13. ABSTRACT

Conceptual design for an airdrop system from a 500 ft. altitude for payloads from 2,000 to 35,000 lb using a spinning Ballute for cargo extraction and initial rotor spin-up and an autorotating inflatable flexible rotor for terminal descent are reported. Ballute weights and rotor system size and weights are evaluated for systems with and without a flare maneuver to meet acceptable impact velocity conditions. Operational requirements and a preliminary estimate of reliability are presented. Design and free-flight testing of a 5-ft. diameter model inflatable rotor is described.

14. KEY WORDS	LINK A		LINK B		LINK C	
	ROLE	WT	ROLE	WT	ROLE	WT
Air-drop operations	8					
Delivery	8					
Descent	8					
Payload	9					
Aircraft	9					
Ballute	10					
Rotary Wings	10					
Low altitude	8					